Intercellular Communication During Human Pluripotent Stem Cell Lineage Specification

by © Grace A. Christopher B.Sc.

A Thesis Submitted to the School of Graduate Studies in partial fulfilment

of the requirements for the degree of

Masters of Science in Medicine (Cancer and Development).

Division of Biomedical Sciences, Faculty of Medicine

Memorial University of Newfoundland

October 2021

St. John's, Newfoundland and Labrador

Abstract

During embryonic germ layer development, cells must communicate with each other and their environment to ensure proper lineage specification and tissue development. Proteins of the connexin (Cx) or pannexin (PANX) protein families mediate cellular communication. Cx's facilitate direct cell-cell communication through gap junction channels, while PANXs release small molecules into the extracellular space for autocrine or paracrine signalling. While previous reports suggest that gap junctional intercellular communication may contribute to germ layer formation, there have been no comprehensive expression analyses or genetic ablation studies on either Cxs or PANXs during human pluripotent stem cell (PSC) specification to the three embryonic germ lineages. I screened the mRNA profile and select protein expression of human Cx and PANX isoforms in undifferentiated human induced pluripotent stem cells and after directed differentiation into the three embryonic germ lineages: ectoderm, endoderm and mesoderm. RT-qPCR analysis of control iPSCs revealed upregulation of Cx62 in iPSC-derived ectoderm cells, Cx45 upregulation in ectoderm and mesoderm cells, and enrichment of Cx30.3, Cx31, Cx32, Cx36, Cx37 and Cx40 in endoderm. However, Cx43 and PANX1 remain highly expressed in iPSCs as well as cells of each germ lineage. Despite high expression levels, both the Cx43 and the PANX1 CRISPR-Cas9 knockout iPSCs each successfully differentiated into cells of all three germ layers, suggesting that Cx43 and PANX1 are dispensable during directed iPSC lineage specification. This is the first comprehensive analysis of Cx and PANX isoform expression throughout iPSC germ layer segregation. Future studies will

reveal whether other Cx or PANX isoforms compensate for the loss of Cx43 and/or PANX1 in the generated knockout iPSCs cells during germ lineage specification.

Lay Summary

Just as communication is essential to people and societies, the cells that make up our bodies are in constant communication with each other. Very early in human embryonic development, cells must decide what sort of adult cell type they will become. While making fate decisions, cells communicate with each other to ensure that every individual cell is properly placed and functioning appropriately. When something goes wrong in this process, human developmental disorders can arise. In order to learn more about how cells communicate with each other during human embryonic development, this project will mimic the first embryonic cell fate decisions using human-induced pluripotent stem cells. Induced pluripotent stem cells are created by "reprogramming" adult skin cells into stem cells, which can then become any cell type in the body. With the development of straightforward gene-editing techniques (CRISPR-Cas9), genes that are involved in cell communication can easily be deleted or mutated. It is hypothesized that when the cells cannot communicate with each other, human stem cell fate decisions will be compromised. Herein is shown that deletion of heavily studies communication proteins, Cx43 or PANX1, does not impact early fate decisions of stem cells. This vital work will help us better understand human developmental disorders and hopefully one day uncover treatments and preventative measures.

Co-Authorship Statement

Versions of Figures 3.7 through 3.10 (with slight modification) were published within Frontiers in Cell and Developmental Biology:

Noort RJ*, Christopher GA*, and Esseltine JL. Pannexin 1 influences lineage specification of human iPSCs. Frontiers in Cell and Developmental Biology. Volume 9. doi: https://doi.org/10.3389/fcell.2021.659397. *contributed equally. Contributing authors retain copyright to materials presented in this paper, including that presented in Figures 3.7 through 3.10 of this thesis.

Dr. Jessica L. Esseltine designed and engineered the *GJA1-/-* and *PANX1-/-* human iPSCs used throughout this study. Rebecca Frohlich (Noort) and Jessica Esseltine designed the RT-qPCR primer sets, and Rebecca performed primer validation. Differentiation and RNA harvest for RT-qPCR presented in Figure 3.1 was carried out by myself. Rebecca Frohlich performed one biological replicate while I completed the rest of the data set. Sequencing of the *PANX1-/-* iPSC line and identification of induced mutations presented in Figure 3.10 was carried out by Rebecca Frohlich. All remaining experiments and data analysis were conducted myself.

Acknowledgements

I would first like to extend much gratitude and thanks to my supervisor Dr. Jessica Esseltine whose guidance has been instrumental in the development of this project. Secondly, to my committee members, Dr. Ken Kao and Dr. Laura Gillespie, for providing expert insight and opinions of benefit to this project. I am indebted to the current and former members of the Esseltine research group for their direction, encouragement, and aid throughout my master's program. In specific I would like to thank Rebecca Frohlich for acting as both a mentor and friend during the last two years.

This project was largely supported by several faculty members, including Dr. Jacqueline Vanderluit, Dr. Qui Yuan, and Dr. Karren Mearrow, as well as members of the CORE facility Stephanie Tucker and Chris Corkum.

Finally, this work was supported through the Natural Sciences and Engineering Research Council Discovery Grant RGPIN-2019-04345, Memorial University Faculty of Medicine startup funds and the Medical Research Endowment Fund to Jessica L. Esseltine.

Table of Contents

Abstract ii

Lay Summary iv

Co-Authorship Statement v

Acknowledgements vi

List of Tables xi

List of Figures xii

List of Abbreviations and Symbols xiii

1 Introduction 1

1.1 Human Embryonic Development 1

1.2 Embryonic Gastrulation and Development of the Embryonic Germ Layers 2

1.3 Stem Cells 8

1.4 Cellular Differentiation 12

1.5 Cellular Communication 14

1.6 Gap Junctional Intercellular Communication 15

1.7 GJIC in embryonic development and disease 19

1.8 Connexins influence stem cell reprogramming and cell fate specification 19

1.9 Cell-cell communication through the Pannexin family of large pore channels 21

1.10 Pannexin channels in human development and disease 23

1.11 Genetic Engineering 26
1.12 Rationale and objectives 27
1.13 Summary of Findings 28
2 Materials & Methods 29
2.1 Cell Lines 29
2.2 Stem Cell Maintenance 29
2.3 Directed Differentiation 30
2.4 Spontaneous Monolayer Differentiation 31
2.5 Immunofluorescence 32
2.6 Confocal Microscopy 33
2.7 Image Analysis 33
2.8 Western Blotting 35
2.8.1 Cell Lysis, Protein Extraction, and Protein Quantification 35
2.8.2 SDS PAGE 36
2.8.3 Immunoblotting 37
2.8.4 Western Blot Imaging 37
2.9 RNA Analysis 39
2.9.1 Cell Lysis and RNA Extraction 39
2.9.2 cDNA Conversion 40

2.9.3 Quantitative RT-PCR (RT-qPCR) 40

2.10 Statistical Analysis 42

3 Results 44

3.1 Connexin isoforms are differentially expressed during human iPSC specification to the three germ lineages 44

3.2 Cx43 protein expression persists throughout lineage specification 48

3.3 Human iPSCs tolerate *GJA1* CRISPR-Cas9 manipulation 51

3.4 Cx43-eGFP iPSCs differentiate into all three germ lineages 52

3.5 Cx43 is Dispensable During Lineage Specification 58

3.6 Cx32 is Retained Intracellularly in iPSCs and Germ Lineages 61

3.7 PANX1 is expressed in human iPSCs and cells of the three germ layers 64

3.8 PANX1 is alternatively glycosylated in cells from the three germ layers 64

3.9 PANX1 is differentially localized in Human Germ Lineages 65

3.10 *PANX1*-/- human iPSCs remain viable and morphologically comparable to WT iPSCs 71

3.11 PANX1 is not required for iPSCs Germ Lineage Commitment 74

4 Discussion: 77

4.1 Cell-cell communication in human pluripotent stem cells. 77

4.2 The connexin mRNA profile of human iPSC derived germ lineages 81

4.2.1 Connexins in ectoderm 81

4.2.2 Connexins in mesoderm 83

4.2.3 Connexins in endoderm 84

4.3 Pannexin1 in human stem cells and cell fate decisions 87

4.4 Pannexin1 is alternatively glycosylated and localized in iPSC-derived germ lineages 88

4.5 PANX1 is not essential for iPSC directed differentiation into the germ lineages 89

4.6 Study limitations 90

4.7 Conclusions 91

4.8 Perspectives and future directions 95

5 References 97

6 Appendix A 128

List of Tables

Table 2.1: Primary and Secondary Antibodies Used in Immunofluorescence 34

Table 2.2: Primary and Secondary Antibodies Used in Western Blotting.....38

Table 2.3: Thermocycler settings for RT-qPCR.....40

Table 2.4: Complete Primer Sets and Sequences used in RT-qPCR Analysis 55

List of Figures

Figure 1.1 - Human pluripotent stem cells differentiate into multipotent and terminal cell types. 4

Figure 1.2 - Signalling cascades and lineage markers involved in lineage specification. . 23

Figure 1.3 - Hexameric connexin hemichannels mediate gap junctional intercellular communication. 33

Figure 1.4 - Pannexin proteins form heptameric transmembrane channels. 24

Figure 3.1 - Connexin expression during iPSC lineage specification. 46

Figure 3.2 - Cx43 protein expression and localization in iPSCs and cells of each germ lineage. 49

Figure 3.3 - CRISPR-Cas9 manipulation of *GJA1* in human iPSCs. 54

Figure 3.4 - Cx43 Localization in spontaneously differentiated Cx43-eGFP CRISPR knock-in iPSCs. 56

Figure 3.5 - Directed differentiation of *GJA1-/-* iPSCs to the three germ layers. 59

Figure 3.6 - Cx32 localization in iPSCs and endoderm cells 62

Figure 3.7 - PANX1 is differentially glycosylated in the three germ layers. 67

Figure 3.8 - PANX1 is differentially localized in the three embryonic germ layers. 69

Figure 3.9 - PANX1 expression and CRISPR-Cas9 gene ablation in human iPSCs. 72

Figure 3.10 - *PANX1-/-* iPSCs Trilineage Differentiation. 75

Figure 4.1 - Connexin expression profile described in literature. 90

Figure 4.2 - Expression and localization of connexin and pannexin proteins in iPSCs and the three germ layers. 102

List of Abbreviations and Symbols

ANOVA - Analysis of variance

ATP- Adenosine triphosphate

BMP - Bone morphogenic protein

BSA - Bovine serum albumin

Ca^{2+} - Calcium ion

Cas - CRISPR associated proteins

cDNA - Complementary deoxyribonucleic acid

CO_2 - Carbon Dioxide

CRISPR - Clustered regularly interspaced short palindromic repeats

crRNA - CRISPR ribonucleic acid

Fig - Figure

% - Percent

°C - Degrees Celsius

ANOVA - Analysis of variance

ATP- Adenosine triphosphate

BMP - Bone morphogenic protein

BSA - Bovine serum albumin

Ca^{2+} - Calcium ion

Cas - CRISPR associated proteins

cDNA - Complementary deoxyribonucleic acid

cm^2 - centimetres squared

CO_2 - Carbon Dioxide

CRISPR - Clustered regularly interspaced short palindromic repeats

crRNA - CRISPR ribonucleic acid

Cx - Connexin

Cx26 - Connexin 26/*GJB2*

Cx30 - Connexin 30/*GJB6*

Cx30.3 - Connexin 30.3/*GJB4*

Cx31 - Connexin 31/*GJB3*

Cx31.1 - Connexin 31.1/*GJB5*

Cx32 - Connexin 32/GJB1

Cx36 - Connexin 36/*GJD2*

Cx37 - Connexin 37/*GJA4*

Cx40 - Connexin 40/*GJA5*

Cx43 - Connexin 43/*GJA1*

Cx45 - Connexin 45/*GJA1*

Cx62 - Connexin 62/*GJA10*

DABCO - 1,4-Diazabicyclo[2.2.2]octane

DAPI - 4′,6-diamidino-2-phenylindole

DIC - Differential interference contrast

DKK1 - Dickkopf-related protein 1

DMEM - Dulbecco's Modified Eagle Medium

DNA - Deoxyribonucleic acid

DNase - Deoxyribonuclease

Ecto - Ectoderm

Endo - Endoderm

ER - Endoplasmic reticulum

ESC - Embryonic stem cell

FGF - Fibroblast growth factor

FOXA2r - Forkhead box protein A2

GAPDH - Glyceraldehyde 3-phosphate dehydrogenase

GFP - Green fluorescent protein

GJIC - Gap junction intercellular communication

Gly - Glycolysis

gRNA - Guide ribonucleic acid

HCl - Hydrochloric acid

HRP – Horseradish peroxidase

ICM - Inner cell mass

iPSC - Induced pluripotent stem cells

JACop – Just another colocalization plugin

KCl - Potassium chloride

KH_2PO_4 - Potassium dihydrogen phosphate

Klf4 - Krüppel-like factor 4

KO - Knockout

Meso - Mesoderm

min - minute

MIXL1 - Mix Paired-Like Homeobox

ml - millilitre

mM - millimolar

NA - Numerical aperture

Na_3VO_4 - Sodium orthovanadate

NaCl - Sodium chloride

NaFl - Sodium fluoride

nm - nanometer

NPC - Neural precursor cell

PANX - Pannexin

PAX6 - Paired box protein 6

PBS - Phosphate buffered saline

pH - The potential of hydrogen or power of hydrogen

PSC - Pluripotent stem cells

RNA - Ribonucleic acid

RNase - Ribonuclease

ROCKi - Rho-kinase inhibitor

RPM - Revolutions per minute

RT-qPCR - Quantitative real-time polymerase chain reaction

SDS-PAGE - Sodium dodecyl sulphate polyacrylamide gel electrophoresis

siRNA - Short interfering ribonucleic acids

SOX2/SOX17 - SRY box transcription factor

TBS-T - Tris-buffered saline with Tween 20

TGF-β - Transforming growth factor-beta

tracrRNA - trans-activating CRISPR ribonucleic acid

ug - microgram

ul - microliter

um - micrometre

V - Volts

WNT - Combination name including Wingless (Wg) and integration site (Int)

1 Introduction

1.1 Human Embryonic Development

The development of a complex multicellular organism from a single fertilized cell relies on the tight orchestration of several events, including cellular migrations and rearrangements, cellular morphology changes and cell fate specification (Chan et al., 2017; Kumar et al., 2017). Cellular communication between neighbouring cells is highly regulated; specific timing and localization of signalling enables patterning and organization of the developing embryo. As such, the loss of cellular communication can be detrimental to processes including lineage specification, tissue patterning, and organogenesis (Perrimon et al., 2012). Upon oocyte fertilization, human embryonic development begins with a series of cell divisions called cleavage that results in 8 equivalent blastomeres (Figure 1.1). Each of these blastomeres retains the potential to form the entire living organism. Once the embryo extends past the 16 cell stage, cellular compaction and expression of adhesion molecules produces a morula. Cells within the morula develop polarity, and subsequent cell rearrangements and lineage restriction events produce a hollow ball of cells known as a blastocyst. Cellular specification within the blastocyst restricts cells to either the trophoblast, which gives rise to extra-embryonic tissues, or the inner cell mass (ICM), yielding the embryo proper. Implantation begins the next stage of embryo development and results in epiblast formation (Wolpert, 2015). In the weeks post-implantation, localized signalling gradients across the embryo will trigger large cellular rearrangements that coordinate the formation of the primitive streak and subsequent gastrulation. The three tissue layers that arise during gastrulation (ectoderm, mesoderm and

endoderm) are collectively known as the embryonic germ layers and will give rise to select organs unique to each lineage (Figure 1.1; (Tam & Loebel, 2007). For example, the ectoderm forms the skin and central nervous system, while mesoderm gives rise to muscle and connective tissue, and endoderm contributes to internal organs, including the pancreas and intestines (Kiecker et al., 2016; Zorn & Wells, 2009). Endodermal cell populations exist within both extraembryonic and embryonic structures. To give distinction between extraembryonic and embryonic endoderm, populations derived from the trophoblast are considered primitive endoderm while the epiblast-derived germ layer is considered embryonic or definitive endoderm.

1.2 Embryonic Gastrulation and Development of the Embryonic Germ Layers

In the developing embryo, Activin, Nodal, bone morphogenic protein (BMP), and WNT signalling induce gastrulation (Chhabra et al., 2019; Nostro et al., 2008; Tam & Loebel, 2007). WNT3 induces primitive streak formation and subsequent mesendoderm formation. Segregation towards mesoderm relies on prolonged WNT3 and BMP signalling while definitive endodermal lineages emerge in response to elevated levels of expression of Nodal and Activin A (Figure 1.2; (Tam & Loebel, 2007). Activation of the BMP pathways through Activin A induces Nodal signalling, to promote the expression of various endoderm-specific transcription factors such as FOXA2, GATA4, and SOX17 (Zorn & Wells, 2009). SOX17 is a robust marker for definitive endoderm formation (Wang et al., 2011). Loss of SOX17 in mice reduces definitive endoderm populations, limiting downstream foregut, hindgut, and midgut differentiation (Kanai-Azuma et al., 2002). In

light of its strong implications in endoderm development SOX17 is widely used to validate the formation of endoderm during development.

Active WNT and bone morphogenic protein (BMP) and transforming growth factor-β (TGF-β) signalling permit mesoderm formation (Figure 1.2). Differentiating pluripotent stem cells (PSCs) fail to produce mesoderm when treated with the potent WNT inhibitor Dickkopf-related protein 1; DKK1 (Lindsley et al., 2006; Tam & Loebel, 2007). Furthermore, BMP/TGF-β induces the expression of known mesoderm and lineage markers *MIXL1* (encoding for mix paired-like homeobox 1; MIXL1) and *T* (encoding for Brachyury). Treatment of embryos with BMP inhibitor Noggin downregulates *T* expression, while BMP4 actively promotes the formation of SMAD2/3-containing DNA binding complex that promotes expression of *MIXL1* (Raymond et al., 2014; Sharma et al., 2017). It is therefore common to use MIXL1 as a marker of mesendoderm induction.

Prior to the formation of the primitive streak, a wave of Nodal expression migrates across the cells of the epiblast, inducing Lefty in its wake. As an effective inhibitor of WNT, active Lefty prevents specific cells from ingressing along the primitive streak (Engert et al., 2013). Partnered with Nodal, TFG-β and BMP inhibition, these cells differentiate into ectoderm (Figure 1.2; (Tam & Loebel, 2007; Tchieu et al., 2017). Premature neurectoderm development results from the absence of Nodal (Tam & Loebel, 2007). Thus the formation of ectoderm is reliant the on presence of Nodal and the absence of endoderm and mesoderm drivers.

Figure 1.1 – Cell potency is progressively lost as lineage specification occurs during embryogenesis or *in vitro* stem cell differentiation. Human development begins with the fertilization of the oocyte. A series of cleavages produces a 2-cell then a 4-cell embryo. Continued segregation events and cellular reorganization form the preimplantation embryo, comprised of the trophectoderm, the blastocoel, and the inner cell mass. Cells of the inner cell mass are pluripotent and develop into the embryo proper. After implantation, the developing embryo undergoes gastrulation forming the three germ layers that give rise to the early embryo cell types and tissues. Generation of human pluripotent stem cells for culture begins with either the isolation of undifferentiated cells of the preimplantation embryos inner cell mass (embryonic stem cells, ESCs) or reprogramming of terminally differentiated cells (induced pluripotent stem cells, iPSCs). Pluripotent stem cells (PSCs) have the capacity to form all cell types of the embryo. Lineage specification restricts pluripotent stem cells to the three germ layers. Resident cells of the three germ lineages are multipotent as they are only capable of producing cell types specific to one lineage. Multipotent cells respond to environmental signals, continuing to divide and differentiate until they reach terminal differentiation. Terminally differentiated cells are limited to one form and function. This figure was generated through the use of *BioRender.com*

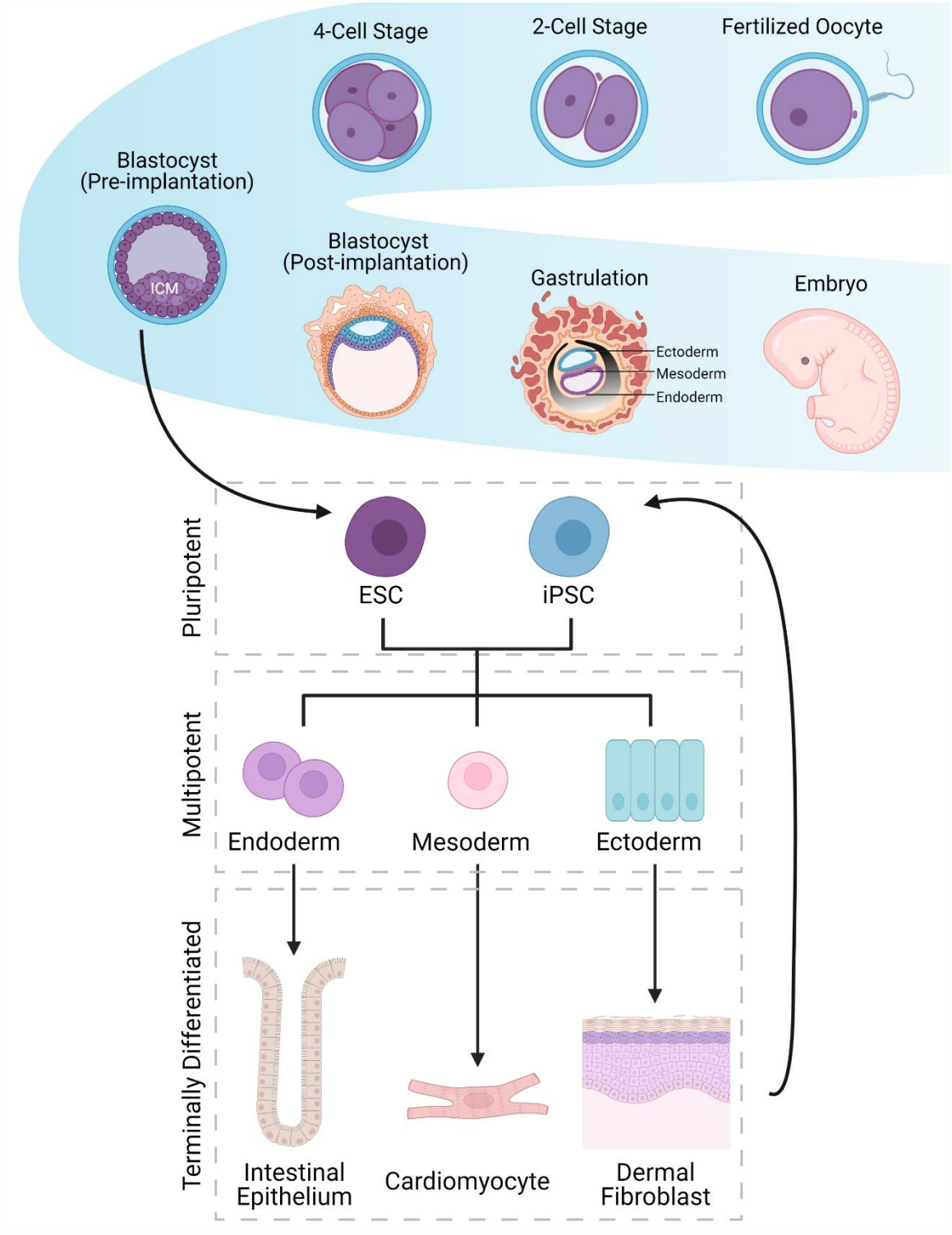
4-Cell Stage
2-Cell Stage
Fertilized Oocyte
Blastocyst
(Pre-implantation)
ICM
Blastocyst
(Post-implantation)
Gastrulation
Ectoderm
Mesoderm
Endoderm
Embryo
Pluripotent
ESC
iPSC
Multipotent
Endoderm
Mesoderm
Ectoderm
Terminally Differentiated
Intestinal
Epithelium
Cardiomyocyte
Dermal
Fibroblast

Figure 1.2 - Signalling cascades and lineage markers involved in germ lineage specification. Human pluripotent stem cells, including ESCs and iPSCs express SOX2 and *POU5F1* encoding for OCT4 as undifferentiated state markers. Loss of TGF-β and FGF-2 signalling allows PSCs to begin differentiating towards the three germ layers. PSCs with active WNT develop into mesendoderm marked by MIXL1 and *T* encoding for Brachyury. Continued WNT and BMP activity permit mesoderm development and continued expression of lineage marker Brachyury. Formation of endoderm is marked by SOX17 expression and relies on NODAL and Activin A activity. Inhibition of NODAL, BMP and TGF-β signalling prevents the formation of mesendoderm, and instead results in early ectoderm. This figure was generated through the use of *BioRender.com*

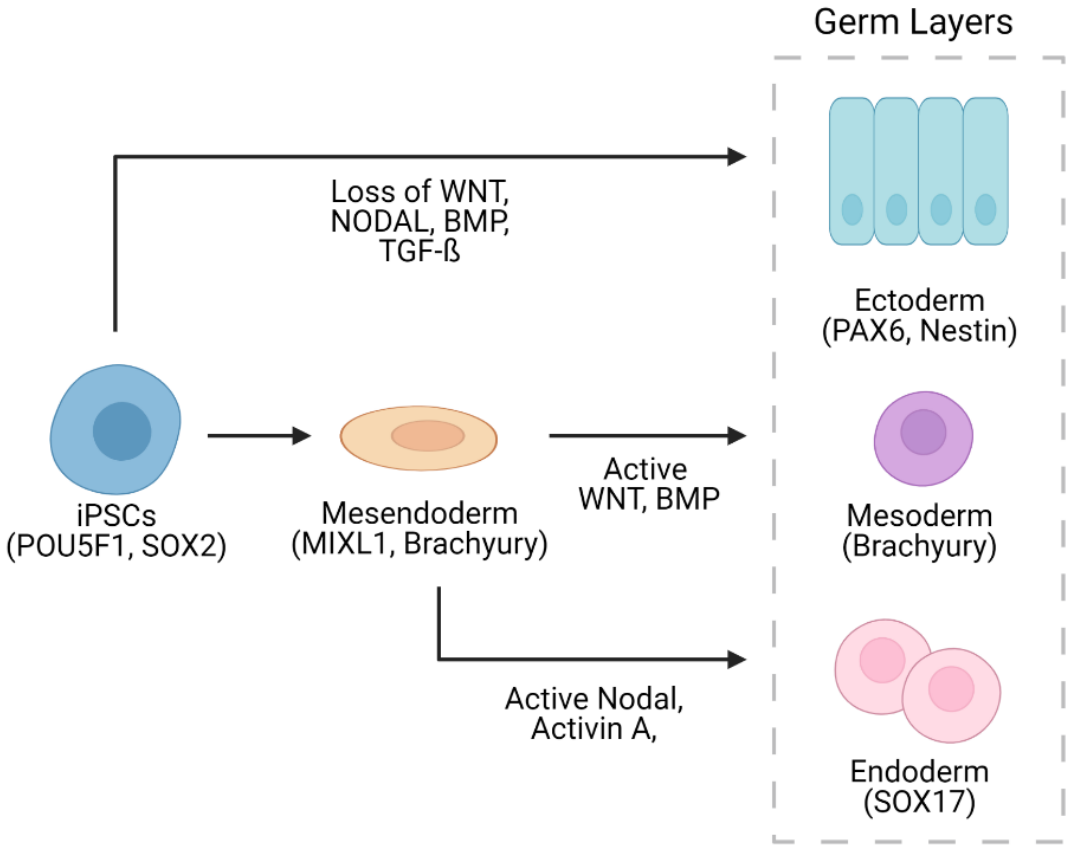
Germ Layers
Loss of WNT,
NODAL, BMP,
TGF-ß
Ectoderm
(PAX6, Nestin)
iPSCs
(POU5F1, SOX2)
Mesendoderm
(MIXL1, Brachyury)
Active
WNT, BMP
Mesoderm
(Brachyury)
Active Nodal,
Activin A,
Endoderm
(SOX17)

1.3 Stem Cells

Model organisms have yielded seminal discoveries toward understanding embryogenesis. Recent advancements in the isolation and generation of human PSCs permit human-specific investigations into human developmental processes such as cellular differentiation and germ linage specification (Shahbazi, 2020; Tam & Loebel, 2007).

The term “stem cell” refers to a unique classification of cells marked by their ability to self-renew and give rise (differentiate) to specialized cell types as determined by their potency (Biehl & Russell, 2009; Singh et al., 2016). Stem cells can divide both symmetrically and asymmetrically. Stem cells maintaining their potency will undergo symmetric division, which yields two daughter cells phenotypically identical to the parent cell. Asymmetric division of stem cells produces morphologically different daughter cells, leading to differentiation. Stem cells undergoing asymmetric division must exit the cell cycle and prevent cell death while altering their gene activity and morphology (Soufi & Dalton, 2016). Successful asymmetric division allows cells to progressively lose potency, and in this manner, can mediate cellular differentiation (Shahriyari & Komarova, 2013). Differentiation proceeds in a stepwise manner towards lineage commitment, the crucial stage that results in the emergence of the three embryonic germ layers. Signals from neighbouring cells can dramatically influence this process and subsequent cellular differentiation. For example, partial disruption of intercellular communication using Cre-loxP deletion of Cx43/Cx45 in ESCs prevents primitive endoderm formation, a crucial specifier of later embryonic cell types; endoderm, ectoderm, and mesoderm (Wörsdörfer et al., 2017). Similarly, chemical disruption of intercellular communication prevents ESC to

hepatocyte maturation and activity (Qin et al., 2016). Due to their nature and response to changes in cellular communication, stem cells are a sophisticated model system with widespread applications.

Potency describes the breadth of downstream cell types into which a stem cell can differentiate. Classification of a stem cell as either totipotent, pluripotent, multipotent or unipotent can be influenced by a stem cell's source (Biehl & Russell, 2009; Raveh-Amit et al., 2013). Multipotent tissue-resident stem cells, somatic stem cells, are the most specialized type of stem cell. These cells reside in areas of the body requiring high turnover rates to maintain tissue integrity and functionality (Biehl & Russell, 2009). For example, one of the most proliferative somatic stem cell niches resides in the small intestine. The human intestinal epithelial lining is entirely replaced every 4 to 5 days by resident stem cells within intestinal crypts (Umar, 2010). Thus, somatic stem cells are considered multipotent, as they are restricted to select cell types specific to their resident tissue.

By contrast, pluripotent stem cells, including embryonic stem cells and induced pluripotent stem cells, are capable of forming any of the three primordial germ lineages. ESCs are generated through the isolation and culture of inner cell mass cells from the preimplantation blastocyst (Evans & Kaufman, 1981; Thomson & Odorico, 2000). Embryonic stem cells can be cultured *in vitro* indefinitely, remaining in undifferentiated proliferative states for over a year without replicative senescence (Rosler et al., 2004). Theoretically ESCs can differentiate into any cell type of the body as they originate from the preimplantation blastocyst inner cell mass (Thomson et al., 1998; Thomson & Odorico, 2000). As isolation of inner cell mass cells destroys the human embryo, ethical concerns

surround the generation and use of human ESCs. For a comprehensive review and discussion of the ethics surrounding the use of human embryonic stem cells please see (de Wert & Mummery, 2003; Lo & Parham, 2009). Without an abundantly available ethical source, the application of human ESCs is limited. Out of this ethical controversy and increased demand for personalized regenerative medicine came another source for pluripotent stem cells.

Induced pluripotent stem cells are a unique tool in cellular biology as they are produced through the reprogramming of terminal cell types such as dermal fibroblasts, leukocytes, or urinary endothelial cells (Takahashi et al., 2007). iPSCs have become the favoured model system for disease modelling or personalized regenerative medicine as they can be easily sourced from genetically matched donors without ethical debate (Zhao et al., 2013). Derived from healthy individuals as well as patients with disease, iPSCs represent a valuable model for human disease progression and pathogenesis. Similar to ESCs, iPSCs retain their ability to produce any cell type of the body while dividing in culture (Zhu & Huangfu, 2013). Forced expression of reprogramming factors c-Myc, OCT4, Klf4, and SOX2 ("Yamanaka factors") reverts tissue-specific restrictions producing undifferentiated pluripotent cells (Takahashi et al., 2007). Effective cellular reprogramming requires dramatic genetic, epigenetic, morphological, and metabolic changes to occur within the cell while escaping apoptosis and senescence (Buganim et al., 2013). OCT4 and SOX2 strongly reinforce pluripotency, often ensuring their own expression through an autoregulatory positive feedback loop (Schmidt & Plath, 2012). SOX2 is the best described interacting partner of OCT4, often binding a composite OCT-SOX element within regulatory elements of pluripotency genes (Shi & Jin, 2010). Simultaneously binding this element SOX2 and

OCT4 cooperate to elevate expression of *POU5F1, SOX2, Nanog, FGF-4, UTF1, ZFP206,* all of which modulate pluripotency (Ambrosetti et al., 1997; Chew et al., 2005; Nishimoto et al., 1999; Rodda et al., 2005; Wang et al., 2007).

The chromatin topology of terminally differentiated cells can prevent these pluripotency transcription factors from binding their targets (Takahashi et al., 2007). Present theories suggest the role of c-Myc and Klf4 during reprogramming is to promote an active chromatin environment rather than inducing pluripotency (Schmidt & Plath, 2012; Takahashi et al., 2007). c-Myc is thought to bind enhancer regions of essential pluripotency genes, where it recruits chromatin opening factors, including Klf4 and others (Chappell & Dalton, 2013; Takahashi et al., 2007). Once the chromatin is made available, pluripotency activating transcription factors such as OCT4 and SOX2 can actively bind their targets, promoting a gene-environment similar to ESCs (Chappell & Dalton, 2013; Schmidt & Plath, 2012; Takahashi et al., 2007). Often SOX2 and OCT4 can be used as markers of the pluripotent state using common methodologies such as Western blotting, RT-qPCR and immunofluorescence.

Human PSCs require very few exogenous signals to maintain their pluripotency *in vitro*. iPSCs reprogrammed from somatic cells behave similarly to ESC, relying on FGF-2 and TGF-β signalling to maintain pluripotency (Lotz et al., 2013; Mullen & Wrana, 2017). FGF-2 is capable of binding all FGF receptors to regulate key transcription factors that act to promote the expression of SOX2, OCT4, and Nanog while stimulating the release of TGF-β (Mossahebi-Mohammadi et al., 2020). In PSCs, TGF-β manipulates the activity of the SMAD proteins, which bind promoter regions of *SOX2*, *POU5F1* and *NANOG*

(Gordeeva, 2019). The depletion of FGF-2 creates variances of growth factors in culture, increasing the probability of spontaneous differentiation (Lotz et al., 2013). Complete loss of FGF-2 and TGF-β mediates spontaneous differentiation (Lotz et al., 2013; Mullen & Wrana, 2017). Without these regulatory signals, stem cells follow their inherent preference towards the various cell types of the body.

Many functional assays exist to evaluate stem cell pluripotency, including the generation of chimeras, teratomas, embryoid bodies or *in vitro* differentiation assays. *In vivo* fusion of two embryos results in the formation of a chimera. Injection of genetically unique ESCs or iPSCs into a host embryo *in vitro* generates murine chimeras (Matsui et al., 1992; Okita et al., 2007). Similarly, teratomas assess stem cell pluripotency by determining their contribution to tumour formation. Cells are injected into an immunocompromised host, typically mice, and develop a resultant teratoma. Teratomas exhibiting characteristics of all three germ layers are presumed to have been generated from pluripotent stem cells (Singh et al., 2016). The above-described methods have been well established in mice: however, ethical considerations prevent their application in humans. As a result, human stem cell pluripotency is often assessed using embryoid bodies or *in vitro* monolayer differentiation assays (Singh et al., 2016). Used in conjunction with genetic editing, these assays represent powerful tools for analyzing the influence of a gene on pluripotency and cell lineage commitment (Singh et al., 2016).

1.4 Cellular Differentiation

Human PSCs have broad differentiation potential, as they can differentiate into any of the embryonic cell types. PSC differentiation can be directed toward a lineage of interest,

providing a precise way to study early timepoints in human development otherwise unethical or problematic to isolate (Qin et al., 2016). Decades of developmental biology research provide insight into the conditions required for germ layer formation and generally outline the signalling cascades found during embryogenesis as described in section 1.2 (Figure 1.2). Exposure to exogenous growth factors, cytokines, morphogens, or small molecules known to modulate differentiation *in vivo* can constrain cellular differentiation towards a desired cell type (Lam et al., 2014; Singh et al., 2016; Tchieu et al., 2017).

Directed endoderm differentiation protocols use FGF with Activin A to produce endoderm from human PSCs in culture (McLean et al., 2007; Sui et al., 2012). Other protocols use Activin A with a regulator of Wnt and β-Catenin signalling, including the chemical compound CHIR09921 (D'Amour et al., 2006; Pagliuca et al., 2014). Lam et al. describe effective mesoderm differentiation using CHIR09921 alongside Wnt3a or Activin A and BMP4 (Lam et al., 2014). Tchieu et al. 2017 describes a protocol using dual SMAD inhibitors to remove BMP and TGF-β activity, generating PAX6 positive neuroectoderm (Tchieu et al., 2017). Without PAX6 human PSCs fail to differentiate into neuroectoderm (Zhang et al., 2010). PAX6 is well described as a valuable and reliable marker for ectoderm formation.

In contrast to the external cues applied to cells during directed differentiation, spontaneous differentiation enables passive, cell-guided differentiation. Embryoid bodies (EBs) are three-dimensional aggregates of PSCs that attempt to mimic the early embryo's patterning and signalling (Lin & Chen, 2014; Mansergh et al., 2009; Simunovic & Brivanlou, 2017). This method effectively evaluates human stem cell pluripotency by

removing TGF-β and FGF-2, allowing stem cells to undergo spontaneous differentiation (Mullen & Wrana, 2017). Embryoid bodies generally differentiate into cells of all three embryonic germ lineages, although they are not organized in the same manner as a developing embryo (Bratt-Leal et al., 2009; Pettinato et al., 2014). Additionally, the size and input cell number can influence the formation and differentiation of EBs. Large compact EBs inhibit nutrient diffusion and undergo core necrosis, while smaller embryoid bodies fail to thrive in culture (Pettinato et al., 2014). Although monolayer differentiation assays lack many spatial cues present in the above assays, new 3D culture methods and robust kits provide precise tools for investigating influential cellular signals during cell fate specification (Noort et al., 2021; Pettinato et al., 2014).

1.5 Cellular Communication

Cellular communication helps to spatially arrange the activities of nearly every cell in the human body. Cells can communicate with each other and their environment in different ways, including autocrine signalling, endocrine signalling, paracrine signalling, and direct cell-cell communication (Cooper, 2000; Esseltine & Laird, 2016). Endocrine signalling occurs when hormones travel to distant locations through the blood (Cooper, 2000). Autocrine signalling involves the release of signalling molecules intended to bind to their originating cell inducing signal transduction (Przybyla & Voldman, 2012). Paracrine signalling differs in that the released external cues act on neighbouring cells (Franco et al., 2008). Finally, direct cell-cell communication can be facilitated through gap junctions between adjacent cells.

1.6 Gap Junctional Intercellular Communication

Direct cell-cell communication is facilitated by the connexin (Cx) family of gap junction proteins. There are 21 distinct Cx family members, differentially expressed and regulated across various cell and tissue types. Connexins are transmembrane proteins arranged in a hexameric membrane hemichannel that can dock with hemichannels of neighbouring cells to facilitate gap junction intercellular communication (GJIC) (Figure 1.3; (Esseltine & Laird, 2016). Connexin protein assembly, hemichannel oligomerization and trafficking follow the classic secretory pathways for plasma membrane proteins, from the ER to the intermediate compartment, Golgi apparatus and finally the plasma membrane. The process of Cx oligomerization is unique from that of other transmembrane channels. Sequence homology within the third transmembrane domain governs the pairing of different connexin isoforms into hemichannels comprised of one (homomeric) or multiple isoforms (heteromeric) (Kelly et al., 2015; Koval et al., 2014). Once expressed at the cell surface, select residues and motifs in the extracellular loops regulate the interactions of each hemichannel (Bai et al., 2018). This high level of connexin isoform intermixing creates a complex hierarchy of channel selectivity, exponentially regulating cell signalling (Koval et al., 2014).

The ability of connexin hemichannels to dock with hemichannels on adjacent cells can be modulated by select post-translational modifications. Post-translational modifications affect other connexin protein interacting partners and even the biosynthesis and degradation of connexin channels (Johnstone et al., 2012). For example, several different protein kinases phosphorylate Cx43 carboxyl-terminal residues to alter channel

permeability, conductance, and gating (Ek-Vitorin et al., 2006; Lampe et al., 2000). Post-translational modification of Cx proteins is then essential to determining the activity and functionality of gap junction channels.

Figure 1.3 - Connexin channels mediate gap junctional intercellular communication. Connexin (Cx) proteins have four transmembrane domains, two extracellular loops, one intracellular loop and cytoplasmic amino and carboxyl termini. Regions essential for connexins channel formation and gating such as transmembrane domains, N-terminus and extracellular loops are highly conserved. Meanwhile, the C-terminus and intracellular loop are highly variable between different connexin isoforms and appropriate targets for specific antibody detection. Connexin proteins are trafficked to the cell surface as a hexameric unit known as a hemichannel. Once expressed at the cell surface, hemichannels at the interface between adjacent cells can form gap junctions, mediating direct intercellular communication. Depending on the Cx isoform, gap junction channels exhibit different pore permeabilities but are generally permeable to molecules less than 1 kDa in size. This figure was generated through the use of *BioRender.com*

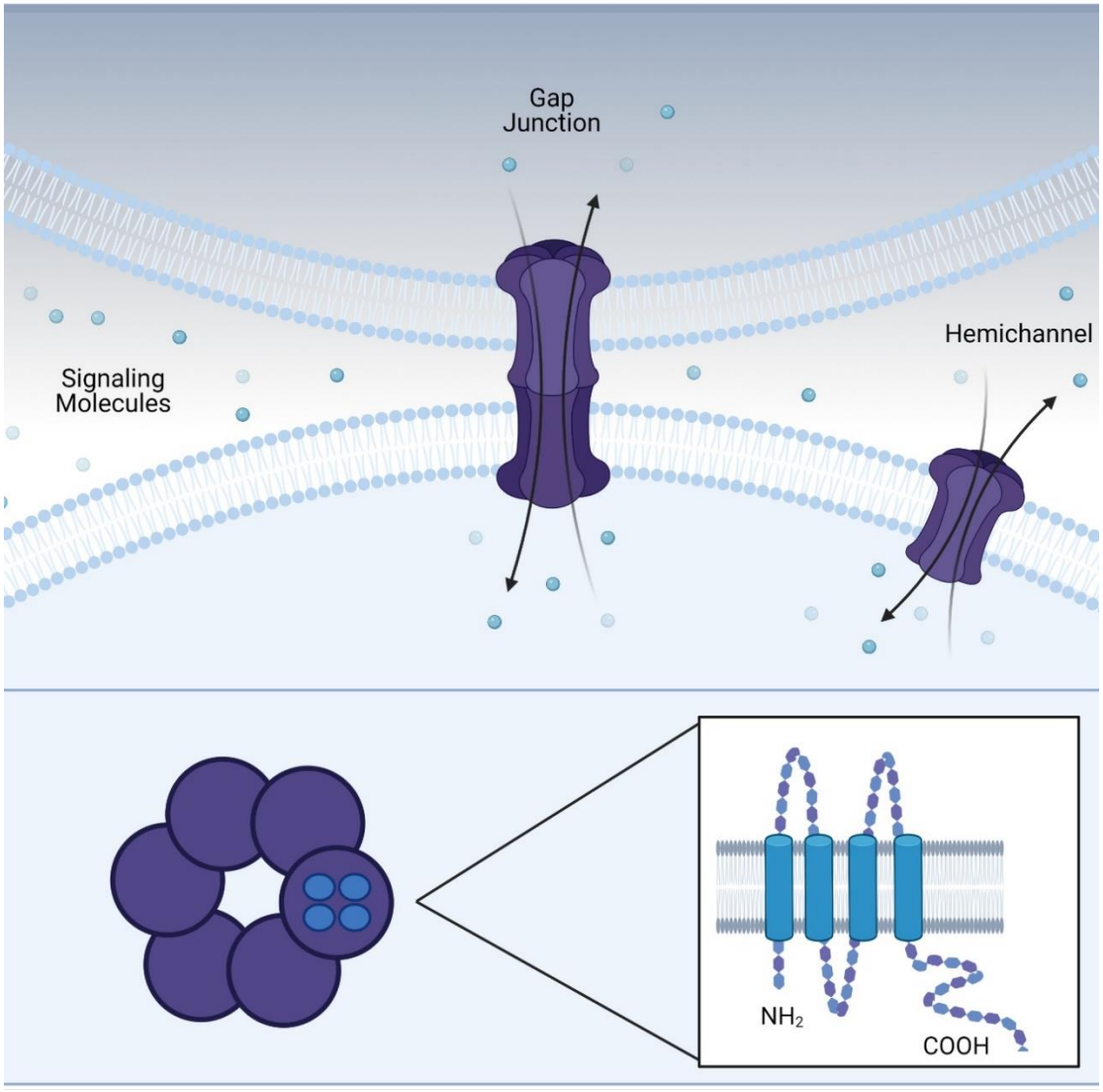
Gap
Junction
Hemichannel
Signaling
Molecules
NH_2
COOH

1.7 GJIC in embryonic development and disease

GJIC is established as early as the 8 cell embryo (Becker et al., 1992). Cx43 is the earliest expressed connexin in development and is widely expressed in adult tissues. The importance of GJIC in human development is exemplified by the numerous human germline Cx mutations which result in developmental disorders (Laird et al., 2017). Mice deficient in Cx43 die after birth due to obstruction of the right ventricular outflow leading to cardiac dysfunction (Lampe & Lau, 2004; Plum et al., 2000; Reaume et al., 1995). Replacement of Cx43 with Cx32 or Cx40 can partially rescue this lethality (Plum et al., 2000). Mutations in human Cx43 lead to atrial fibrillation and oculodentodigital dysplasia (Kelly et al., 2016; Nishii et al., 2014), while mutations in Cx32 cause X-linked Charcot-Marie Tooth disease (Bruzzone et al., 1994; Fairweather et al., 1994). Mouse models lacking Cx32 mimic the aforementioned human neuropathy alongside widespread liver dysfunction (Anzini et al., 1997; Nelles et al., 1996; Temme et al., 1997; Willecke et al., 1999). Embryonic loss of Cx26 in mice results in a lethal defect in transplacental glucose uptake, whereas Cx26 mutation in humans results in deafness and skin disease (Gabriel et al., 1998; Lee & White, 2009; Murgia et al., 1999). Proper establishment of GJIC is then quite evidently influential to the healthy development of the embryo.

1.8 Connexins influence stem cell reprogramming and cell fate specification

Collectively presently available research describes gene expression of Cx25, Cx26, Cx30, Cx30.2, Cx30.3, Cx31, Cx31.1, Cx31.9, Cx32, Cx36, Cx37, Cx40, Cx43, Cx45, Cx46, Cx47, Cx59, Cx62 in human iPSCs (summarized in Figure 4.1; (Ke et al., 2013; Oyamada et al., 2013). Despite the availability of several Cx transcripts, Cx40, Cx43, and

Cx45 are the only Cx described at the protein level in human ESCs (Huettner et al., 2006). Human PSC survival, pluripotency, and terminal differentiation rely on GJIC, and ectopic expression of Cx43 and Cx45 enhances the efficiency of iPSC reprogramming (Czyż et al., 2017; Dbouk et al., 2009; Esseltine et al., 2017; Ke et al., 2013; Ke et al., 2017). Furthermore, changes in GJIC can alter the differentiation potential of PSCs. For example, Cx43 has recently been shown to be upregulated during human ESC primitive endoderm differentiation, and Cx43-deficient PSCs exhibit compromised endoderm formation (Wörsdörfer et al., 2017; Yang et al., 2019). On the other hand, simultaneous overexpression of Cx32 and knockdown of Cx43 promotes ESC differentiation to hepatocytes (Pei et al., 2017; Qin et al., 2016). Such research highlights the dynamic relationship between GJIC and cell fate specification.

Cx32 and Cx43 both exert protective effects on hematopoietic stem cells (Hirabayashi et al., 2007b; Taniguchi Ishikawa et al., 2012). Mice lacking Cx32 possess higher counts of undifferentiated hematopoietic stem cells and as a result fewer hematopoietic progenitor cells, suggesting that dynamic expression of Cx32 may control the timing of hematopoietic progenitor cell maturation (Hirabayashi et al., 2007a, 2007b). Cx43 knockout mice, on the other hand, exhibit defects in blood cell formation, implicating Cx43 in hematopoiesis (Montecino-Rodriguez et al., 2000). Overexpression of Cx43 in human ESCs positively mediates cardiac differentiation, while mesenchymal stem cells deficient in Cx43 exhibit decreased osteoblast differentiation potential (Lin et al., 2018; Moore et al., 2008). Conversely, expression of Cx32 markedly decreases in the early stages of adipose-derived stem cell differentiation (Mannino et al., 2020). Therefore, it is apparent that connexins are

important for the maintenance and downstream specification of somatic stem cell populations.

1.9 Cell-cell communication through the Pannexin family of large pore channels

Pannexins (PANX1, PANX2, PANX3) are large pore-forming membrane channels that mediate paracrine signalling through the passage of small molecules between the cytosol and extracellular space (Figure 1.4; (Esseltine & Laird, 2016; Scemes et al., 2007; Shao et al., 2016) . PANX1 is widely expressed, including throughout tissues derived from all three germ layers. PANX2 is primarily expressed in the nervous system, while PANX3 is restricted to skin, bone, and connective tissues (Crespo Yanguas et al., 2017); (Uhlén et al., 2015). Pannexin proteins have four membrane-spanning domains, two intracellular and two extracellular loops, an intracellular N-terminal loop and a cleavable C-terminus (Michalski et al., 2020). Recent Cryogenic electron microscopy based studies have demonstrated that PANX1 channels exist as a heptamer (Michalski et al., 2020; Qu et al., 2020). Pannexins were initially classified as gap junction proteins along with connexins; however, identifiable differences in localization, protein arrangement, and protein glycosylation have led to the reclassification of pannexins as single membrane-spanning large pore channels.

PANX1 glycosylation occurs within the extracellular domains, and thus it is unlikely that these proteins are capable of docking to form an intercellular channel (Boassa et al., 2007). PANX1 is initially glycosylated in the endoplasmic reticulum before passing to the Golgi apparatus. Here the glycosylated protein can be further modified before being trafficked to the plasma membrane (Boassa et al., 2008). It is now widely accepted that PANX1 has three different glycosylation states Gly-0, unglycosylated; Gly-1, high

mannose; Gly-2, complex carbohydrate (Figure 1.4). Several studies have demonstrated that these three main PANX1 glycosylation states can be resolved via Western blot as distinct molecular weight bands (Boassa et al., 2008; Penuela et al., 2007; Penuela et al., 2009). The level of glycosylation has been suggested to influence the trafficking of PANX1. Gly-0 PANX1 generally localizes to the endoplasmic reticulum, Gly-1 is found in the Golgi apparatus, while Gly-2 is expressed at the cell surface (Boyce et al., 2018). Pharmacological inhibition of glycosylation or site-directed mutagenesis of the N254Q glycosylation site blocks PANX1 cell surface expression (Boassa et al., 2008). Glycosylation of PANX1 can now be commonly detected using simple methods such as Western blotting.

Many mouse models implicate pannexins in disease development or progression, including Crohn's and colitis, Alzheimer's disease, various cancers, and ischemia (Aquilino et al., 2019; Diezmos et al., 2013a; Orellana et al., 2011; Penuela et al., 2014). One of the most well-defined roles of PANX1 is in cell death. When cells are stressed, open PANX1 channels allow the free flow of small molecules, including ATP out of the cell, thus accelerating apoptosis and potentially triggering the cell death of neighbouring cells (Crespo Yanguas et al., 2017). In contrast to their role mediating cell death, pannexins may support tissue-resident stem cell populations. PANX1 has been shown to regulate the self-renewal or differentiation of murine skeletal muscle satellite cells, neural precursor cells (NPCs) and adipose-derived stromal cells (Lee et al., 2018; Pham et al., 2018; Wicki-Stordeur et al., 2012; Wicki-Stordeur et al., 2016). PANX1 is therefore an attractive target for the investigation of endoderm related developmental diseases.

1.10 Pannexin channels in human development and disease

PANX1 is expressed in human oocytes and 2-cell and 4-cell stage embryos, suggesting a role for this protein in human embryonic development (Esseltine & Laird, 2016; Hainz et al., 2018; Shao et al., 2016). *PANX1* -/- mice remain fertile, producing typical size litters (Sang et al., 2019). However, presence of mutated PANX1 proves more damaging, as several detrimental germline mutations have been presented in humans. Heterozygous *PANX1* mutations lead to decreased PANX1 protein expression, disruption of PANX1 trafficking and post-translational modification and perturbed channel function. These germline mutations lead to female human infertility as a result of primary oocyte death (Sang et al., 2019). The severity of symptoms increases with homozygous *PANX1* mutation with the genetic variant PANX1-R217H causing severe neurological deficits in addition to primary ovarian failure (Shao et al., 2016). Although PANX1 has recently been identified in human oocytes and PSCs (Hainz et al., 2018; Sang et al., 2019), it is currently unknown if PANX1 similarly supports self-renewal or differentiation of human pluripotent stem cells.

Figure 1.4 – Pannexin proteins form transmembrane channels. The pannexin family is comprised of three isoforms PANX1, PANX2, PANX3. Pannexins have four transmembrane domains, two extracellular domains, one intracellular domain, and cytoplasmic amino and carboxyl termini. Glycosylation sites (location denoted by attached carbohydrate; *green*) have been confirmed in the extracellular loops of PANX1, PANX2 and PANX3. PANX1 arranges as a heptameric transmembrane channel, often interacting with cytoplasmic actin filaments (*yellow*). Unlike connexins, external glycosylation prevents the formation of gap junctions. Instead, pannexins act as single membrane channels in autocrine or paracrine signalling. This figure was generated through the use of *BioRender.com*

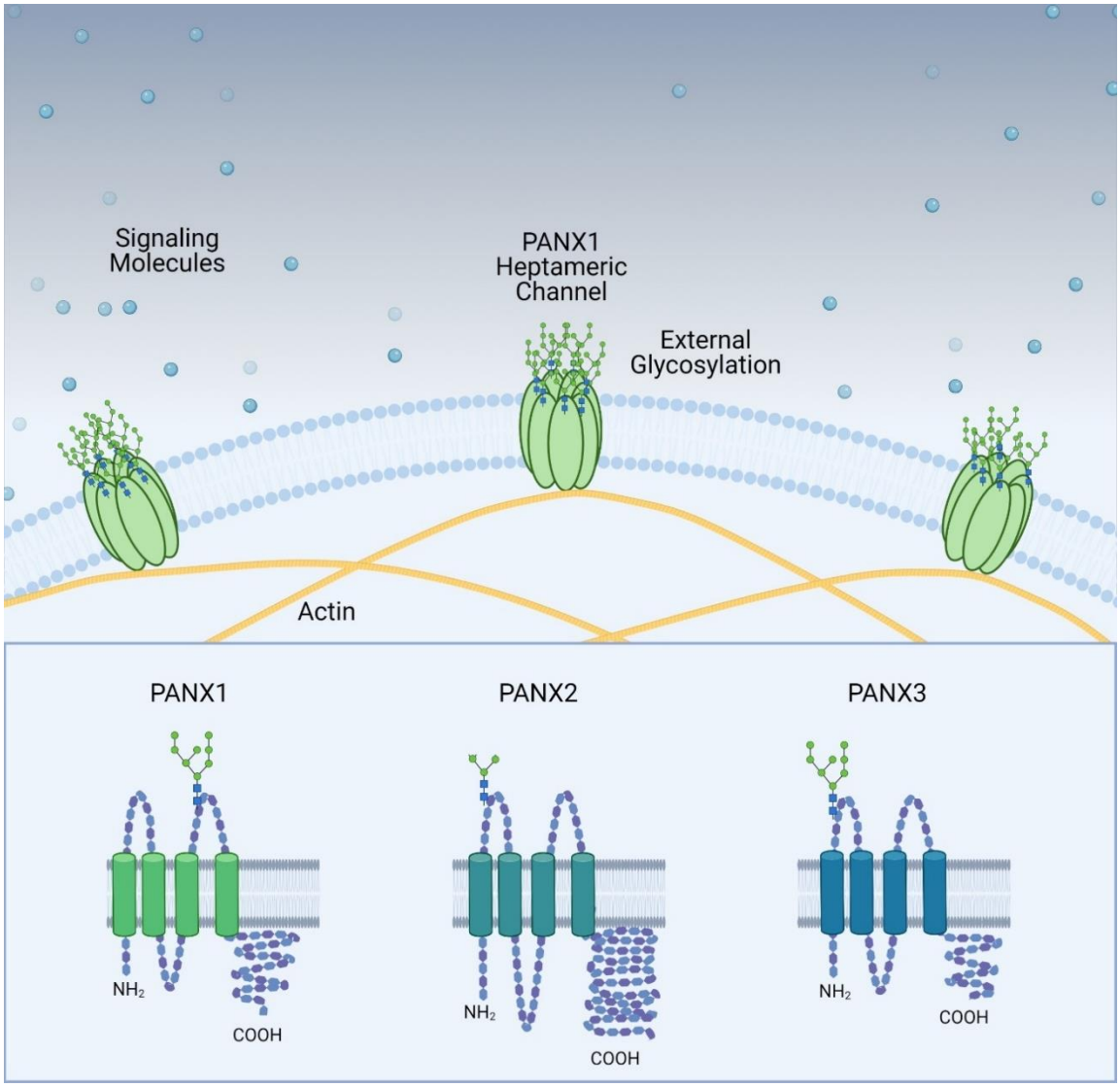
Signaling Molecules
PANX1 Heptameric Channel
External Glycosylation
Actin
PANX1
PANX2
PANX3
NH2
COOH
NH2
COOH
NH2
COOH

1.11 Genetic Engineering

CRISPR-Cas9 systems can be manipulated to allow for the induction of targeted genetic mutations. CRISPR guide RNAs (gRNA) contain a transactivating crRNA (tracrRNA) fused to a CRISPR RNA (crRNA) designed explicitly in compliment to a sequence of interest (Joberty et al., 2020). By predetermining the crRNA sequence, Cas9 activity and location of induced DNA breaks can be directed. Such DNA damage is repaired by either non-homologous end joining or through the homology-directed repair pathway (Hsu et al., 2014). Non-homologous end-joining can introduce small insertion or deletion mutations (indels), disrupting the reading frame and silencing the gene of interest (Guo et al., 2018). Meanwhile, homology-directed repair can be used to insert precise DNA sequences. Donor DNA sequences with homologous arms can introduce novel genes at the site of induced DNA breaks or encode fluorescent tag-fused proteins (Sharma et al., 2018; Verma et al., 2017). This technology is especially beneficial to uncovering how specific genes influence pluripotent stem cell reprogramming, survival, and cell fate specification. For example, targeting of select genes in hematopoietic stem and progenitor cells by CRISPR-Cas9 enables retention of multilineage differentiation potential (Mandal et al., 2014). CRISPR-Cas9 genetic engineering can be leveraged for disease modelling by either inducing or repairing human genetic mutation within pluripotent stem cells (Song et al., 2015; Tang et al., 2021). With this CRISPR systems advances genetic editing, making phenotypic analyses more precise with complete ablation in place of residual expression.

1.12 Rationale and objectives

As highlighted above, connexins and pannexins are widely expressed throughout the early embryo as well as adult tissues. Moreover, cell-cell communication impacts stem cell self-renewal and fate specification. Due to the early and widespread embryonic expression of Cx43, and the numerous diseases associated with Cx43 malfunction, ***it is hypothesized that complete genetic ablation of GJA1 (Connexin 43) will negatively impact germ lineage specification. Specifically, it is hypothesized that mesoderm and endoderm differentiation will be compromised in Cx43 knockout iPSCs compared to control.***

Similarly, because PANX1 is identifiable in the earliest stages of embryonic development and is most highly expressed in ectodermal-derived tissues, including brain and skin, ***it is hypothesized that PANX1 knockout iPSCs will exhibit impaired ectodermal lineage differentiation compared to control.*** In order to test these hypotheses, this project has three main objectives:

1) Characterize select connexin and pannexin expression in human iPSCs through RT-qPCR, Western blot, and immunofluorescent analysis.

2) Identify differences in select connexin and pannexin expression and subcellular localization in cells of the three germ lineages by differentiating control iPSCs into ectoderm, mesoderm, and endoderm cells.

3) Evaluate the effect of CRISPR-Cas9 genetic ablation of either *PANX1* or *GJA1* on the differentiation capacity of human iPSCs to the three embryonic germ lineages.

1.13 Summary of Findings

Gene expression analysis using RT-qPCR identified transcripts for 11 of the 21 connexin isoforms in iPSCs and the three germ layers. Transcripts for Cx62 were enriched in ectodermal cell types, while transcripts encoding for Cx45 increased post mesoderm and ectoderm formation. Endoderm populations had elevated transcripts encoding Cx30.3, Cx31, Cx32, Cx36, Cx37 and Cx40 transcripts. Western blot revealed persistent expression of Cx43 and PANX1 throughout lineage specification. Interestingly our results suggest PANX1 is alternatively glycosylated and differentially localized across cells of each germ layer. *PANX1-/-* and *GJA1-/-* iPSCs generated using CRISPR-Cas9 gene ablation maintain characteristics of PSCs, and successfully differentiate into ectoderm, mesoderm, or endoderm under directed differentiation. It was therefore concluded that neither Cx43 nor PANX1 are essential during lineage specification.

2 Materials & Methods

2.1 Cell Lines

Human female control, *GJA1-/-* (Cx43) and *PANX1-/-* induced pluripotent stem cells (iPSCs) were obtained through a material transfer agreement with The University of Western Ontario (London, Ontario, CA) (Esseltine et al., 2020; Esseltine et al., 2017; Shao et al., 2019). Human male iPSCs were acquired from the NIGMS Human Genetic Cell Repository (GM25256*e, NIGMS Human Genetic Cell Repository). Mono-allelic EGFP insertion behind the endogenous *GJA1* allele of GM25256*e iPSCs (Cx43-eGFP) was performed by The Allen Institute for Cell Science (AICS-0053-016iPSC, Allen Cell Collection).

2.2 Stem Cell Maintenance

Stem cells were housed in a humidified 37°C cell culture incubator supplemented with 5% CO_2. iPSCs were fed daily with either Essential 8 media (Cat# A1517001, ThermoFisher, Waltham, Massachusetts, US) or mTeSR + (Cat# 05825, Stem Cell Technologies, Vancouver, British Colombia, CA). Healthy iPSCs in culture exist as large colonies, approximately 6mm in diameter, of tightly packed cells with high nucleus to cytoplasmic ratios, a pronounced nucleolus, and highly refractive colony borders (Nagasaka et al., 2017; Wakui et al., 2017). Stem cell cultures were passaged when colonies were large, round, and exhibited white multilayering at the center, typically every five days. Before passaging, regions of differentiation were identified through visual inspection and were aspirated from culture. Spent media was then removed, and the cells washed with

phosphate-buffered saline (PBS) (Cat# 311-011-CL, Wisent, St-Bruno, Quebec, CA). Stem cell colonies were dissociated to clumps at room temperature using Gibco™ enzyme-free cell dissociation buffer (Cat# 13151014, ThermoFisher). Dissociation was allowed to progress until gaps in colonies were visible under the microscope while ensuring the cells remained attached to the dish, approximately 3 minutes. Dissociation was stopped by aspirating buffer from cells and adding 1ml of Essential 8 to the well. Stem cells were scraped from the culture ware using sterile cell scrapers and re-plated at a split ratio of 1:20. Cultureware was pre-coated for one hour by diluting cold Geltrex (1:100) (Cat# A1413302, ThermoFisher) or Matrigel (Cat# 08-774-552, ThermoFisher), according to manufacturer's instructions in cold plain DMEM (Cat# 319-015-CL, Wisent).

For experiments requiring passage of single cells, stem cells were incubated at 37°C in Stem Pro Accutase (Cat# A1370701, ThermoFisher) for 5 to 8 minutes or until colonies float from culture ware. Colonies were dissociated to single cells by triturating suspension. The dissociation reaction was stopped by resuspending the single-cell suspension in plain DMEM. Cells were pelleted via centrifugation at 300x gravity for 5 minutes and resuspended in mTeSR+ containing Y-27632 (ROCKi) at a final concentration of 10 uM (Cat#1254, Tocris, Oakville, Ontario, CA) to promote cell survival as single cells adhere to the polymerized Geltrex matrix (Claassen et al., 2009).

2.3 Directed Differentiation

Directed iPSC differentiation toward definitive endoderm, mesoderm, or ectoderm followed the protocol of the STEMDiff™ Trilineage Differentiation kit (Cat# 05230, Stem Cell Technologies). iPSCs used in endoderm differentiation were enriched in mTeSR+

iPSC maintenance media (Cat# 05825, Stem Cell Technologies) for five days before setup. Colonies reached approximately 80% in confluency, exhibiting multilayering and round edges before being taken for set up. Cultures containing minimal differentiation, 1 to 5%, were selected for directed differentiation. Accutase-digested single cells were plated at 50,000 cells/cm^2 for mesoderm or 200,000 cells/cm^2 for ectoderm and endoderm. Viable cell counts were determined in duplicate using Trypan Blue Solution, 0.4% (Cat#15250061, ThermoFisher) and counted using a TC20 Automated Cell Counter (Cat# 1450102, BioRad, Hercules, California, US). Required volumes of single-cell suspension per plate were determined using the following equation:

(Total Required Number of Cells / Average Viable Cell Concentration per mL) x 1000 = Volume Cell Suspension Required (µL)

Single cells were incubated in mTeSR+ with ROCKi for 24 hours to promote single-cell survival. The next day, spent media was aspirated and replaced with STEMDiff™ Endoderm, Mesoderm, or Ectoderm Medium. Cultures were fed daily with fresh media until day five (Mesoderm, Endoderm) or day eight (Ectoderm), where differentiated cells were harvested for protein, RNA, or immunofluorescence as detailed below. Cells were fed 4 hours prior to harvest to ensure optimal cell viability and marker expression (Esseltine et al., 2020).

2.4 Spontaneous Monolayer Differentiation

iPSCs were seeded into Geltrex-coated Nunc™ Lab-Tek™ II CC2™ Chamber Slides (Cat# 154739, Thermo Scientific) or Matrigel-coated glass coverslips. The following day, iPSC maintenance media (Essential 8) was changed to Essential 6 (A1516401,

ThermoFisher), which lacks the crucial pluripotency factors TGF-β and FGF-2 (Mullen et al., 2017). Media was changed every 1 to 2 days during the spontaneous differentiation process (Gholamitabar Tabari et al., 2019). Differentiation was allowed to progress until day nine before processing for immunocytochemistry.

2.5 Immunofluorescence

Media from live cells was aspirated, and cells were washed twice with room temperature PBS solution pH 7.4 (140 mM NaCl (600-082-DG, Wisent), 2.6 mM KCL (P330-500, Fisher Scientific, Ottawa, Ontario, CA), 1.4 mM KH_2PO_4 (BP362500, Fisher Scientific). Cells were fixed at room temperature for 30 minutes, with 10% normal buffered formalin pH 7.13 (CA71007-344, VWR, Radnor, Pennsylvania, US). Formalin was aspirated, and cells washed twice with PBS.

Fixed cultures were incubated in primary antibodies (Table 1) diluted in blocking/permeabilization solution for 1 hour at room temperature or overnight at 4°C. Blocking/permeabilization solution consisted of PBS with 3% bovine serum albumin (BSA) (800-095-EL, Wisent) to block non-specific antibody binding and 0.1% Triton™ X-100 (T8532, Sigma-Aldrich, St. Louis, Missouri, US) to permeabilize cell membranes.

After incubation with primary antibodies, the cells were washed twice for 10 minutes with homemade PBS before adding dyes and secondary antibodies (Table 1). Fluorescently-conjugated secondary antibodies and dyes were diluted in the same blocking/permeabilization buffer described above. Secondary antibodies and cellular stains were incubated at room temperature in the dark for one hour to allow primary: secondary conjugation. The solution was aspirated, and cells were washed with PBS. Cover glass #1.5

was adhered to the slide with either Prolong™ Diamond Antifade Mountant (P36962, Life Technologies), containing DAPI nuclear stain or prepared Mowiol 4-88 (Cat# 81381, Sigma-Aldrich) mounting media containing DABCO (Cat# D013425G, Fisher Scientific). Slides were dried and stored in the dark at 4°C before imaging.

2.6 Confocal Microscopy

Acquisition of confocal images used an Olympus Fluoview FV10i-W3 confocal microscope (Olympus, Tokyo, JPN) running Fluoview v2.1.1.7 software, equipped with 60x/1.2 NA and 10x/0.4 NA water immersion lenses. Imaging used the following lasers to visualize fluorophores: DAPI/Hoechst 33342 (405 nm laser); Alexa Fluor 488/eGFP (473 nm laser); Phalloidin/Alexa Fluor 555 (559 nm laser); Alexa Fluor 647 (635 nm laser). Laser power and sensitivity were adjusted to visualize immunofluorescence and minimize background signal. Additional sample imaging used an Olympus Fluoview FV1000 confocal microscope fitted with 10X0.4 NA, 20X/0.75NA or 40X/0.95NA and the following lasers: 405 nm, 458 nm, 568 nm, 633 nm. Images were analyzed using Fiji open-source software. When deemed necessary, fluorescent confocal images were subjected to brightness/contrast enhancement.

2.7 Image Analysis

Images were analyzed and pseudo-coloured with Fiji software (Schindelin et al., 2013). The generation of composite images used Fiji Software. Brightness and contrast were equally adjusted for optimal visualization in all images using Fiji software. Quantitative analysis of protein colocalization used Fiji plugin JACoP (Just another colocalization plugin) to determine Mander's coefficient values as described in Bolte et al.

2006 (Bolte & Cordelières, 2006). In this case Mander's coefficient was selected for this analysis as it measures co-occurrence of signals in addition to correlation and focuses on high intensity combinations. Thresholds were set for images subjected to colocalization assay were to minimize noise prior to analysis with JACoP.

Table 2.1: Primary and Secondary Antibodies Used in Immunofluorescence

Target Protein	Host Species	Type of Antibody & Fluorophore	Concentration	Vendor and Cat#
Connexin 43	Rabbit	Primary	1:1000	C6219, Sigma-Aldrich
Connexin 32	Rabbit	Primary	1:250	AP20645OU-N, OriGene
PANX1	Rabbit	Primary	1:500	Laird Laboratory
SOX17	Goat	Primary	1:500	AF1924, R&D Systems
KDEL	Mouse	Primary	1:500	AB12223, Abcam
SOX2	Mouse	Primary	1:200	AF2018, R&D Systems
Brachyury	Rabbit	Primary	1:1000	EPR18113, Abcam
Nestin	Mouse	Primary	1:500	14-9843-82, Invitrogen
Nuclei	DAPI	Cell Stain	-	P36962, ThermoFisher
Nuclei	Hoechst 33342	Cell Stain	1:1000	H3570, Fisher Scientific
Rabbit	Donkey	Secondary (AF488)	1:500	A21206, Invitrogen
Mouse	Donkey	Secondary (AF488)	1:500	A31572, Invitrogen
Rabbit	Donkey	Secondary (AF555)	1:500	31572, Invitrogen
Mouse	Donkey	Secondary (AF555)	1:500	31570, Invitrogen

Actin	Phalloidin	Cell Stain (AF555)	1:500	A34055, Invitrogen
Rabbit	Donkey	Secondary (AF647)	1:500	A31573, Invitrogen
Goat	Donkey	Secondary (AF555)	1:500	AS32816, Invitrogen
Goat	Donkey	Secondary (AF647)	1:500	A21082, Invitrogen
Mouse	Goat	Secondary (AF647)	1:500	A32728, Invitrogen

2.8 Western Blotting

2.8.1 Cell Lysis, Protein Extraction, and Protein Quantification

Cultures were placed on ice and washed twice with cold PBS. Cells were lysed with ice-cold lysis buffer (50 mM tris HCL (Cat# M-26956, Fisher Scientific) pH 8, 150 mM NaCl, 0.02% NaN_3 (Cat# S2002, Sigma-Aldrich), 0.1% Triton X-100 (Cat# T8532, Sigma-Aldrich), protease inhibitors: 2 ug/mL leupeptin (Cat# AAJ6188MB, Fisher Scientific) and 2 ug/mL aprotinin (Cat# AAJ11388MB, Fisher Scientific) and the phosphatase inhibitors: NaF (10 mM) (Cat# S299-100, Fisher Chemical) and Na_3VO_4 (1 mM) (Cat# 81104, AlfaAesar). Wells were scraped, and the suspension homogenized by pipetting before transfer to a microcentrifuge tube. Lysates were centrifuged at 12,000 RPM for 10 minutes at 4°C to pellet insoluble material. Supernatant containing soluble proteins was transferred to a fresh tube and frozen at -20°C until protein concentration determination and subsequent analysis.

Protein concentration was determined in duplicate using the Pierce BCA protein kit (Cat# PI23225, ThermoFisher). Standard curves were generated using Bovine Serum Albumin (BSA) (0 ug, 0.17 ug, 0.25 ug, 0.5 ug, 1 ug, and 2 ug). Final absorbance was read

at 562 nm using a VICTOR Multilabel Plate Reader (model 2030, Perkin Elmer, Waltham, Massachusetts, US). Protein concentrations were extrapolated from the generated standard curve using the following formula y = mx + b. 20 ug of total protein was diluted into the same volume with PBS to ensure equal protein concentration. Protein denaturation occurred via addition 4x loading buffer pH 6.81 (10% sodium dodecyl sulfate (SDS) (Cat# 800-100-CG, Wisent), 0.5% bromophenol blue (Cat# AC403140050, ACROS Organics™, Geel, BE), 20% 2-mercaptoethanol (Cat# BP176100, Fisher Scientific) and 50% glycerol (Cat# G33-4, Fisher Scientific)) at 1:4 of the total sample volume. Samples were incubated at room temperature for 30 minutes to ensure protein denaturation before separation via SDS-PAGE.

2.8.2 SDS PAGE

Proteins were separated via SDS-PAGE on a 7.5% polyacrylamide gel (Cat# EC890, National Diagnostics, Atlanta, Georgia, US). Gels were run in a BioRad Mini-PROTEIN® Tetra Cell (Cat# 1658005) and the chamber filled with Running electrophoresis buffer pH 8.26 (25 mM tris (Cat# 1610719, BioRad), 190 mM glycine (Cat# 800-045-IK, Wisent), and 0.1% SDS (Cat# 800-100-CG, Wisent)) Gels were run at 100 V supplied by a PowerPac^{TM} Basic Power Supply (Cat# 1645050, BioRad). Protein separation was determined in reference to the migration of 5ul of Precision plus all Blue standard (Cat# 1610393, BioRad). Post-separation, the protein samples were transferred to a nitrocellulose membrane, pore size of 0.45 um (Cat# 1620115, BioRad). Gel transfer used 100 V run in ice-cold transfer buffer pH 8.12 (25 mM tris base, 192 mM glycine, and 20% methanol (Cat# BP1105-4, Fisher Scientific)) at 4°C for one hour using BioRad Mini-

Protean transfer cell (Cat# 1703930, BioRad). Transfer was conducted at 100 V for one hour using a PowerPac™ Basic Power Supply (Cat# 1645050, BioRad).

2.8.3 Immunoblotting

The nitrocellulose membrane was blocked in 3% milk solution (instant skim milk powder, Carnation®) prepared in TBS-T solution pH 7.6 (15.2 mM Tris HCL (BP153-1, Fisher Scientific), 46.2 mM Tris base (Cat# 1610719, BioRad), 150.6 mM NaCl (Cat# 600-082-DG, Wisent), and 0.1% Tween 20 (Cat# BP337100, Fisher BioReagents)). Primary antibodies were diluted in 3% milk in TBS-T and incubated at 4°C overnight on a rotating platform (Table 2). After removing primary antibodies, membranes were washed three times in TBS-T for 5 mins each at room temperature on a rotating platform. The membrane was then incubated for 1hr at room temperature with secondary antibody solutions in 3% milk in TBS-T (Table 2). Membranes were washed three times in TBS-T for 5 minutes each.

2.8.4 Western Blot Imaging

Proteins were visualized with Clarity Western ECL Substrate (1705061, BioRad) and imaged on a GE ImageQuant LAS 4000 (28 9558 10, GE Healthcare, Chicago, Illinois, US). A comparison of the experimental bands to the protein ladder determined approximate molecular weight of proteins. Protein expression was normalized to the housekeeping gene GAPDH to account for protein loading across samples. All samples were run on one blot and probed for individual proteins of interest. When re-probing the same blot with antibodies of different host species, previous HRP was deactivated through the addition of 0.05% sodium azide to the primary antibody solution. Blots were stripped between

antibodies of the same host species by washing twice with fresh mild stripping buffer (1.5% glycine (Cat# 800-045-IK, Wisent), and 0.1% SDS (Cat# 800-100-CG, Wisent) 1% Tween 20 (Cat# BP337100, Fisher BioReagents)) adjusted pH of 2.2) for 5 to 10 each wash. Followed by two ten-minute washes in PBS and two five minute washes in TBS-T. Loss of residual signal was ensured by redeveloping and exposing stripped blots.

Quantitative analysis of resolved Western blots was conducted using Fiji Software. Protein bands were normalized to internal loading control GAPDH. Prospective glycosylation states were determined by measuring total PANX1, followed by individual bands corresponding in size to the predicted molecular weight of each PANX1 glycosylation state (Boassa et al., 2008; Penuela et al., 2007; Penuela et al., 2009). Therefore, the intensity of each band is presented as a percent of total PANX1 in that sample.

Table 2.2: Primary and Secondary Antibodies Used in Western Blotting

Target	Host Species/Dye	Antibody & Fluorophore	Concentration	Vendor and Cat#
Rabbit	Goat	Secondary (HRP)	1:1000	31460, ThermoFisher
Goat	Donkey	Secondary (HRP)	1:1000	Mearow Laboratory
Mouse	Goat	Secondary (HRP)	1:1000	31430, ThermoFisher
Connexin 43	Rabbit	Primary	1:2000	C6219, Sigma-Aldrich
PANX1	Rabbit	Primary	1:1000	AP20645OU-N, OriGene
SOX17	Goat	Primary	1:1000	AF1924, R&D Systems
PAX6	Rabbit	Primary	1:1000	ab195045, Abcam

Brachyury (T)	Rabbit	Primary	1:1000	ab209665, Abcam
GAPDH	Mouse	Primary	1:5000	MAB374, MilliporeSigma
GFP	Rabbit	Primary	1:5000	ab290, Abcam

2.9 RNA Analysis

2.9.1 Cell Lysis and RNA Extraction

Media was aspirated, and cells washed with PBS. According to the manufacturer's instructions, RNA extraction was conducted using the Purelink™ RNA Mini Kit (12183025, Thermofisher Scientific). Briefly, cultures were scraped and passed five to ten times through a 28G insulin syringe (Cat# BD329424, ThermoFisher) or homogenized via a Qiashredder (79654, Qiagen). 70% ethanol was added to homogenized samples to precipitate nucleic acid. Precipitated RNA was collected on RNA spin collection columns before on-column DNA digestion using the Purelink™ DNase Set (12185010, Thermofisher Scientific). Washed and purified RNA was eluted from the spin column into a prelabelled collection tube using 30 ul of RNAse free water. Samples stored at -80ºC for long-term storage.

RNA concentration and purity were evaluated using the Nanodrop™ 1000 spectrophotometer running Nanodrop™ Operating Software version 3.81. Samples were measured at 260 nm using the 260/280 nm and the 260/230 ratio to measure nucleic acid purity. A 260/230 or 260/280 value of ≥ 2.0 is expected for pure RNA samples as lower values could indicate carryover of isolation reagents including phenol (Johnson et al., 2012).

2.9.2 cDNA Conversion

Five hundred nanograms of extracted RNA was converted to complementary DNA (cDNA) using the High-Capacity cDNA Reverse Transcription Kit according to manufacturer's instructions (4368814, Thermofisher Scientific). cDNA conversion was conducted in a T100 thermocycler (Cat# 1861096, BioRad). The generated cDNA was stored at -20°C for long-term storage.

2.9.3 Quantitative RT-PCR (RT-qPCR)

Quantitative reverse transcription-polymerase chain reaction (RT-qPCR) analysis was performed using intercalating dye technology (ssoAdvanced SYBR green supermix) (Cat# 1725274, BioRad) according to the manufacturer's instructions. Primer sets and sequences added can be seen in Table 4. PCR reactions were run on a ViiA™ 7 (ThermoFisher) running QuantStudio Real-Time PCR Software version 1.3 (Applied Biosystems). Cycle conditions are detailed in Table 3.

Table 2.3: Thermocycler settings for RT-qPCR

Stage of Reaction	Duration (seconds)	Temperature (°C)
Initial Denature	30	95
Denature	15	95
Anneal	45	60-62
Repeat 40x	Steps 2-3	-
Melt Curve Step 1.	15	95

Melt Curve Step 2.	60	60
Melt Curve Step 3.	30 (incremental then hold)	95
Melt Curve Step 4.	15	60

Table 2.4: Complete Primer Sets and Sequences used in RT-qPCR Analysis

Target or Gene Name	Primer Sequence	Anneal Temp (°C)	Product Size (bp)
GJB2 (Cx26)	F: CCCGACGCAGAGCAAAC	60	200
	R: CAGGGTGCAGACAAAGT		
GJB6 (Cx30)	F: GAAGGGTCAGGTGTTAGGAA	60	94
	R: AGAGGGCGTACAAGTTAGAA		
GJB4 (Cx30.3)	F: TGTGGTGGACGTACTTGCTG	60	101
	R: GCGGGGCATGTCATAATCCT		
GJB3 (Cx31)	F: CACTCTCTGGCATGGCTTCA	60	96
	R: GTAGGTCGGGCAATGTAGCA		
GJB5 (Cx31.1)	F: AAACAAGACGACCTCCTTTC	60	111
	R: CCCTCACAAGATGGTTTTCT		
GJB1 (Cx 32)	F: TTCCCCATCTCCCATGTGC	60	145
	R: CCCTCAAGCCGTAGCATTTTC		
GJD2 (Cx36)	F: AGCAGCACTCCACTATGATCG	60	286
	R: GTAGAGTAGCGGCGTTCTCG		
GJA4 (Cx37)	F: TCAGCACACCCACCCTGGTCT	60	189
	R: GGATGCGCAGGCGACCATCTT		
GJA5 (Cx40)	F: CCCAGTATACGAAGCCTTTC	60	136

	R: TTTGGTATGCTGCTGGTATG			
GJA1 (Cx43)	F: GGTCTGAGTGCCTGAACTTGCCT		60-62	184
	R: AGCCACACCTTCCCTCCAGCA			
GJC1 (Cx45)	F: TACACCGAACTGTCCAATGC		60-62	271
	R: TCCCATCCCCTGATTTGCTA			
GJA10 (Cx62)	F: AGGCAACTTGAACTAGACCCTT		60	197
	R: GCCGTAGTTGTACCTAGCCA			
GAPDH	F: TGCTTTTAACTCTGGTAAAG		50-62	198
	R: CACTTGATTTTGGAGGGATC			
SOX17	F: GAGCCAAGGGCGAGTCCCGTA		62	141
	R: CCTTCCACGACTTGCCCAGCAT			
T (Brachyury)	F: CGTCTCCTTCAGCAAAGTCAA	Hs.PT.58.12439 65	60	98
	R: CTATGTGGATTCGAGGCTCATAC			
POUF1 (Oct 4)	F: GAGAACCGAGTGAGAGGCAACC		62	78
	R: CATAGTCGCTGCTTGATCGCTTG			
NESTIN	F: CTGCGGGCTACTGAAAAGTT		60	161
	R: TCCAGGAGGGTCCTGTACG			

2.10 Statistical Analysis

Statistical analysis and plotting of raw data used Graph Pad Prism v.8. Graphs presented as ± standard error of the mean (SEM). Unless otherwise stated $n \geq 3$ independent biological replicates. Statistical analysis between two groups used paired student's t-test. Larger data sets of three or more groups were analyzed using analysis of variance (ANOVA). Statistical

significance was identified by running a Tukey's multiple comparisons test. * $p < 0.05$, ** $p < 0.01$, *** $p < 0.001$, **** $p < 0.0001$.

3 Results

3.1 Connexin isoforms are differentially expressed during human iPSC specification to the three germ lineages

Given that aberrant GJIC is linked to numerous disease conditions, I investigated the expression of 11 connexin isoforms in human control iPSCs and after directed differentiation toward the three embryonic germ layers: ectoderm, endoderm and mesoderm (Figure 3.1; (Laird et al., 2017). Directed differentiation was conducted using the StemDiff Trilineage Differentiation kit (StemCell Technologies, Vancouver, British Colombia, CA), and resultant populations were routinely screened via RT-qPCR, Western blotting and immunofluorescence to ensure proper lineage-specific gene expression. Expression of transcripts encoding Cx26, Cx31.1, and Cx43 showed no significant fluctuation during ectoderm, mesoderm, or endoderm restriction compared to start iPSC expression levels ($p > 0.05$) (Figure 3.1). Cx62 was 30.68 ± 20.94 fold higher in ectoderm as compared to undifferentiated iPSCs ($p < 0.01$) (Figure 3.1). Similarly, Cx45 is 1.451 ± 0.3097 fold higher post-ectoderm formation ($p < 0.05$) (Figure 3.1). Meanwhile, restriction of iPSCs to mesoderm significantly increased transcripts of Cx45 1.681 ± 0.3129 fold over iPSCs ($p < 0.01$) (Figure 3.1). Compared to undifferentiated iPSCs, endoderm specification resulted in increased transcript levels of Cx30.3 (6.439 ± 1.963 fold ($p < 0.01$)); Cx31 (2.819 ± 1.063 fold ($p < 0.01$)); Cx32 (7.51 ± 6.007 fold ($p < 0.01$)); Cx36 (3.964 ± 2.016 fold ($p < 0.05$)); Cx37 (5.826 ± 4.144 fold ($p < 0.05$)) and Cx40 (1.974 ± 0.2959 fold ($p < 0.01$)) (Figure 3.1). I continued my study with Cx43 and Cx32 due to the wide expression of Cx43 as well as Cx32's implication in endoderm and ectoderm-related disorders

(Sargiannidou et al., 2009; Scherer & Kleopa, 2012). These results describe the presence of transcripts for several Cx isoforms some for the first time in iPSCS, ectoderm, mesoderm or endoderm providing a suggestive background for future work.

Figure 3.1 – Connexin expression during iPSC lineage specification. Quantitative RT-PCR (RT-qPCR) expression of mRNA transcripts that encode 11 of the 21 human connexin isoforms in human control iPSCs (*grey dotted line*) and after directed differentiation into ectoderm, endoderm and mesoderm. Data represent the standard error of the mean of 3 to 5 independent experiments. *, $p < 0.05$; **, $p < 0.01$ compared to iPSC.

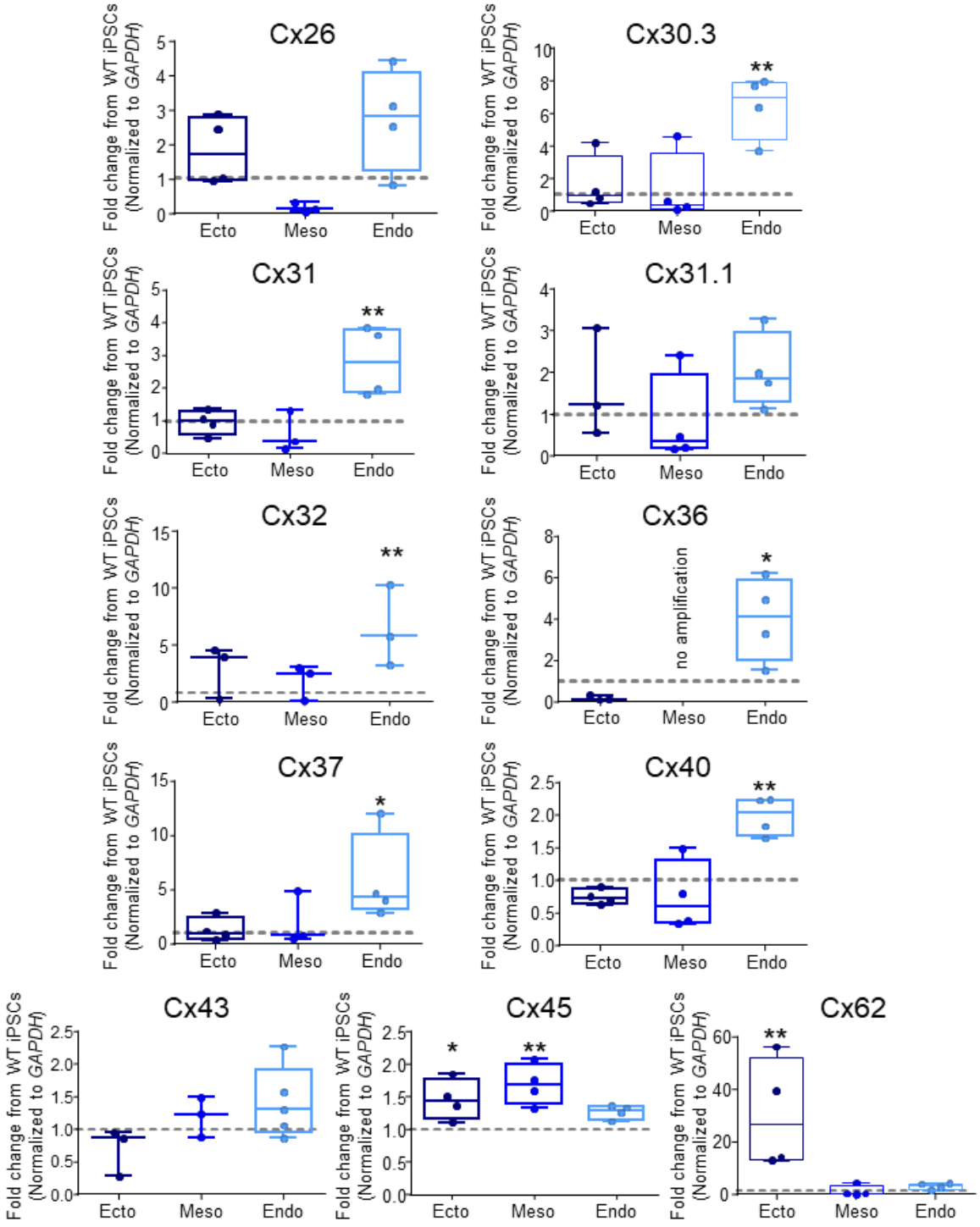
Cx26
Cx30.3
Cx31
Cx31.1
Cx32
Cx36
Cx37
Cx40
Cx43
Cx45
Cx62
Fold change from WT iPSCs (Normalized to GAPDH)
Ecto
Meso
Endo
**
*
no amplification

3.2 Cx43 protein expression persists throughout lineage specification

In line with the broad expression of Cx43 throughout the developing embryo, I found that Cx43 transcript abundance was comparable across control iPSCs and all three embryonic germ lineages (Figure 3.1). Due to the widely reported role of Cx43 in stem cell differentiation, along with my findings that Cx43 (*GJA1*) transcripts remained high during iPSC lineage commitment, I focused on this protein's expression and localization across the three germ lineages. While transcript abundance for Cx43 remained constant throughout lineage specification, I sought to determine if this was reflected in protein expression (Figure 3.2). Representative Western blots and immunofluorescence of lineage-specific proteins demonstrate the successful differentiation of iPSCs into ectoderm (PAX6 or Nestin), endoderm (SOX17), and mesoderm (Brachyury) (Figure 3.2A, B). Cx43 in all examined cell types was localized to small puncta at the interface between cells, indicative of gap junction plaques (Figure 3.2A). This result is consistent with multiple reports using a broad range of cell types confirming Cx43 localization to the cell surface (Hillis et al., 1997; Ke et al., 2013; Lin et al., 2018; Peng et al., 2019; Shao et al., 2019; Söhl et al., 2010; Wörsdörfer et al., 2008; Yang et al., 2019). In contrast to results presented with RT-qPCR, I found that Cx43 protein was similarly expressed in iPSCs, ectoderm and endoderm, but significantly increased in mesoderm (iPSCs 1.00 ± 0.0, Mesoderm 1.607 ± 0.222; Figure 3.2B, C).

Figure 3.2 – Cx43 protein expression and localization in iPSCs and cells of each germ lineage. (A) Representative immunofluorescent confocal micrographs demonstrating Cx43 (merged overlay; *green*) localization to large puncta (*white arrows*) at cell-cell interfaces, indicative of gap junction formation in cells differentiated into the three germ layers (SOX2, iPSCs; Nestin, ectoderm; Brachyury, mesoderm; SOX17, endoderm: merged overlay; *purple*) nuclei (Hoechst, nuclei: merged overlay; *blue*). Scale bars = 50 µm. Images representative of n=2 (endoderm), n=1 (iPSCs, ectoderm and mesoderm). Equal adjustments to brightness and contrast were made in Fiji. All images presented at the same magnification, zoom panels represent cropped and enlarged sections of original images. **(B)** Representative Western blots show Cx43 expression in PAX6-positive ectoderm, Brachyury-positive mesoderm, and SOX17-positive endoderm. **(C)** Densitometry revealed that total Cx43 protein expression remains comparable between iPSCs and cells of each germ layer. Data represent the standard error of the mean of 3 to 9 independent experiments analysed using one-way ANOVA.

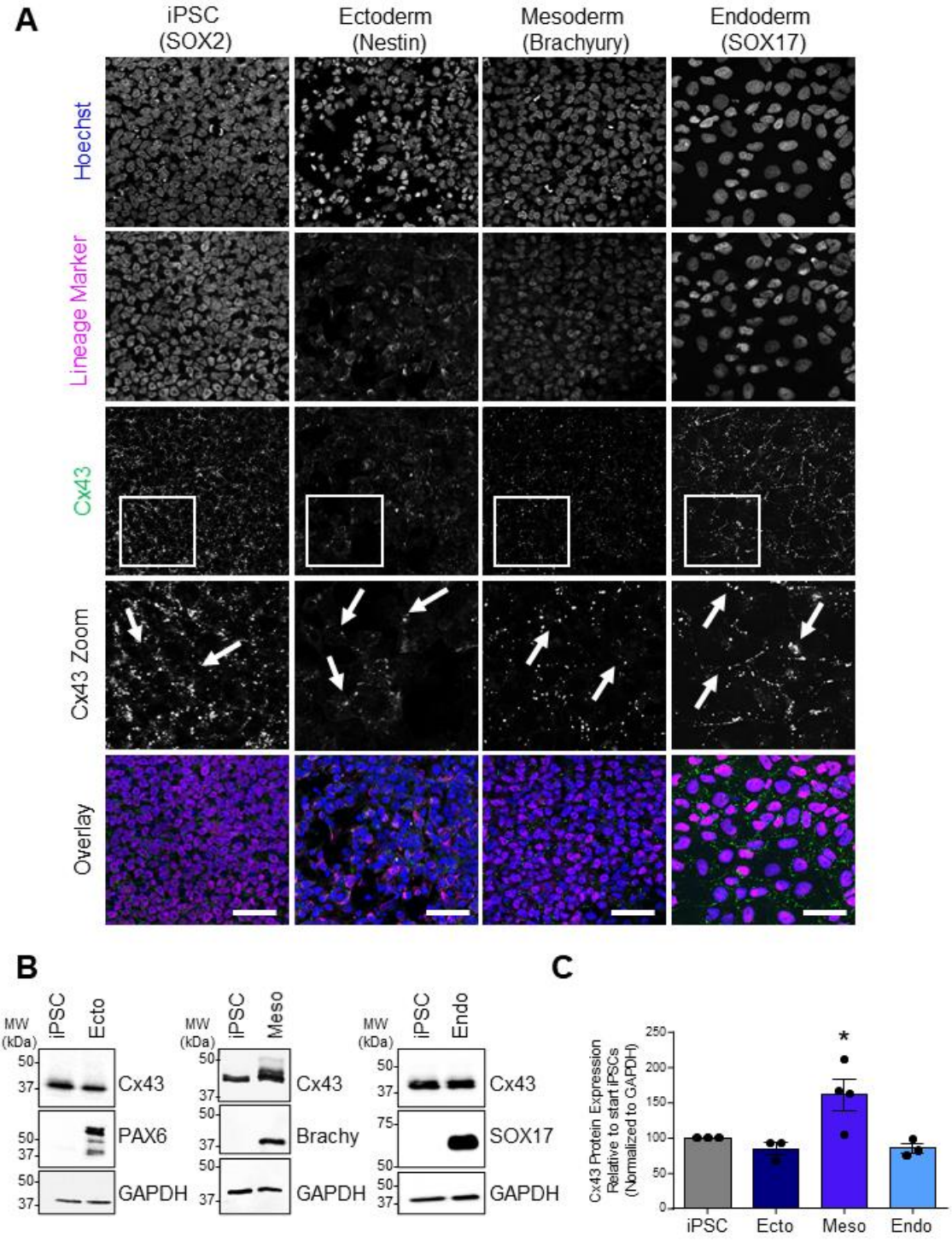
A
iPSC (SOX2)
Ectoderm (Nestin)
Mesoderm (Brachyury)
Endoderm (SOX17)
Hoechst
Lineage Marker
Cx43
Cx43 Zoom
Overlay
B
MW (kDa)
iPSC
Ecto
Cx43
PAX6
GAPDH
Meso
Brachy
Endo
SOX17
C
Cx43 Protein Expression Relative to start iPSCs (Normalized to GAPDH)
iPSC
Ecto
Meso
Endo

3.3 Human iPSCs tolerate *GJA1* CRISPR-Cas9 manipulation

Previous studies determined that Cx43 was dispensable for human iPSC survival and pluripotency gene expression (Esseltine et al., 2020). However, due to the wide expression profile and early developmental expression of Cx43, I sought to determine whether this protein plays a role in cell fate specification. Dr. Esseltine generated a *GJA1-/-* (encoding for Cx43) iPSC line via CRISPR Cas9 gene-editing (Esseltine et al., 2020; Shao et al., 2019). Figure 3.3A shows the alignment between generated CRISPR guide RNA (gRNA) and the *GJA1* genomic sequence. Cx43 ablation was confirmed by immunofluorescence and Western blotting (Figure 3.3B, C). Meanwhile, the Cx43-eGFP reporter cell line was generated via CRISPR-Cas9 gene editing by the Allen Institute for Cell Science. Resultant iPSCs harbour a heterozygous insertion of the Cx43-eGFP construct at the endogenous *GJA1* allele, that results in iPSCs with one wild-type *GJA1* allele and one genetically altered to express Cx43-eGFP (Figure 3.3B, C). It is important to note that the Cx43-eGFP edited iPSCs are not overexpressing the reporter construct; instead, CRISPR-Cas9 editing allows the replacement of the endogenous allele with the edited construct. Produced cells express similar levels of Cx43 as the unedited cells normally would. Confocal fluorescent microscopy of control, *GJA1-/-* and Cx43eGFP iPSCS revealed no observable difference in cellular morphology of the edited iPSCs compared to control (Figure 3.3C). Western blotting revealed bands of appropriate size for Cx43 (~ 43 kDa) in control iPSCs, which is absent in *GJA1-/-* iPSCs (Figure 3.3B). On the other hand, the Cx43-eGFP reporter cell line exhibits two distinct protein species corresponding to the unedited Cx43 allele (~43 kDa) and the Cx43-eGFP CRISPR knock-in allele (~60 kDa) (Figure 3.3B). Indeed, immunoblotting with a GFP-specific primary

antibody confirms that the 60 kDa band in the Cx43-eGFP cells corresponds to a GFP fusion protein. As noted above, immunofluorescence confirmed that Cx43 protein is expressed at the cell surface in wild-type human iPSCs, where it forms large puncta at opposing cell membranes, indicative of gap junction plaques containing hundreds of clustered gap junction channels (Figure 3.3C). Here I used the F-actin binding protein phalloidin to delineate the actin cytoskeleton and determine Cx43 gap junction plaque localization. As would be expected of gene knockout, this punctate staining pattern is absent in *GJA1-/-* iPSCs (Figure 3.3C). The generated Cx43-eGFP demonstrates comparable Cx43 localization to control cells (WT iPSCs 75.78 ± 7.14; Cx43-eGFP 72.76 ± 1.68) with large plasma membrane puncta, confirming that the addition of eGFP did not affect Cx43 expression or localization (Figure 3.3C). Taken together, these three human iPSC lines (control, *GJA1-/-* and Cx43-eGFP) enable a comprehensive evaluation of Cx43 during iPSC lineage commitment and differentiation.

3.4 Cx43-eGFP iPSCs differentiate into all three germ lineages

Aside from verifying the correct GFP insertion in the Cx43-eGFP reporter line, no other cell line validation was completed by the Allen Institute for Cell Science. As genetic manipulation can alter the inherent differentiation capacity of iPSCs, I wanted to ensure that the Cx43-eGFP iPSCs performed like control cells. Therefore, I performed passive spontaneous iPSC differentiation to evaluate the inherent differentiation potential of the Cx43-eGFP iPSCs. Contrary to directed differentiation, spontaneous differentiation does not involve exogenous signals, thus enabling the cells to undergo self-guided differentiation. Cx43-eGFP iPSCs, cultured in the absence of external pressures such as

strong morphogens and growth factors used in directed differentiation, successfully differentiated into cell types from all three germ layers. This was determined through the identification of regions rich in SOX17 positive nuclei indicating endoderm formation, Brachyury positive nuclei indicative of mesoderm formation, and regions of Nestin expression denoting ectoderm formation (Figure 3.4). As observed after differentiation of unedited control iPSCs, the spontaneously differentiated Cx43-eGFP cultures expressed Cx43 across cells of each germ layer and formed the typical puncta indicative of gap junction plaques (Figure 3.4).

Figure 3.3 – CRISPR-Cas9 manipulation of *GJA1* in human iPSCs. (A) Alignment of CRISPR-Cas9 gRNA targeted to the second exon of *GJA1* antisense strand reference sequence, generated using NCBI gene and Clustal Omega. PAM sequence indicated in red. **(B)** Representative Western blots of Cx43 and GFP protein expression in WT, *GJA1-/-* and Cx43-eGFP iPSCs along with loading control GAPDH. n=5 WT and *GJAI-/-* iPSC; n=2 Cx43-eGFP iPSCs. **(C)** Immunofluorescence confirms the absence of Cx43 (merged overlay; *green*) in *GJA1-/-* iPSCs and shows Cx43 forms gap junction plaques (*white arrows*) and localizes to the cell surface in WT iPSCs and Cx43-eGFP iPSCs. Actin (phalloidin, merged overlay; *grey)*; nuclei (Hoechst, merged overlay; *blue*). Scale bar = 50 µm. Images representative of n=3. All images presented at the same magnification, zoom panels represent cropped and enlarged sections of original images. Fiji analysis was used to apply equal brightness, contrast adjustments where necessary. **(D)** Manders' coefficient of Cx43 percent colocalization with phalloidin. Data representative of three biological replicates averaged from 1 to 6 individual images.

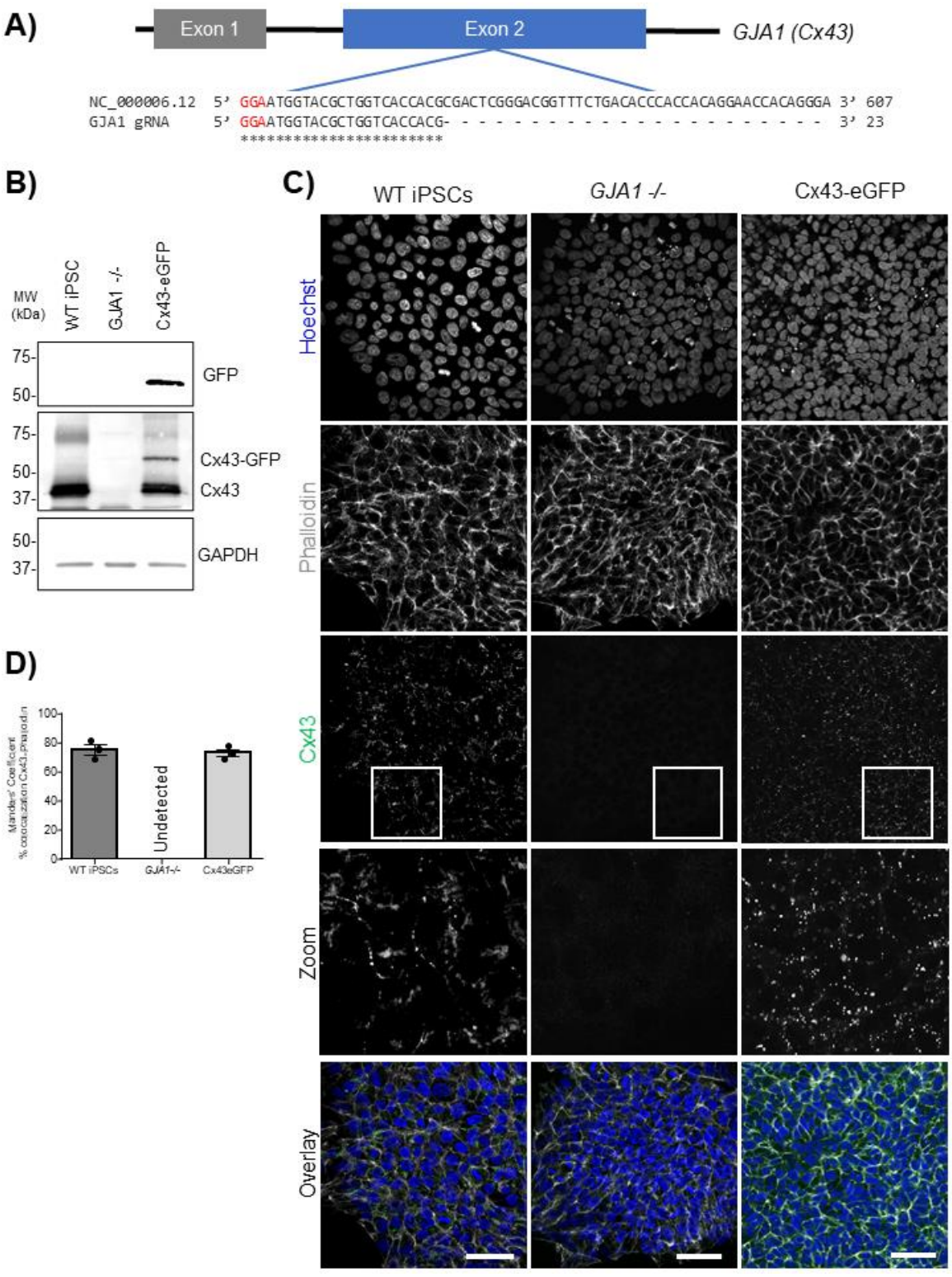
A)
Exon 1
Exon 2
GJA1 (Cx43)
NC_000006.12 5' GGAATGGTACGCTGGTCACCACGCGACTCGGGACGGTTTCTGACACCCACCACAGGAACCACAGGGA 3' 607
GJA1 gRNA 5' GGAATGGTACGCTGGTCACCACG- 3' 23
****
B)
MW (kDa)
WT iPSC
GJA1 -/-
Cx43-eGFP
75-
50-
GFP
75-
50-
37-
Cx43-GFP
Cx43
50-
37-
GAPDH
C)
WT iPSCs
GJA1 -/-
Cx43-eGFP
Hoechst
Phalloidin
Cx43
Zoom
Overlay
D)
Undetected
WT iPSCs
GJA1-/-
Cx43eGFP

Figure 3.4 – Cx43 Localization in spontaneously differentiated Cx43-eGFP CRISPR knock-in iPSCs. Representative immunofluorescent confocal micrographs demonstrating Cx43-eGFP (merged overlay; *green*) localization to regions of spontaneously differentiated ectoderm (Nestin, merged overlay; *purple*), mesoderm (Brachyury, merged overlay; *purple*) or endoderm (SOX17, merged overlay; *purple*) cells. Nuclei (Hoechst, merged overlay; *blue*). Cx43 forms large plaques (*white arrows*) at the cell surface. Scale bars = 50 µm. Images representative of n=3. Equal brightness, contrast adjustments were made in Fiji.

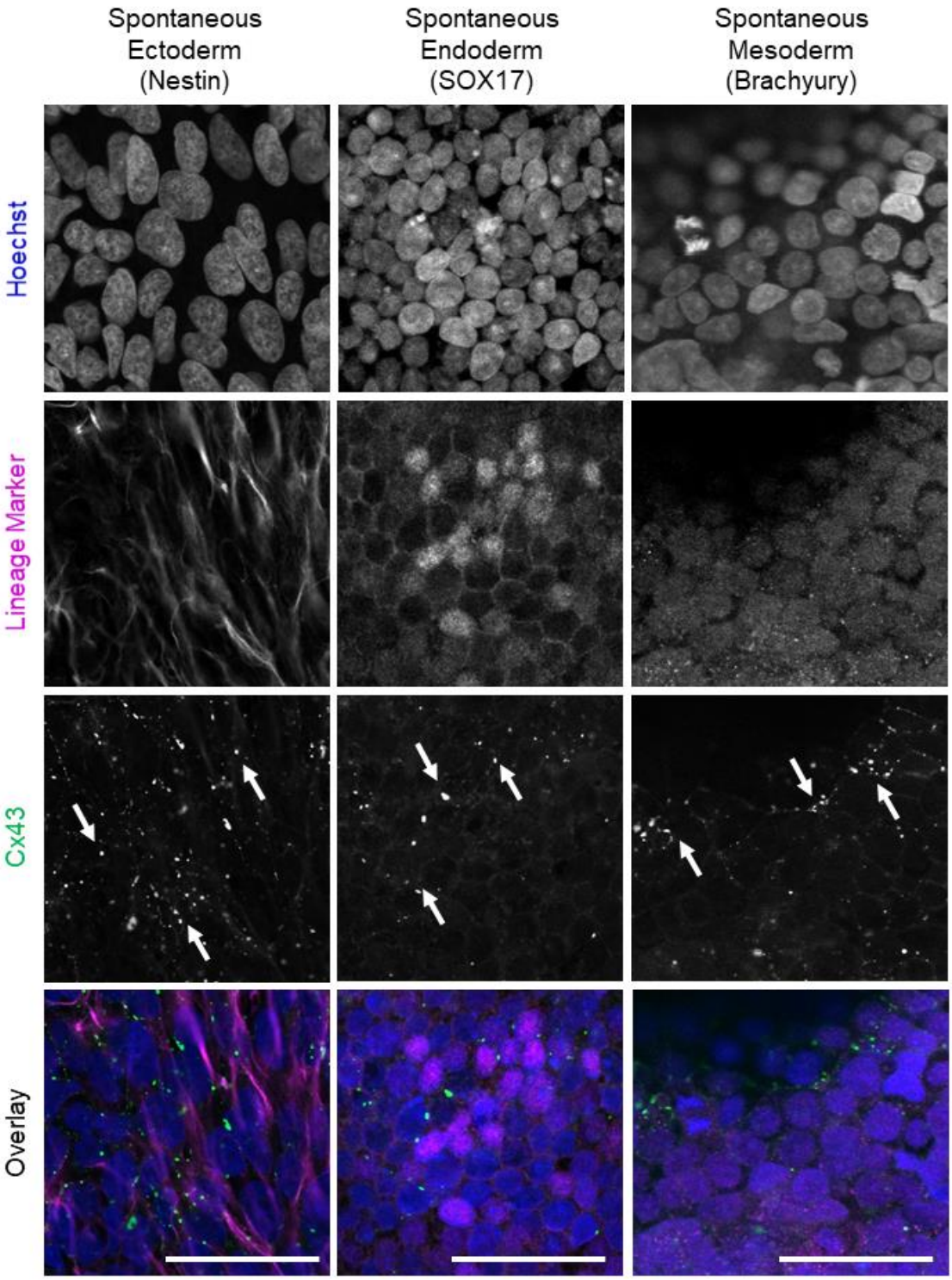
Spontaneous Ectoderm (Nestin)
Spontaneous Endoderm (SOX17)
Spontaneous Mesoderm (Brachyury)
Hoechst
Lineage Marker
Cx43
Overlay

3.5 Cx43 is Dispensable During Lineage Specification

Previous reports using pharmacological gap junction blockers or Cx43 siRNA knockdown suggested that Cx43 influenced human and mouse PSC germ lineage specification (Peng et al., 2019; Yang et al., 2019). To determine whether *GJA1-/-* iPSCs exhibited similar changes in germ lineage differentiation, I differentiated control and *GJA1-/-* iPSCs into ectoderm, endoderm, or mesoderm (STEMdiff™ Trilineage Differentiation kit, STEMCELL Technologies; Figure 3.5). In contrast to previous studies, I found no significant difference in ectoderm (PAX6), mesoderm (Brachyury) or endoderm (SOX17) cells differentiated from control or *GJA1-/-* iPSCs (Figure 3.5). As *GJA1-/-* iPSCs successfully differentiated into all three germ lineage under directed conditions, I concluded that Cx43 is dispensable during lineage specification.

Figure 3.5 – Directed differentiation of *GJA1-/-* iPSCs to the three germ layers. Representative Western blot and densitometry of differentiated WT and *GJA1-/-* iPSCs. **(A)** Ectoderm formation indicated by expression of PAX6, while **(B)** mesoderm evaluated by Brachyury expression and **(C)** endoderm formation confirmed by SOX17. Data represent the standard error of the mean of three independent experiments. ns: no significance.

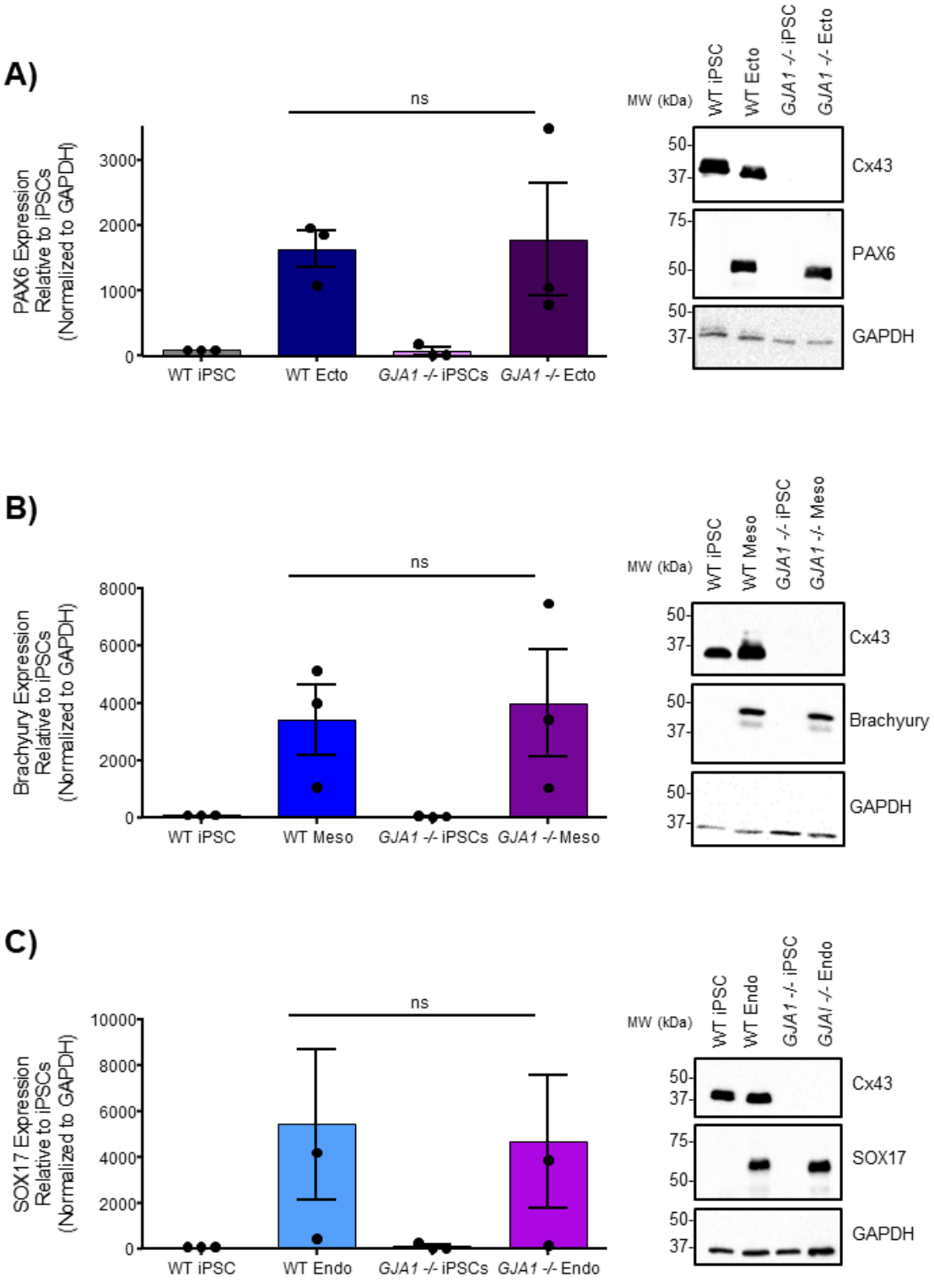
A)
ns
PAX6 Expression Relative to iPSCs (Normalized to GAPDH)
3000
2000
1000
0
WT iPSC
WT Ecto
GJA1 -/- iPSCs
GJA1 -/- Ecto
MW (kDa)
WT iPSC
WT Ecto
GJA1 -/- iPSC
GJA1 -/- Ecto
50
37
Cx43
75
50
PAX6
50
37
GAPDH
B)
ns
Brachyury Expression Relative to iPSCs (Normalized to GAPDH)
8000
6000
4000
2000
0
WT iPSC
WT Meso
GJA1 -/- iPSCs
GJA1 -/- Meso
MW (kDa)
WT iPSC
WT Meso
GJA1 -/- iPSC
GJA1 -/- Meso
50
37
Cx43
50
37
Brachyury
50
37
GAPDH
C)
ns
SOX17 Expression Relative to iPSCs (Normalized to GAPDH)
10000
8000
6000
4000
2000
0
WT iPSC
WT Endo
GJA1 -/- iPSCs
GJA1 -/- Endo
MW (kDa)
WT iPSC
WT Endo
GJA1 -/- iPSC
GJAI -/- Endo
50
37
Cx43
75
50
SOX17
50
37
GAPDH

3.6 Cx32 is Retained Intracellularly in iPSCs and Germ Lineages

While the prototypical Cx43 has been extensively studied, there are other intriguing and less well-known connexins expressed in human iPSCs. I specifically evaluated Cx32 after iPSC differentiation toward the three germ layers based on previous studies linking it to PSC lineage commitment as well as presented RT-qPCR evidence that it may be elevated in endoderm-derived cells (Figure 3.1; (Qin et al., 2016). As a proxy for plasma membrane localization, I analyzed the co-localization of Cx43 (Figure 3.3C) and Cx32 (Figure 3.6) with the actin binding molecule phalloidin. Mander's co-localization coefficient confirms that the majority of Cx43 staining is co-localized with phalloidin in iPSCs (75.78 ± 7.14) (Figure 3.3C). Conversely, significant ($p < 0.01$) decreases in manders coefficient demonstrate that Cx32 colocalizes less with phalloidin, indicating that a large population of the Cx32 protein appears to be retained intracellularly (50.80 ± 6.36% iPSCs; 49.30 ± 7.75% ectoderm; 45.16 ± 3.49% mesoderm; 33.23 ± 8.89 endoderm; Figure 3.6). Future work will determine the specific subcellular localization of Cx32, which could illuminate its potential participation in lineage specification.

Figure 3.6 – Cx32 localization in iPSCs and cells of the three germ lineages. (A) Representative immunofluorescent confocal micrographs of Cx32 (merged overlay; *green)* along with actin (phalloidin, merged overlay; *red*) in undifferentiated iPSCs (left), after directed differentiation into ectoderm (middle left), mesoderm (middle right) endoderm (right). Inset: zoomed region of Cx32 and phalloidin localization. Cx32 forms differentially localized gap junction plaques (*white arrows*). SOX17-endo, Nestin-ecto, Brachyury-meso, SOX2-iPSC (merged overlay; *purple*); nuclei (Hoechst, merged overlay; *blue*). All images presented at the same magnification, zoom overlay represent cropped and enlarged sections of original Cx32 and phalloidin images used in Mander's coefficient analysis. Scale bars = 50 µm. Images are representative of one biological replicate. **(B)** Manders' coefficient of Cx32 percent colocalization to phalloidin. Data presented as standard error of the mean and represents analysis of 3 to 6 images taken from one biological replicate.

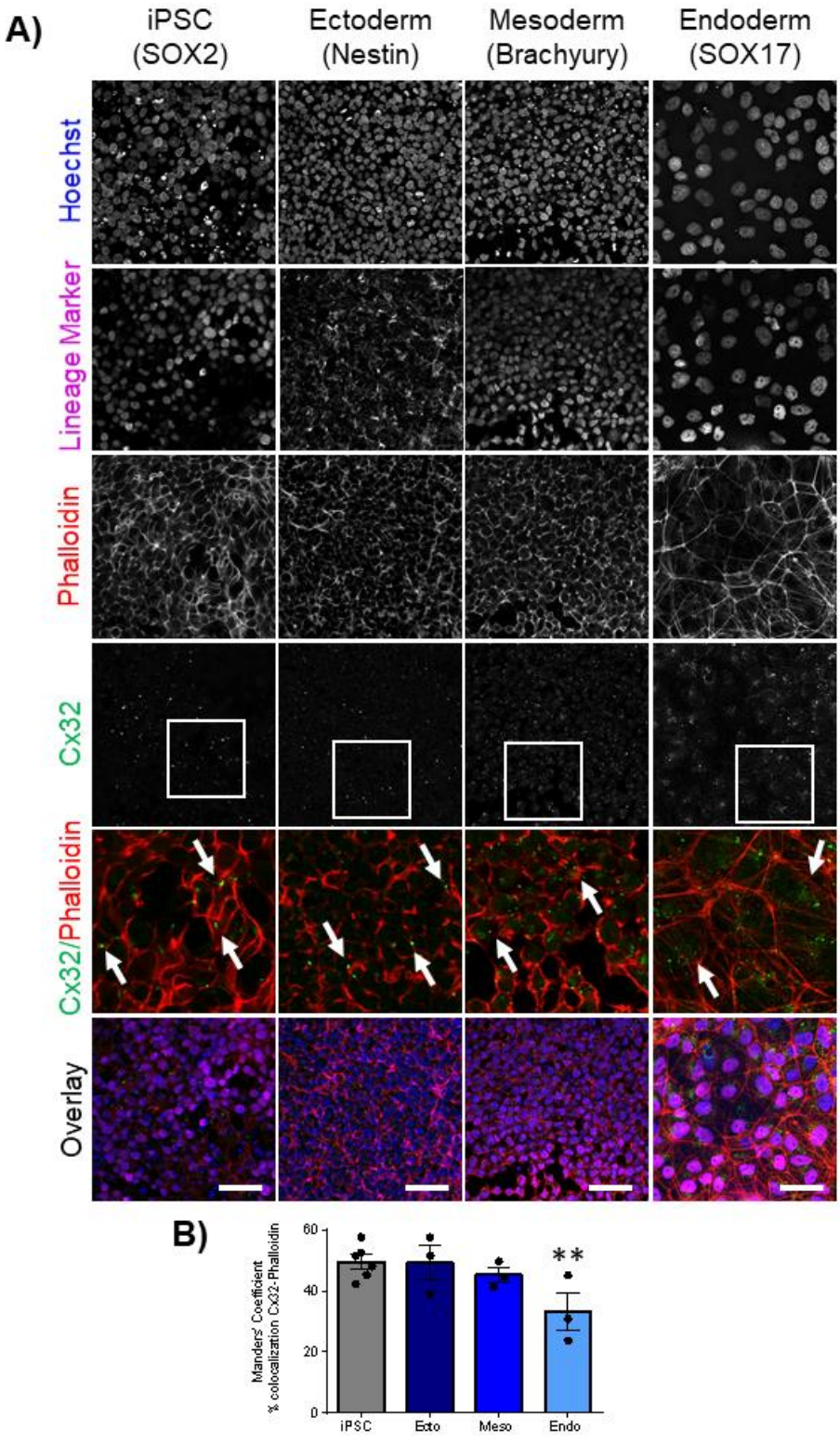
A)
iPSC (SOX2)
Ectoderm (Nestin)
Mesoderm (Brachyury)
Endoderm (SOX17)
Hoechst
Lineage Marker
Phalloidin
Cx32
Cx32/Phalloidin
Overlay
B)
Manders' Coefficient % colocalization Cx32-Phalloidin
60
40
20
0
**
iPSC
Ecto
Meso
Endo

3.7 PANX1 is expressed in human iPSCs and cells of the three germ layers

In addition to connexins, recently human iPSCs were reported to express mRNA of the Pannexin (PANX) family of large pore membrane channels (Hainz et al., 2018). The PANX1 protein has been widely described in various terminal tissue types derived from the three embryonic germ layers. Therefore, I examined PANX1 protein expression in iPSCs as well as after ectoderm, endoderm, or mesoderm differentiation (Figure 3.7). Western blot shows expression of PANX1 in all three germ layers: PAX6 positive ectoderm, SOX17 positive endoderm, and Brachyury positive mesoderm (Figure 3.7A, B). Total PANX1 protein expression remains comparable between undifferentiated iPSCs and differentiated germ lineage cultures (Figure 3.7A).

3.8 PANX1 is alternatively glycosylated in cells from the three germ layers

The migration of PANX1 is well established, resolving as three distinct molecular weight bands on a Western blot, and these three bands have been shown to correspond to the three primary glycosylation species of PANX1 (Boassa et al., 2008; Penuela et al., 2007; Penuela et al., 2009). Thus, PANX1 glycosylation states are commonly inferred from Western blot analysis based on molecular weight. Although total PANX1 protein does not change after germ lineage differentiation, densitometric analysis of the molecular weight species corresponding to specific PANX1 glycosylation states revealed significant differences across the three germ layers. Similar to what was observed in iPSCs, 37.15 ± 2.47% of ectoderm PANX1 migrates on a Western blot corresponding to the molecular weight of the fully glycosylated isoform, while the high mannose molecular weight band comprises 25.59 ± 2.91% total protein and 37.24 ± 3.28% of PANX1 protein runs according

to the unglycosylated molecular weight (Figure 3.7B, C). Interestingly, one-way ANOVA (α=0.05) analysis showed the molecular weight band corresponding to fully glycosylated PANX1 is significantly elevated in mesoderm cells compared to iPSCs (61.25 ± 1.29% Gly2, 22.71 ± 7.58% Gly1 and 16.01 ± 6.43% Gly0). On the other hand, endoderm cells appeared to have a significant reduction in the bands corresponding to the Gly1 and Gly2 species. 61.09 ± 5.84% of endodermal PANX1 resolves as the correct molecular weight of the unglycosylated PANX1 species, while only 22.38 ± 2.35% correspond to the correct molecular weight of the fully glycosylated, with complex carbohydrate, species (Figure 3.7B, C).

3.9 PANX1 is differentially localized in Human Germ Lineages

PANX1 glycosylation reportedly regulates its trafficking to the plasma membrane (Boassa et al., 2007; Boassa et al., 2008). As the generated Western blots suggest that PANX1 may be differentially glycosylated across each germ lineage, I evaluated the subcellular distribution of PANX1 across these different lineages. As noted above, I used the actin-binding molecule phalloidin to delineate the cytoskeleton and determine PANX1 protein intracellular localization. In SOX2-positive iPSCs, Nestin-positive ectoderm and Brachyury-positive mesoderm cells, immunofluorescence shows PANX1 overlapping with Phalloidin-AF555 (72.01 ± 4.89% iPSC, 76.37 ± 6.84% colocalization ectoderm; 71.17 ± 0.62% colocalization mesoderm; Figure 3.8, inset, yellow regions). However, in SOX17 positive endoderm cells, PANX1 localized mainly to intracellular compartments with much less overlap with phalloidin (42.90 ± 8.78% colocalization endoderm; Figure 3.8 inset, white arrowheads). One-way ANOVA confirmed a significant decrease ($p < 0.0001$) in

Manders coefficient values evaluating PANX1 colocalization with actin. Therefore, it can be concluded that PANX1 resides primarily at the cell surface in undifferentiated iPSCs as well as ectoderm and mesoderm cells, while endoderm formation redistributes PANX1 to intracellular locations (Figure 3.8, inset).

Figure 3.7 - PANX1 is differentially glycosylated in the three germ layers. (A) Densitometric analysis of total PANX1 protein expression in iPSCs, ectoderm, mesoderm, and endoderm cells. **(B)** Representative Western blots with respective lineage markers. Western blot resolves PANX1 protein as three individual bands of different sizes corresponding with the molecular weight of the non-glycosylated protein (Gly0), high mannose (Gly1) or complex carbohydrate addition (Gly2). **(C)** Densitometric analysis of the three PANX1 glycosylation states as a percent of total PANX1. Data represent the standard error of the mean of 3 to 9 independent experiments. ns: no significance; * $p < 0.05$; ** $p < 0.01$ compared to iPSCs.

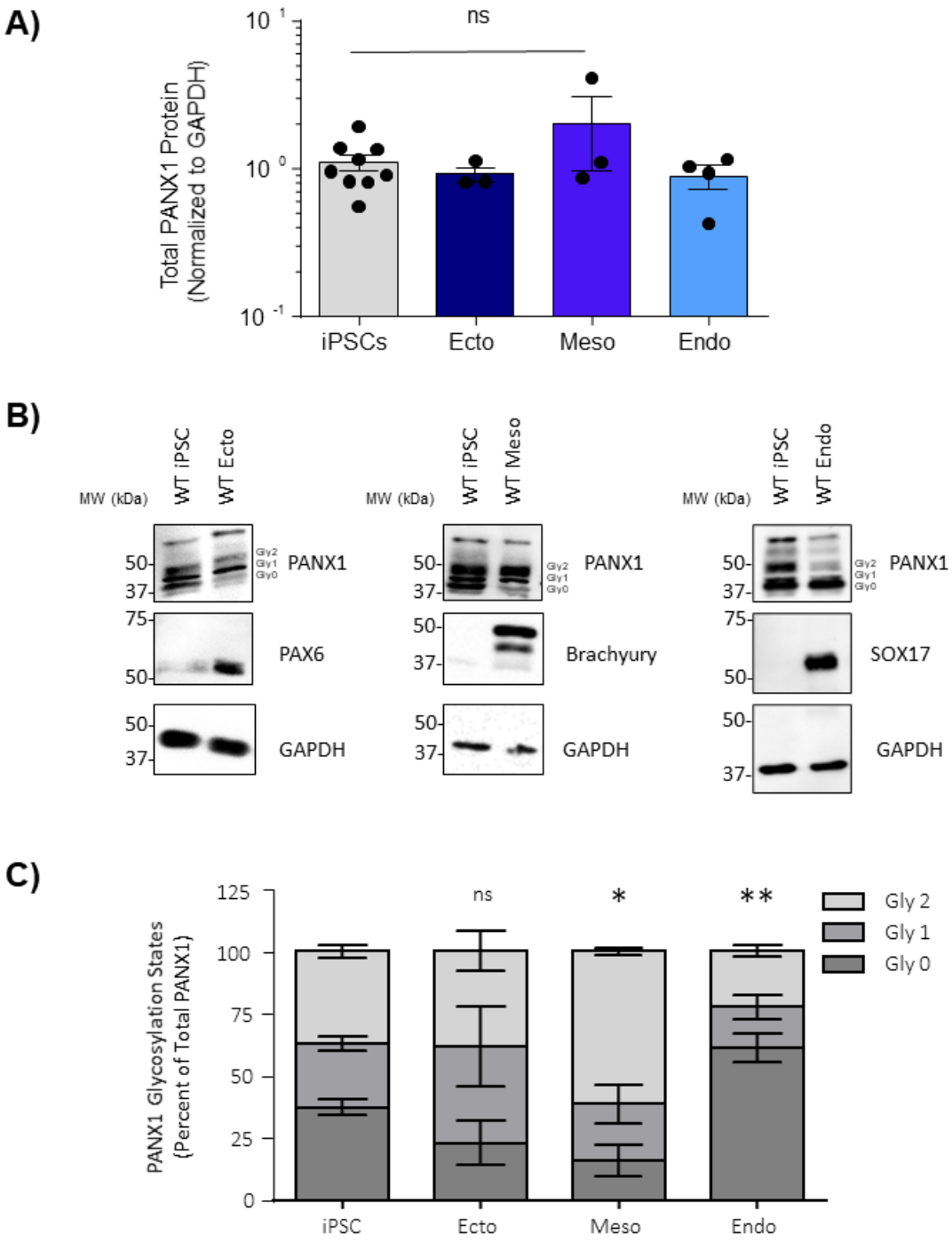
A)
ns
Total PANX1 Protein
(Normalized to GAPDH)
10 1
10 0
10 -1
iPSCs
Ecto
Meso
Endo
B)
MW (kDa)
WT iPSC
WT Ecto
WT Meso
WT Endo
PANX1
PAX6
Brachyury
SOX17
GAPDH
Gly2
Gly1
Gly0
50-
37-
75-
C)
PANX1 Glycosylation States
(Percent of Total PANX1)
125
100
75
50
25
0
ns
*
**
Gly 2
Gly 1
Gly 0
iPSC
Ecto
Meso
Endo

Figure 3.8 - PANX1 is differentially localized in the three embryonic germ layers. Representative immunofluorescent confocal images of PANX1 (merged overlay; *green*) along with actin (phalloidin, merged overlay; *red*) in iPSCs, ectoderm and mesoderm. Nuclei (Hoechst, merged overlay; *blue)*; lineage markers (SOX2, Nestin, Brachyury, SOX17, merged overlay; *magenta*). Inset: regions of interest cropped and enlarged to highlight regional PANX1 localization. Arrows highlight intracellular PANX1 localization in endodermal cells. Scale bar = 50 µm, n=3 endoderm, n=1 ectoderm, mesoderm.

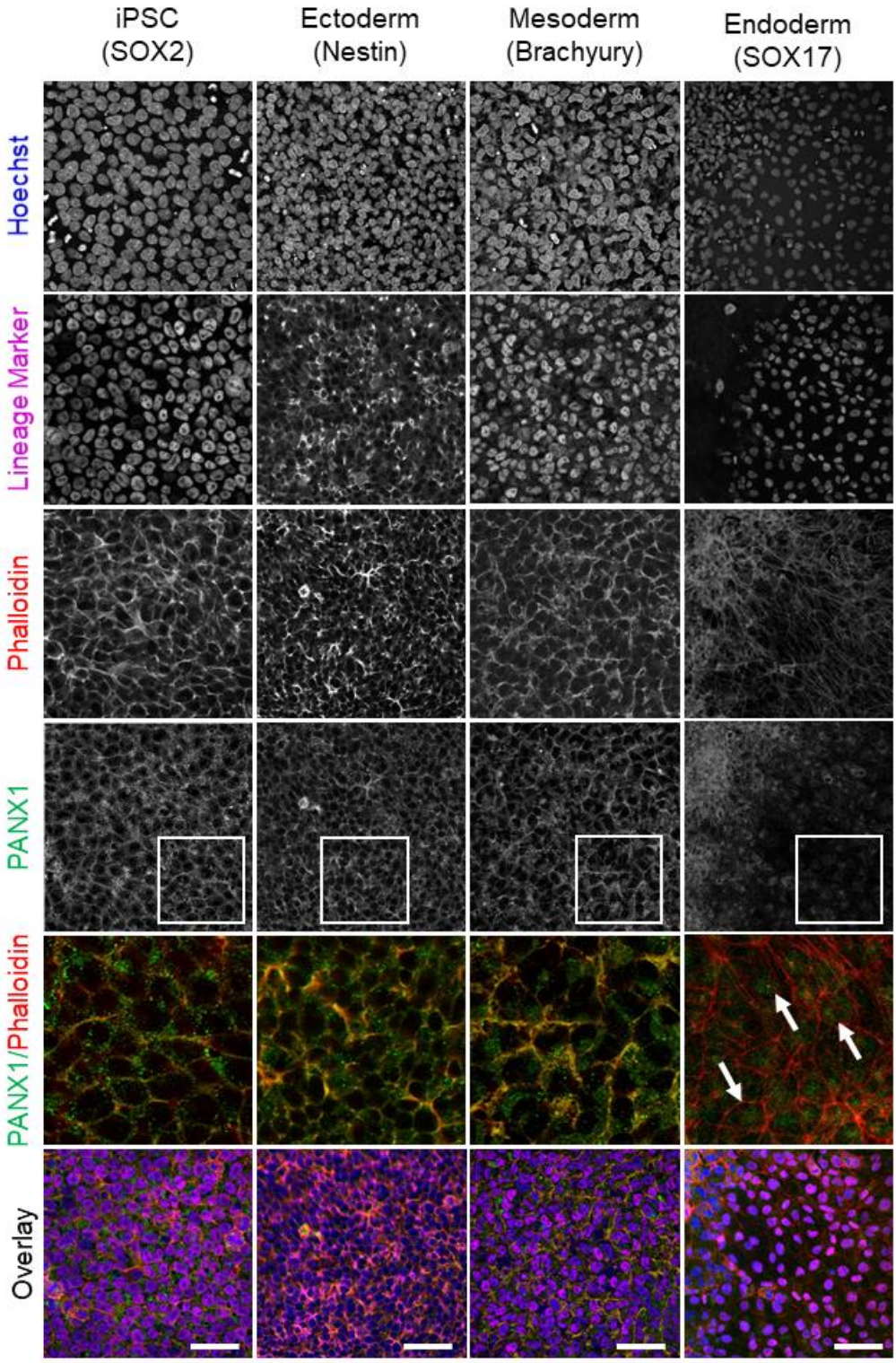
iPSC
(SOX2)
Ectoderm
(Nestin)
Mesoderm
(Brachyury)
Endoderm
(SOX17)
Hoechst
Lineage Marker
Phalloidin
PANX1
PANX1/Phalloidin
Overlay

3.10 *PANX1*-/- human iPSCs remain viable and morphologically comparable to WT iPSCs

As I found above that PANX1 is expressed in undifferentiated iPSCs as well as all three embryonic germ lineages, I next questioned whether iPSCs can tolerate the loss of PANX1. CRISPR-Cas9 was used to genetically ablate *PANX1* in iPSCs (Figure 3.9). A single base pair deletion in the third exon of *PANX1* produced a frameshift mutation and up to 15 early stop codons (Figure 3.9A). Western blot and immunofluorescence reveal successful CRISPR-Cas9 gene ablation, as *PANX1-/-* iPSCs no longer express PANX1 protein (Figure 3.9B, C). Other members of our research group have confirmed loss of PANX1 protein and mRNA through flow cytometry and RT-qPCR (Noort et al., 2021). As seen in the Western blots, non-specific bands in the *PANX1* knockout cells are occasionally detected. Depending on PANX1 expression and total protein loaded onto gels, I have found that these non-specific bands generally appear when longer exposure times were necessary to capture sufficient PANX1 protein signal. However, these bands were consistent across different samples and therefore considered non-specific. Thus, I am confident that the *PANX1-/-* iPSCs are indeed knocked out. *PANX1-/-* iPSCs appear morphologically indistinguishable from control cells and continue to grow as large colonies of tightly packed cells characteristic of human pluripotent stem cells (Figure 3.9C).

Figure 3.9 - PANX1 CRISPR-Cas9 gene ablation in human iPSCs. (A) Gene schematic of CRISPR-Cas9 gRNA target site and induced mutations. CRISPR-Cas9 gene ablation targeting the second PANX1 exon resulted in a single base pair deletion (*red box*), thus interrupting the reading frame and producing several early stop codons (*red boxes*). **(B)** Successful gene ablation and loss of PANX1 protein expression is demonstrated by representative Western blot and immunofluorescence. **(C)** Immunofluorescence images were acquired using consistent parameters and are representative of more than 5 replicate experiments. PANX1 (merged overlay; *green*); Nuclei (Hoechst, merged overlay; *blue*); Actin (Phalloidin, merged overlay; *grey*). Scale bar = 50 μm.

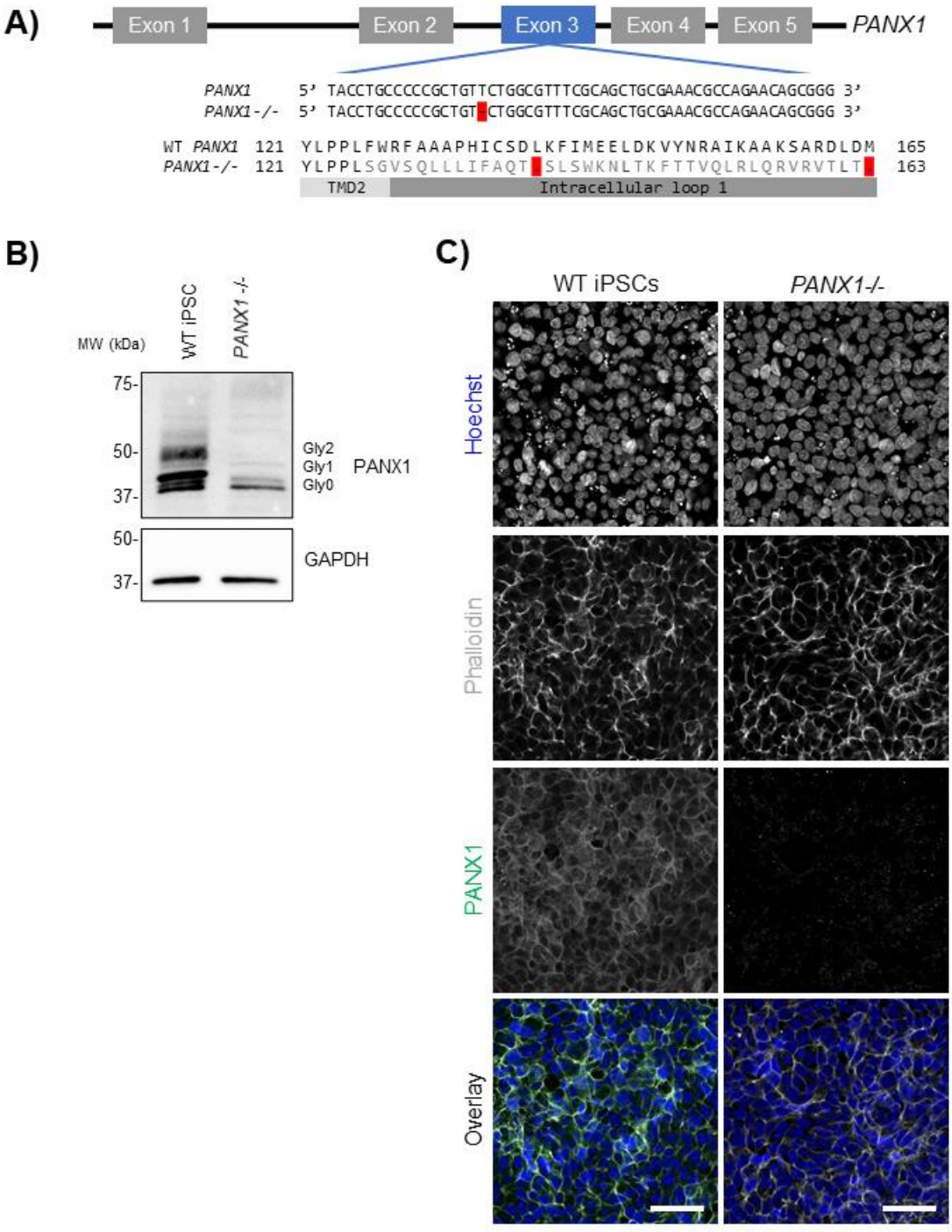
A)
Exon 1
Exon 2
Exon 3
Exon 4
Exon 5
PANX1
PANX1 5' TACCTGCCCCCGCTGTTCTGGCGTTTCGCAGCTGCGAAACGCCAGAACAGCGGG 3'
PANX1-/- 5' TACCTGCCCCCGCTGTCTGGCGTTTCGCAGCTGCGAAACGCCAGAACAGCGGG 3'
WT PANX1 121 YLPPLFWRFAAAPHICSDLKFIMEELDKVYNRAIKAAKSARDLDM 165
PANX1-/- 121 YLPPLSGVSQLLLIFAQTSLSWKNLTKFTTVQLRLQRVRVTLT 163
TMD2
Intracellular loop 1
B)
MW (kDa)
WT iPSC
PANX1 -/-
75-
50-
37-
Gly2
Gly1
Gly0
PANX1
50-
37-
GAPDH
C)
WT iPSCs
PANX1-/-
Hoechst
Phalloidin
PANX1
Overlay

3.11 PANX1 is not required for iPSCs Germ Lineage Commitment

Elevated expression of PANX1 in human oocytes and embryos suggests a potential role of this protein during embryogenesis (Esseltine & Laird, 2016; Hainz et al., 2018; Shao et al., 2016). To determine whether loss of PANX1 impacted directed germ lineage differentiation, control and *PANX1-/-* iPSCs were differentiated into the three embryonic germ lineages (STEMdiff™ Trilineage Differentiation kit, STEMCELL Technologies). Western blot densitometric analysis showed similar ectoderm (PAX6), mesoderm (Brachyury) and endoderm (SOX17) expression between control and *PANX1-/-* iPSCs, indicating equal efficiency of germ lineage production in the absence of PANX1 protein (Figure 3.10). Directed differentiation to the three germ layers is therefore not reliant on PANX1 expression.

Figure 3.10 – *PANX1*-/- iPSCs Trilineage Differentiation. Representative Western blots and densitometric analysis of WT and *PANX1*-/- iPSCs differentiated into **(A)** ectoderm, **(B)** mesoderm and **(C)** endoderm. Data represent the standard error of the mean of three independent experiments. ns, no significance.

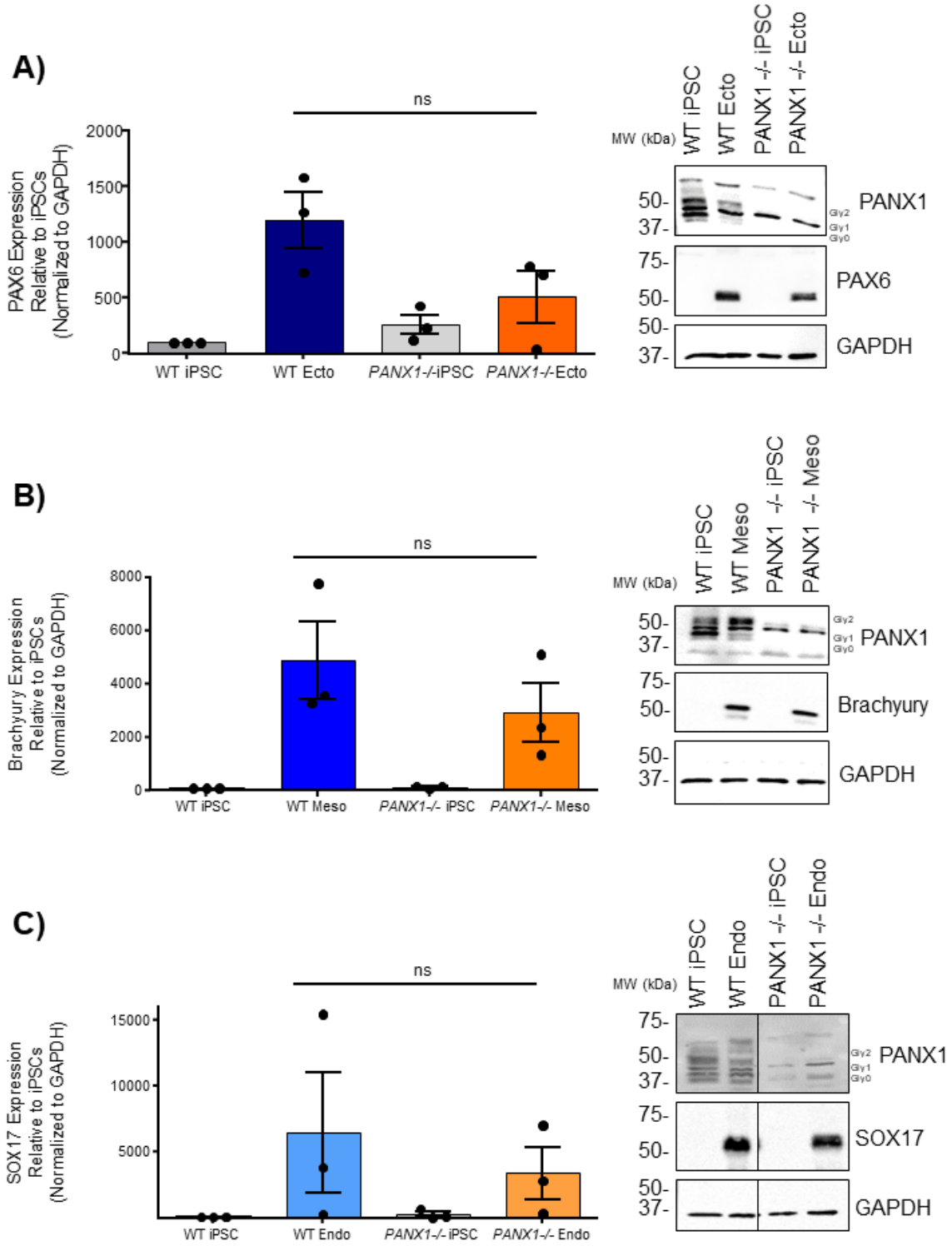
A)
ns
PAX6 Expression Relative to iPSCs (Normalized to GAPDH)
2000
1500
1000
500
0
WT iPSC
WT Ecto
PANX1-/-iPSC
PANX1-/-Ecto
MW (kDa)
WT iPSC
WT Ecto
PANX1 -/- iPSC
PANX1 -/- Ecto
50-
37-
PANX1
Gly2
Gly1
Gly0
75-
50-
PAX6
50-
37-
GAPDH
B)
ns
Brachyury Expression Relative to iPSCs (Normalized to GAPDH)
8000
6000
4000
2000
0
WT iPSC
WT Meso
PANX1-/- iPSC
PANX1-/- Meso
MW (kDa)
WT iPSC
WT Meso
PANX1 -/- iPSC
PANX1 -/- Meso
50-
37-
PANX1
Gly2
Gly1
Gly0
75-
50-
Brachyury
50-
37-
GAPDH
C)
ns
SOX17 Expression Relative to iPSCs (Normalized to GAPDH)
15000
10000
5000
WT iPSC
WT Endo
PANX1-/- iPSC
PANX1-/- Endo
MW (kDa)
WT iPSC
WT Endo
PANX1 -/- iPSC
PANX1 -/- Endo
75-
50-
37-
PANX1
Gly2
Gly1
Gly0
75-
50-
SOX17
50-
37-
GAPDH

4 Discussion:

In this study, I examined the gene expression profile of 11 connexin isoforms as well as pannexin1 in wild-type human iPSCs and, after directed differentiation into cells of the three embryonic germ layers. I found that several connexins are dynamically expressed across the different germ lineages and ultimately focused my studies on Cx43, Cx32 and PANX1. CRISPR-Cas9 gene ablation was used to uncover how the loss of cell-cell communication through Cx43 or PANX1 impacted iPSC lineage commitment.

4.1 Cell-cell communication in human pluripotent stem cells.

Uniquely, connexin proteins form gap junctions at the interface between two cells facilitating direct passage of small molecules important for cell fate decisions. Previous work in human iPSCs revealed gene expression of Cx25, Cx26, Cx30, Cx30.2, Cx30.3, Cx31, Cx31.1, Cx31.9, Cx32, Cx36, Cx37, Cx40, Cx43, Cx45, Cx46, Cx47, Cx59, Cx62 (summarized in Figure 4.1; (Ke et al., 2013; Oyamada et al., 2013). On the other hand, only Cx40, Cx43, and Cx45 have been identified at the protein level in human ESCs (Huettner et al., 2006). My RT-qPCR screen revealed expression of Cx26, Cx30.3, Cx31, Cx31.1, Cx32, Cx36, Cx37, Cx40, Cx43, Cx45 Cx62 in wild type human iPSCs (Figure 3.1). Similar to previous reports, I find that Cx43 is by far the highest expressed connexin isoform in undifferentiated iPSCs and can be readily detected at the protein level in cells from all three germ lineages (Peng et al., 2019; Yang et al., 2019). However, given the connexin expression profile revealed by ourselves and others, it remains possible that

several different connexin isoforms work together to coordinate cell-cell communication in human iPSCs.

Several reports dispute the role of connexins in the establishment, survival, and maintenance of human PSCs (Esseltine et al., 2020; Esseltine et al., 2017; Ke et al., 2013; Ke et al., 2017; Oyamada et al., 2013; Peng et al., 2019; Sharovskaya et al., 2012; Wong et al., 2006). For example, dye transfer assays demonstrate reestablishment of GJIC during iPSC reprogramming (Sharovskaya et al., 2012), and siRNA knockdown of either Cx43 or Cx45 has been shown to negatively impact iPSC reprogramming efficiency (Esseltine et al., 2017; Ke et al., 2013; Ke et al., 2017). While broad-spectrum GJIC pharmacological inhibition kills human iPSCs, it appears as though this occurs independently from Cx43 as the Cx43-/- iPSCs survive well in culture (Figure 3.3; (Esseltine et al., 2020). Comprehensive evaluation of the contribution of different connexin isoforms to human PSC survival and potency will help to resolve these discrepancies.

Figure 4.1 - Connexin expression profile described in literature. iPSCs reprogrammed from dermal fibroblasts express transcripts for Cx25, Cx26, Cx30, Cx30.2, Cx30.3, Cx31, Cx31.1, Cx31.9, Cx37, Cx40, Cx45, Cx46, Cx47, Cx59, and Cx62 (Ke et al., 2013; Oyamada et al., 2013). Meanwhile, connexins 26, 32, 40, 43 have been reported in endoderm (Beyer et al., 2012; Peng et al., 2019; Qin et al., 2016; Saund et al., 2012; Yang et al., 2019). Connexins 36, 42, 43, and 45 are present in mesoderm cell populations (Berthoud et al., 2004; Wörsdörfer et al., 2017). Finally, available literature shows expression of connexins 26, 32, and 43 in ectoderm (Dicke et al., 2011; Raymond et al., 2014). This study suggests stable mRNA expression of Cx26, Cx30.3, Cx31.1, Cx36, Cx37, Cx43 and Cx62 iPSCs and after differentiation into all three germ lineages. Significant increases in prospective mRNA transcripts products for Cx62 were viewed in ectoderm, Cx45 in mesoderm, and Cx31, Cx32, and Cx40 in endoderm.

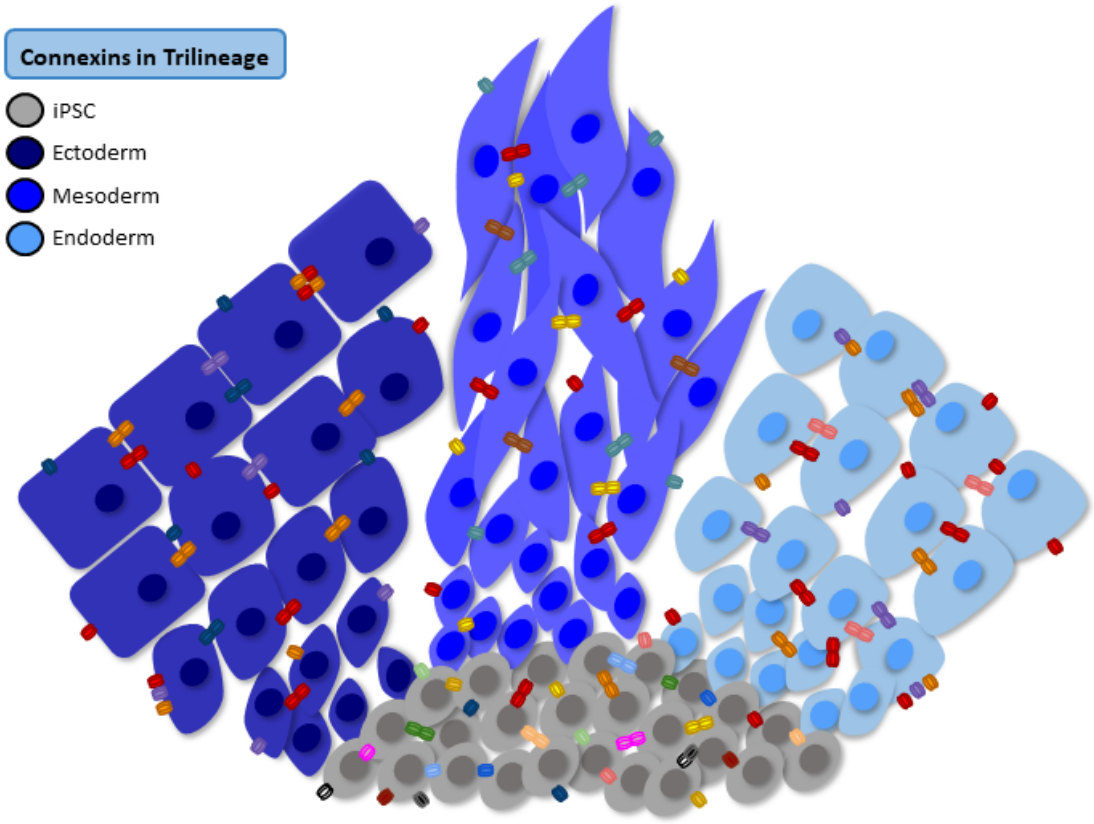

Connexin	Reference	Connexin	Reference
Cx25	(Ke et al., 2013; Oyamada et al., 2013)	Cx37	(Ke et al., 2013; Oyamada et al., 2013)
Cx26	(Beyer et al., 2012; Dicke et al., 2011; Fukanaga et al., 2016; Oyamada et al., 2013; Qin et al., 2016)	Cx40	(Oyamada et al., 2013; Saund et al., 2012)
Cx30	(Fukanaga et al., 2016; Oyamada et al., 2013)	Cx42	(Berthoud et al., 2004;)
Cx30.2	(Ke et al., 2013; Oyamada et al., 2013)	Cx43	(Yang et al., 2019; Berthoud et al., 2004; Ke et al., 2013; Laird et al., 1992; Oyamada et al., 2013; Peng et al., 2019; Qin et al., 2016; Raymond et al., 2014; Saund et al., 2012; Wörsdörfer et al., 2016)
Cx30.3	(Ke et al., 2013; Oyamada et al., 2013)	Cx45	(Berthoud et al., 2004; Ke et al., 2013; Oyamada et al., 2013; Wörsdörfer et al., 2016)
Cx31	(Ke et al., 2013; Oyamada et al., 2013)	Cx46	(Ke et al., 2013; Oyamada et al., 2013)
Cx31.1	(Ke et al., 2013; Oyamada et al., 2013)	Cx47	(Ke et al., 2013; Oyamada et al., 2013)
Cx31.9	(Ke et al., 2013; Oyamada et al., 2013)	Cx59	(Ke et al., 2013; Oyamada et al., 2013)
Cx32	(Beyer et al., 2012; Dicke et al., 2011; Laird et al., 1992; Qin et al., 2016)	Cx62	(Ke et al., 2013; Oyamada et al., 2013)
Cx36	(Berthoud et al., 2004)		

4.2 The connexin mRNA profile of human iPSC derived germ lineages

Several connexin isoforms have been implicated in stem cell lineage commitment. The following section will discuss the connexins implicated in each individual germ lineage.

4.2.1 Connexins in ectoderm

The ectoderm is the germ layer responsible for forming the epidermis, brain, spinal cord, retina, inner ear, and peripheral nerves (Anthwal & Thompson, 2016; Gilbert, 2000b; Graw, 2010). My results suggest Cx26, Cx30.3, Cx31, Cx31.1, Cx32, Cx36, Cx37, Cx40, Cx43, Cx45, and Cx62 expression in human iPSC-derived ectoderm cells. My results are consistent with previous reports that Cx26, Cx30, Cx30.3, Cx31, Cx31.1, Cx37, Cx43, Cx45 are all expressed in the various regions of the human epidermis (Di et al., 2005; Di et al., 2001; Lucke et al., 1999; Salomon et al., 1994; Scott et al., 2012; Wiszniewski et al., 2000). Cx26 and Cx32 have been found in mouse embryonic ectoderm, and Cx43 protein expression has been documented in mouse ESC-derived ectoderm (Dicke et al., 2011; Parekkadan et al., 2008; Peng et al., 2019). Furthermore, Cx43-/- mouse ESCs show defective lineage specification causing aberrant neuroectoderm formation (Parekkadan et al., 2008). My analysis suggests the upregulation of Cx45 and Cx62 mRNA transcripts post-ectoderm specification, which has not yet been described.

Defective GJIC underlies several ectodermal disorders, including congenital deafness, several skin disorders, neuropathies and others. Cx26 and Cx30 are essential for cochlear function and cell survival, as evidenced by the high incidence of Cx26/30 mutations observed in human congenital deafness (Cohen-Salmon et al., 2002; Laird et al.,

2017). Several skin disorders, including Erythrokeratodermia variabilis et progressiva, are linked to mutations in Cx26, Cx30, Cx30.3, Cx31 and Cx43 (Berger et al., 2014; Fuchs-Telem et al., 2011; Kokotas et al., 2012; Scott et al., 2012; Teubner et al., 2003). Mutation and improper establishment of Cx31 have been linked to the development of peripheral neuropathies and deafness (Au et al., 2020; López-Bigas et al., 2001). Meanwhile, mutation of the *GJB1* Cx32 encoding gene triggers the X-linked form of a debilitating demyelinating peripheral neuropathy (Bruzzone et al., 1994; Fairweather et al., 1994; Nelles et al., 1996). Cx36 is documented to regulate neuronal differentiation from neural progenitor cells (Hartfield et al., 2011). Furthermore, mRNA transcripts for Cx62 have been identified in human and mouse retinal tissue (Söhl et al., 2010). My results suggest significant upregulation of Cx62 (*GJA10*) post-ectoderm specification. Aside from being expressed in the human retina, platelet cells, skeletal muscle, and the heart, little is known about Cx62 (or its mouse ortholog Cx57) or its link to human disease (Sahli et al., 2021; Söhl et al., 2010; Söhl et al., 2003). Thus, additional work is needed to characterize Cx62's role in ectoderm differentiation and potential downstream cell types. Investigation of Cx45 expression during embryonal and early fetal stages shows consistent expression throughout the spinal cord and developing ganglia (Jurić et al., 2020). Conditional knockout of Cx45 restricted neural precursor cell proliferation in mice making this isoform a key determinant of murine neural development (Khodosevich et al., 2012). The early expression of Cx45 in the human embryonic brain and the results presented in this thesis provide a strong foundation for further study of Cx45 during ectoderm differentiation.

4.2.2 Connexins in mesoderm

Mesoderm is responsible for muscle, blood progenitors, bone, cartilage and adipose tissue (Gilbert S, 2000; Prummel et al., 2020). The connexin profile in mesoderm is suggested to include Cx36, Cx42, Cx43, and Cx45 (Berthoud et al., 2004; Krüger et al., 2000; Peng et al., 2019; Wörsdörfer et al., 2017). My results suggest that human iPSC-derived mesoderm expresses Cx26, Cx30.3, Cx31, Cx31.1, Cx32, Cx36, Cx37, Cx40, Cx43, Cx45, and Cx62.

Cx43 shRNA knockdown in spontaneously differentiated human ESCs results in under-representation of mesoderm populations, suggesting a role for Cx43 in mesoderm specification (Peng et al., 2019). Similarly, embryoid bodies generated with Cx43/Cx45 deficient mouse ESCs fail to spontaneously differentiate into mesoderm and endoderm. Interestingly, the formation of endoderm and mesoderm can be rescued through singular overexpression of Cx43 or Cx45, indicating that Cx43 and Cx45 might compensate for one another during lineage specification (Wörsdörfer et al., 2017). The results within this thesis revealed a significant increase in protein abundance of Cx43 in iPSC-derived mesoderm cells along with the upregulation of mRNA transcript for Cx45 in mesoderm. Continued work on *GJA1-/-* iPSC will identify possible compensation by Cx45 or other connexin isoforms in Cx43-knockout mesoderm cells.

Connexins display differential expression across the various chambers of the human heart. To date, the human heart has been found to express Cx37, Cx40, Cx43, and Cx45 (van der Velden & Jongsma, 2002; van Veen et al., 2001; Vozzi et al., 1999). Cx43 knockout mice die postnatally as a result of atrial malformations (Liao et al., 2001). Cx40,

Cx43 and Cx45 were considered as potential mesoderm targets as these connexins are expressed throughout the cell types of the heart and mutations which compromise the function of these isoforms can result in arrhythmias and other heart malfunctions (Desplantez, 2017). GJIC has been heavily implicated in cardiac development. The results in this study agree with literature reports that Cx45 is important for mesoderm development. Furthermore, a broad description of Cx's in mesoderm specification could help identify targets for future work.

4.2.3 Connexins in endoderm

Resident cells of the endoderm develop into the liver, gallbladder, pancreas, parts of the respiratory system, small intestine, colon, and stomach (Gilbert, 2000a). Previous reports have identified Cx26, Cx32, Cx40 and Cx43 expression in endodermal-derived tissues and cells (Beyer et al., 2012; Peng et al., 2019; Saund et al., 2012; Yang et al., 2019). These results suggest that Cx30.3, Cx31, Cx32, Cx36, Cx37 and Cx40 are upregulated after iPSC differentiation into endoderm cells. Although several of these isoforms are known to be implicated in later-stage endoderm development, this is the first report of Cx30.3, Cx31, Cx36, Cx37 and Cx40 upregulation post human iPSC definitive endoderm specification.

Cx30.3 was previously described in human pancreatic islet cells (Serre-Beinier et al., 2009), and Cx30.3 overexpression in islet cells inhibits proliferation, enhances apoptosis and lowers insulin secretion heightening the risk of developing type II diabetes (Gässler et al., 2020). Similarly, Cx36 has been identified in late-stage endoderm cell types, including β-cells of the pancreas, where it participates in maintenance of insulin secretion

(Bosco et al., 2011). Therefore, early upregulation of Cx36 may act as a preventative effect against endodermal disorders.

Cx40 has been identified in the mouse and rat liver as well as the rat colon. Meanwhile, Cx31 and Cx37 are found in the small intestine, Cx31 in the colon and Cx37 in the liver (Maes et al., 2015). In contrast to the harmful effects caused by nonfunctional Cx31 proteins in humans, *GJB3-/-* mice fail to exhibit developmental deficiencies (Plum et al., 2001). Further work is necessary to elucidate the role and interactions of Cx31 in early endoderm development.

Cx32 has a well-documented role in late-stage endodermal differentiation. Cx32 protein expression has been identified in endoderm-derived tissues including the kidney, colon, and gallbladder (Wilgenbus et al., 1992). Pharmacological inhibition of Cx32 decreased human ESC differentiation toward hepatocytes (Qin et al., 2016). My RT-qPCR analysis described transcripts encoding Cx32 at comparative levels in iPSC, ectoderm, and mesoderm; however, Cx32 mRNA transcripts significantly increase in endoderm populations (Figure 3.1). Unlike Cx43, I found that a large proportion of Cx32 existed within intracellular pools with partial cell surface expression indicated by the presence of fewer small gap junction plaques at the cell surface. This intracellular localization pattern is similar what we find for Cx32-GFP overexpression in human AD293 cells (unpublished work from Mark Hemmings). However, my findings are in contrast to reports in other cell types where Cx32 was found to localize to gap junction plaques at the cell surface (Kojima et al., 2001; Nagy et al., 2003). Future studies will reveal the specific subcellular

compartments occupied by Cx32 in iPSCs and iPSC-derived germ cells, as well as the function of intracellular Cx32 in lineage specification.

I find that Cx43 is comparably expressed in iPSC, endoderm and ectoderm cells (Figures 3.1, 3.2, 3.4). This is in contrast to studies in which Cx43 is upregulated during directed human ESC endoderm differentiation (Peng et al., 2019). Indeed, the role of Cx43 in endoderm formation includes several contrasting reports. Peng et al. 2019 demonstrated that shRNA knockdown of Cx43 has no impact on endoderm formation denoted by typical expression of endoderm markers SOX17, FOXA2, and CXCR4 (Peng et al., 2019). On the other hand, a secondary study demonstrates that siRNA-mediated knockdown impedes definitive endoderm formation from human ESCs. Using CRISPR-Cas9 gene ablation (Yang et al., 2019). I find that Cx43 knockout iPSCs readily differentiate into all three germ lineages, including endoderm. It can therefore be said that Cx43 is dispensable during iPSC restriction to ectoderm, mesoderm, or endoderm. The discrepancies between this study and the previously published reports may be the result of siRNA versus CRISPR-Cas9 gene ablation. CRISPR Cas9 improves upon the previous siRNA knockdown model system as the chances of residual Cx43 expression altering results is minimized. However, up-regulation of other connexins may occur in order to compensate for the loss of Cx43. For example, Cx45 has been shown to compensate for Cx43 downregulation (Peng et al., 2019). Future studies will determine whether the expression of any other connexins are altered in the Cx43 CRISPR-ablated iPSCs.

4.3 Pannexin1 in human stem cells and cell fate decisions

Pannexin channels mediate purinergic paracrine signalling by releasing small molecules to the extracellular environment. PANX1 is best known for mediating the release of ATP in response to mechanical stress, membrane depolarization, or changes in intracellular ion concentration (Penuela et al., 2013). Despite its well-documented role in terminal cell types and adult tissues, much less is known about the mechanisms by which PANX1 impacts embryonic development, stem cell populations or cell fate specification.

Much of what is known regarding PANX1 in stem cell fate decisions arises from work with somatic stem cells. Studies have suggested a role for pannexins in somatic stem cell maintenance and self-renewal. For example, PANX1 channels release ATP in neural precursor cells, activating P2 receptors and positively regulating progenitor cell proliferation (Wicki-Stordeur et al., 2012). PANX1 knockout mice show reduced neural precursor cells within the ventricular zone (Wicki-Stordeur et al., 2016). Meanwhile, pannexin-mediated ATP release from mesenchymal stem cells reportedly activates transcription factors involved in differentiation. For example, PANX1 knockout mice exhibit reduced adipose-derived stromal cell proliferation and increased adipogenic differentiation (Lee et al., 2018). On the other hand, functional PANX3 inhibits osteoprogenitor cell proliferation through inactivation of β-catenin while promoting osteoblast and chondrocyte differentiation through regulated calcium release (Ishikawa et al., 2014; Ishikawa & Yamada, 2017; Iwamoto et al., 2010). These studies suggest that pannexins play important and dynamic roles in the maintenance and differentiation across different somatic stem cell populations. Other members of our research group have found

that *PANX1-/-* iPSCs survive in culture with comparable morphology, proliferation and apoptosis rates to control iPSCs, indicating PANX1 is inessential to iPSC maintenance (Noort et al., 2021). Differences in these results could indicate PANX1 becomes increasingly crucial during late-stage differentiation.

4.4 Pannexin1 is alternatively glycosylated and localized in iPSC-derived germ lineages

PANX1 is expressed in the human oocyte as well as the 2- and 4-cell stage human embryo and its mutation has been linked to infertility and oocyte death (Sang et al., 2019; Shao et al., 2016)). *PANX1* transcripts have recently been identified in human PSCs (Hainz et al., 2018). I therefore, questioned the influence of PANX1 on early cell fate decisions and maintenance of pluripotency. Here I confirm that iPSCs express PANX1 protein at the cell surface (Figure 3.8). I find that PANX1 expression was comparable in iPSCs and throughout endoderm, ectoderm, or mesoderm specification. Cell surface expression of PANX1 was maintained in ectoderm and mesoderm, while endoderm specification internalized PANX1 (Figure 3.8). Similarly, PANX1 is primarily intracellular in primary osteoblasts (Penuela et al., 2008), and intestinal endothelial cells retain a partial intracellular pool in addition to cell surface PANX1 expression (Diezmos et al., 2013b). Intracellular PANX1 may or may not continue to signal from intracellular compartments; some studies suggest that ER-retained PANX1 acts as a calcium leak channel, increasing intracellular movement of Ca^{2+} ions (Vanden Abeele et al., 2006). It remains to be determined by which mechanism PANX1 is internalized in iPSC-derived endoderm cells or if the PANX1 intracellular pool plays a function in endoderm development.

Glycosylation has been suggested to control PANX1 trafficking (Gehi et al., 2011). Indeed, these results suggest that PANX1 internalization in endoderm was matched by decreases in PANX1 Gly1 and Gly2 states. The addition of a glycosylation-deficient PANX1 mutant, or the use of de-glycosylating enzymes including Peptide -N-Glycosidase F, would enable us to determine whether glycosylation is, in fact, the driver of pannexin localization in differentiated endoderm cells. Similarly, continued work would ascertain the exact subcellular localization of PANX1 to elucidate the process of PANX1 redistribution and potentially determine the function of intracellular PANX1.

4.5 PANX1 is not essential for iPSC directed differentiation into the germ lineages

The human protein atlas describes the wide profile of PANX1 expression developmentally relevant tissues that develop from all three germ lineages. Here I report for the first time the generation of a *PANX1-/-* human iPSCs generated using CRISPR-Cas9 systems. Genotyping, immunofluorescence, and Western blot validated loss of this protein in the clonal knockout. Despite confidence in the knockout, additional Western blot bands occasionally appear in the *PANX1-/-* samples when longer exposure times were necessary to resolve PANX1 protein. This typically coincided with less total protein loaded in the gel or longer exposure times necessary to identify PANX1 expression in wild-type cells. However, these additional bands were consistent across multiple samples and therefore considered non-specific. Directed differentiation of *PANX1-/-* iPSCs resulted in the successful formation of all three germ lineages, suggesting that PANX1 is not essential to iPSC differentiation toward the three embryonic germ lineages. However, our recently published article did uncover *PANX1-/-* lineage bias in an embryoid body model of

spontaneous, cell-guided differentiation (Noort et al., 2021). By day 5 of differentiation, *PANX1-/-* EBs become enriched for lineage-specific transcripts, mesendoderm (*MIXL1*), mesoderm (*T, PDGFRA, NCAM1*), and endoderm (*SOX17, HNF1ß*). It remains to be determined if this bias results from decreased ectoderm commitment or variations in cell death or proliferation. Despite evident lineage bias under passive conditions, both Western blot and RT-qPCR confirmed the formation of all three germ lineages in *PANX1-/-* EBs. Exposure to exogenous pressures during directed differentiation supersedes loss of PANX1, indicating that while influential, PANX1 is inessential to germ layer formation Further discussion of these results can be viewed in (Noort et al., 2021).

4.6 Study limitations

Our study took advantage of robust commercially available kits alongside CRISPR-Cas9 gene-editing systems in investigating the role of GJIC during lineage specification. The 2D monolayer culture system utilized in this project may be limited in its representation of lineage specification, as 2D cultures lack many of the spatial and patterning cues present in the developing embryo. Powerful morphogens and exogenous pressures present in directed differentiation might overcome the minor changes in lineage bias that results from *PANX1* or *GJA1* gene ablation. Although my study currently employs 2D spontaneous differentiation, this study would benefit from the addition of passively differentiated 3D embryoid body cultures. The inclusion of 3D cultures like embryoid bodies would allow the investigation of influential signals absent in 2D systems.

Connexins often dynamically regulate their expression and can compensate for the loss of a similar isoform. RT-qPCR analysis of the above discussed Cx isoforms in

CRISPR-Cas9 *GJA1-/-* iPSCs, ectoderm, mesoderm, and endoderm will identify possible compensatory mechanisms in the absence of Cx43. Despite these limitations, my study suggests a baseline of connexin and pannexin expression at a crucial time point in improving future experimental design to investigate potential regulators of germ layer segregation and aberrant mechanisms preceding onset of developmental disease.

4.7 Conclusions

The present study suggests that iPSC-derived germ lineages express a multitude of different connexins. This is the first broad characterization of connexin transcripts in human PSC-derived germ lineage specification. Significant changes in transcript levels point towards a potential role for select connexins in ectoderm, mesoderm, or endoderm specification.

In iPSCs and the three germ layers, Cx43 protein localized to the cell surface, forming large gap junction plaques (Figure 4.2). Despite continued expression throughout differentiation, I find that Cx43 is dispensible to directed germ layer formation. This is in direct contrast to previous reports suggesting Cx43 regulates endoderm or mesoderm differentiation. On the other hand my results suggest that Cx32 was primarily localized intracellularly in each cell type examined. Finally the results presented in this thesis suggest that PANX1 is expressed at the cell surface in iPSCs, mesoderm and ectoderm cells, while endoderm specification results in the redistribution or retention of PANX1 to intracellular compartments. CRISPR-Cas9 *PANX1-/-* iPSCs retain typical morphological characteristics and successfully produce all three germ lineages under directed differentiation. This data

suggests that PANX1 is unnecessary in the maintenance and pluripotency of iPSCs. Furthermore, that lineage specification is not reliant on PANX1.

Figure 4.2 – Expression and localization of connexin and pannexin proteins in iPSCs and the three germ layers. Intercellular communication proteins; Cx32, Cx43, and PANX1 are expressed in iPSCs, endoderm, mesoderm, and ectoderm cells. Cx43 was localized to gap junction plaques at the interface of adjacent cells, while Cx32 remained primarily intracellular. PANX1 was localized to the cell surface in iPSCs, ectoderm and mesoderm while being redistributed to intracellular compartments in endoderm cells. This figure was generated using *BioRender.com*

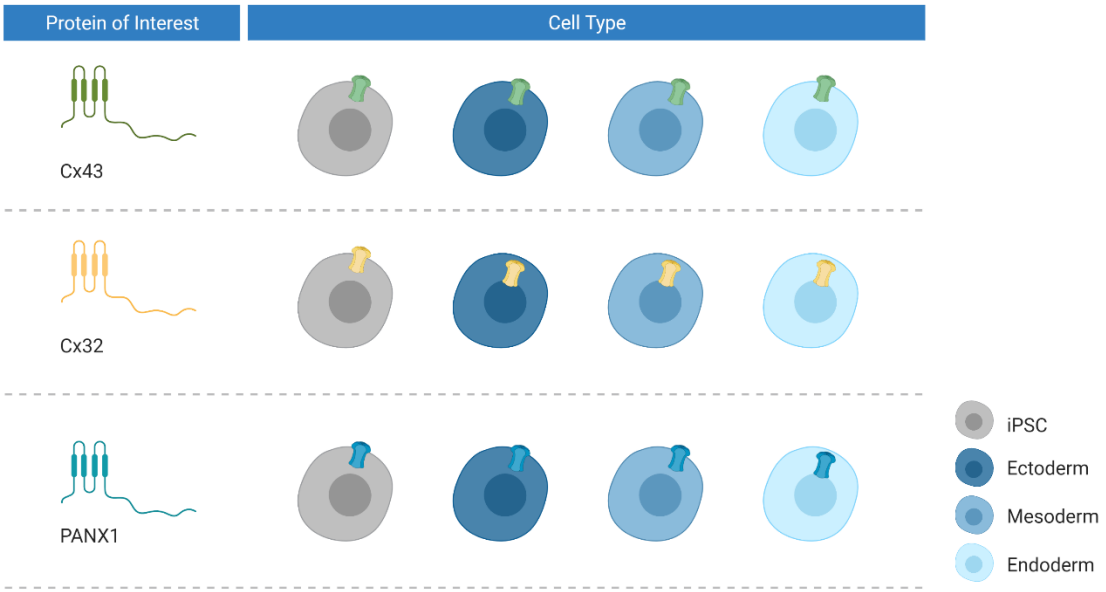
Protein of Interest
Cell Type
Cx43
Cx32
PANX1
iPSC
Ectoderm
Mesoderm
Endoderm

4.8 Perspectives and future directions

Here I report for the first time the expression and localization of several key mediators of cell-cell communication during human iPSC germ lineage commitment. The characterization of Cx expression in human iPSCs helps to validate previous reports and gives insight into possible dynamic changes that control cell fate specification. Herein, I use CRISPR-Cas9 to generate and characterize knockout iPSCs, paving the way for more thorough future investigations into the method by which these proteins influence human stem cell differentiation. As mutant mouse models frequently fail to recapitulate human disease, studies such as this could provide novel insights into the fundamental role of cell-cell communication during human development and disease progression.

Cx43 has been well studied. However, there remains much to learn about Cx32 and PANX1. Given that each of these proteins is associated with human disease, understanding by which means they work at the cellular level will provide necessary insight into disease pathology. PANX1 is widely reported to play an essential role in mouse brains, and dysfunctional PANX1 is implicated in neurodegeneration, seizures, stroke and other brain disorders. Therefore, it would be interesting to determine whether *PANX1-/-* iPSCs can successfully differentiate into neuronal cell types or whether human PANX1 germline mutations alter the function of human PSC-derived neurons. Additional work is needed to identify the subcellular compartment that houses Cx32 in the endoderm, as this could uncover a novel role of intracellular Cx hemichannels. Generation of specific antibodies or CRISPR-Cas9 GFP lines like that used in this thesis would open further avenues for investigation of protein localization and expression levels in the three germ layers.

In summary, these studies provide a strong foundation for research investigating the consequences of cell-cell communication in human stem cell fate decisions and leverage several novel technologies to study the impact of CRISPR-Cas9 genetic engineering on these processes. Future work investigating terminal cell types, engineered tissues or 3-dimensional organoid cultures will reveal the dynamic interplay between cell-cell communication in human cell fate specification, tissue architecture and function.

5 References

Ambrosetti, D. C., Basilico, C., & Dailey, L. (1997). Synergistic activation of the fibroblast growth factor 4 enhancer by Sox2 and Oct-3 depends on protein-protein interactions facilitated by a specific spatial arrangement of factor binding sites. *Mol Cell Biol*, *17*(11), 6321-6329. https://doi.org/10.1128/mcb.17.11.6321

Anthwal, N., & Thompson, H. (2016). The development of the mammalian outer and middle ear. *J Anat*, *228*(2), 217-232. https://doi.org/10.1111/joa.12344

Anzini, P., Neuberg, D. H., Schachner, M., Nelles, E., Willecke, K., Zielasek, J., . . . Martini, R. (1997). Structural abnormalities and deficient maintenance of peripheral nerve myelin in mice lacking the gap junction protein connexin 32. *J Neurosci*, *17*(12), 4545-4551. https://doi.org/https://doi.org/10.1523/jneurosci.17-12-04545.1997

Aquilino, M. S., Whyte-Fagundes, P., Zoidl, G., & Carlen, P. L. (2019). Pannexin-1 channels in epilepsy. *Neurosci Lett*, *695*, 71-75. https://doi.org/10.1016/j.neulet.2017.09.004

Au, A., Shao, Q., White, K. K., Lucaciu, S. A., Esseltine, J. L., Barr, K., & Laird, D. W. (2020). Comparative Analysis of Cx31 and Cx43 in Differentiation-Competent Rodent Keratinocytes. *Biomolecules*, *10*(10). https://doi.org/10.3390/biom10101443

Bai, D., Yue, B., & Aoyama, H. (2018). Crucial motifs and residues in the extracellular loops influence the formation and specificity of connexin docking. *Biochim Biophys Acta Biomembr*, *1860*(1), 9-21. https://doi.org/10.1016/j.bbamem.2017.07.003

Becker, D. L., Leclerc-David, C., & Warner, A. (1992). The relationship of gap junctions and compaction in the preimplantation mouse embryo. *Dev Suppl*, 113-118. https://doi.org/https://doi.org/10.1242/dev.116.Supplement.113

Berger, A. C., Kelly, J. J., Lajoie, P., Shao, Q., & Laird, D. W. (2014). Mutations in Cx30 that are linked to skin disease and non-syndromic hearing loss exhibit several distinct cellular pathologies. *J Cell Sci*, *127*(Pt 8), 1751-1764. https://doi.org/10.1242/jcs.138230

Berthoud, V. M., Singh, R., Minogue, P. J., Ragsdale, C. W., & Beyer, E. C. (2004). Highly restricted pattern of connexin36 expression in chick somite development. *Anat Embryol (Berl)*, *209*(1), 11-18. https://doi.org/10.1007/s00429-004-0416-z

Beyer, T., Thumberger, T., Schweickert, A., & Blum, M. (2012). Connexin26-mediated transfer of laterality cues in Xenopus. *Biol Open*, *1*(5), 473-481. https://doi.org/10.1242/bio.2012760

Biehl, J. K., & Russell, B. (2009). Introduction to stem cell therapy. *J Cardiovasc Nurs*, *24*(2), 98-103; quiz 104-105. https://doi.org/10.1097/JCN.0b013e318197a6a5

Boassa, D., Ambrosi, C., Qiu, F., Dahl, G., Gaietta, G., & Sosinsky, G. (2007). Pannexin1 channels contain a glycosylation site that targets the hexamer to the plasma membrane. *J Biol Chem*, *282*(43), 31733-31743. https://doi.org/10.1074/jbc.M702422200

Boassa, D., Qiu, F., Dahl, G., & Sosinsky, G. (2008). Trafficking dynamics of glycosylated pannexin 1 proteins. *Cell Commun Adhes*, *15*(1), 119-132. https://doi.org/10.1080/15419060802013885

Bolte, S., & Cordelières, F. P. (2006). A guided tour into subcellular colocalization analysis in light microscopy. *J Microsc*, *224*(Pt 3), 213-232. https://doi.org/10.1111/j.1365-2818.2006.01706.x

Bosco, D., Haefliger, J. A., & Meda, P. (2011). Connexins: key mediators of endocrine function. *Physiol Rev*, *91*(4), 1393-1445. https://doi.org/10.1152/physrev.00027.2010

Boyce, A. K. J., Epp, A. L., Nagarajan, A., & Swayne, L. A. (2018). Transcriptional and post-translational regulation of pannexins. *Biochim Biophys Acta Biomembr*, *1860*(1), 72-82. https://doi.org/10.1016/j.bbamem.2017.03.004

Bratt-Leal, A. M., Carpenedo, R. L., & McDevitt, T. C. (2009). Engineering the embryoid body microenvironment to direct embryonic stem cell differentiation. *Biotechnol Prog*, *25*(1), 43-51. https://doi.org/10.1002/btpr.139

Bruzzone, R., White, T. W., Scherer, S. S., Fischbeck, K. H., & Paul, D. L. (1994). Null mutations of connexin32 in patients with X-linked Charcot-Marie-Tooth disease. *Neuron*, *13*(5), 1253-1260. https://doi.org/10.1016/0896-6273(94)90063-9

Buganim, Y., Faddah, D. A., & Jaenisch, R. (2013). Mechanisms and models of somatic cell reprogramming. *Nat Rev Genet*, *14*(6), 427-439. https://doi.org/10.1038/nrg3473

Chan, C. J., Heisenberg, C. P., & Hiiragi, T. (2017). Coordination of Morphogenesis and Cell-Fate Specification in Development. *Curr Biol*, *27*(18), R1024-R1035. https://doi.org/10.1016/j.cub.2017.07.010

Chappell, J., & Dalton, S. (2013). Roles for MYC in the establishment and maintenance of pluripotency. *Cold Spring Harb Perspect Med*, *3*(12), a014381. https://doi.org/10.1101/cshperspect.a014381

Chew, J. L., Loh, Y. H., Zhang, W., Chen, X., Tam, W. L., Yeap, L. S., . . . Ng, H. H. (2005). Reciprocal transcriptional regulation of Pou5f1 and Sox2 via the Oct4/Sox2 complex in embryonic stem cells. *Mol Cell Biol*, *25*(14), 6031-6046. https://doi.org/10.1128/MCB.25.14.6031-6046.2005

Chhabra, S., Liu, L., Goh, R., Kong, X., & Warmflash, A. (2019). Dissecting the dynamics of signaling events in the BMP, WNT, and NODAL cascade during self-organized fate patterning in human gastruloids. *PLoS Biol*, *17*(10), e3000498. https://doi.org/10.1371/journal.pbio.3000498

Claassen, D. A., Desler, M. M., & Rizzino, A. (2009). ROCK inhibition enhances the recovery and growth of cryopreserved human embryonic stem cells and human induced pluripotent stem cells. *Mol Reprod Dev*, *76*(8), 722-732. https://doi.org/10.1002/mrd.21021

Cohen-Salmon, M., Ott, T., Michel, V., Hardelin, J. P., Perfettini, I., Eybalin, M., . . . Petit, C. (2002). Targeted ablation of connexin26 in the inner ear epithelial gap junction network causes hearing impairment and cell death. *Curr Biol*, *12*(13), 1106-1111. https://doi.org/10.1016/s0960-9822(02)00904-1

Cooper, G. M. (2000). *The Cell: A Molecular Approach* (2nd edition ed.). Sinauer Associates.

Crespo Yanguas, S., Willebrords, J., Johnstone, S. R., Maes, M., Decrock, E., De Bock, M., . . . Vinken, M. (2017). Pannexin1 as mediator of inflammation and cell death.

Biochim Biophys Acta Mol Cell Res, *1864*(1), 51-61. https://doi.org/10.1016/j.bbamcr.2016.10.006

Czyż, J., Piwowarczyk, K., Paw, M., Luty, M., Wróbel, T., Catapano, J., . . . Ryszawy, D. (2017). Connexin-dependent intercellular stress signaling in tissue homeostasis and tumor development. *Acta Biochim Pol*, *64*(3), 377-389. https://doi.org/10.18388/abp.2017_1592

Dbouk, H. A., Mroue, R. M., El-Sabban, M. E., & Talhouk, R. S. (2009). Connexins: a myriad of functions extending beyond assembly of gap junction channels. *Cell Commun Signal*, *7*, 4. https://doi.org/10.1186/1478-811X-7-4

de Wert, G., & Mummery, C. (2003). Human embryonic stem cells: research, ethics and policy. *Hum Reprod*, *18*(4), 672-682. https://doi.org/10.1093/humrep/deg143

Desplantez, T. (2017). Cardiac Cx43, Cx40 and Cx45 co-assembling: involvement of connexins epitopes in formation of hemichannels and Gap junction channels. *BMC Cell Biol*, *18*(Suppl 1), 3. https://doi.org/10.1186/s12860-016-0118-4

Di, W. L., Gu, Y., Common, J. E., Aasen, T., O'Toole, E. A., Kelsell, D. P., & Zicha, D. (2005). Connexin interaction patterns in keratinocytes revealed morphologically and by FRET analysis. *J Cell Sci*, *118*(Pt 7), 1505-1514. https://doi.org/10.1242/jcs.01733

Di, W. L., Rugg, E. L., Leigh, I. M., & Kelsell, D. P. (2001). Multiple epidermal connexins are expressed in different keratinocyte subpopulations including connexin 31. *J Invest Dermatol*, *117*(4), 958-964. https://doi.org/10.1046/j.0022-202x.2001.01468.x

Dicke, N., Pielensticker, N., Degen, J., Hecker, J., Tress, O., Bald, T., . . . Willecke, K. (2011). Peripheral lymphangiogenesis in mice depends on ectodermal connexin-26 (Gjb2). *J Cell Sci*, *124*(Pt 16), 2806-2815. https://doi.org/10.1242/jcs.084186

Diezmos, E. F., Sandow, S. L., Markus, I., Shevy Perera, D., Lubowski, D. Z., King, D. W., . . . Liu, L. (2013a). Expression and localization of pannexin-1 hemichannels in human colon in health and disease. *Neurogastroenterol Motil*, *25*(6), e395-405. https://doi.org/10.1111/nmo.12130

Diezmos, E. F., Sandow, S. L., Markus, I., Shevy Perera, D., Lubowski, D. Z., King, D. W., . . . Liu, L. (2013b). Expression and localization of pannexin-1 hemichannels in human colon in health and disease. *J Neurogastroenterology & Motility v25*(6), 1350-1925.

D'Amour, K. A., Bang, A. G., Eliazer, S., Kelly, O. G., Agulnick, A. D., Smart, N. G., . . . Baetge, E. (2006). Production of pancreatic hormone–expressing endocrine cells from human embryonic stem cells. *Nature biotechnology*, *V24*(11). https://doi.org/https://doi.org/10.1038/nbt1259

Ek-Vitorin, J. F., King, T. J., Heyman, N. S., Lampe, P. D., & Burt, J. M. (2006). Selectivity of connexin 43 channels is regulated through protein kinase C-dependent phosphorylation. *Circ Res*, *98*(12), 1498-1505. https://doi.org/10.1161/01.RES.0000227572.45891.2c

Engert, S., Burtscher, I., Liao, W. P., Dulev, S., Schotta, G., & Lickert, H. (2013). Wnt/β-catenin signalling regulates Sox17 expression and is essential for organizer and endoderm formation in the mouse. *Development*, *140*, 3128-3138. https://doi.org/https://doi.org/10.1242/dev.088765

Esseltine, J. L., Brooks, C. R., Edwards, N. A., Subasri, M., Sampson, J., Séguin, C., . . . Laird, D. W. (2020). Dynamic regulation of connexins in stem cell pluripotency. *Stem Cells*, *38*(1), 52-66. https://doi.org/10.1002/stem.3092

Esseltine, J. L., & Laird, D. W. (2016). Next-Generation Connexin and Pannexin Cell Biology. *Trends Cell Biol*, *26*(12), 944-955. https://doi.org/10.1016/j.tcb.2016.06.003

Esseltine, J. L., Shao, Q., Brooks, C., Sampson, J., Betts, D. H., Séguin, C. A., & Laird, D. W. (2017). Connexin43 Mutant Patient-Derived Induced Pluripotent Stem Cells Exhibit Altered Differentiation Potential. *J Bone Miner Res*, *32*(6), 1368-1385. https://doi.org/10.1002/jbmr.3098

Evans, M. J., & Kaufman, M. H. (1981). Establishment in culture of pluripotential cells from mouse embryos. *Nature*, *292*(5819), 154-156. https://doi.org/10.1038/292154a0

Fairweather, N., Bell, C., Cochrane, S., Chelly, J., Wang, S., Mostacciuolo, M. L., . . . Haites, N. E. (1994). Mutations in the connexin 32 gene in X-linked dominant Charcot-Marie-Tooth disease (CMTX1). *Hum Mol Genet*, *3*(1), 29-34. https://doi.org/10.1093/hmg/3.1.29

Franco, R., Panayiotidis, M. I., & de la Paz, L. D. (2008). Autocrine signaling involved in cell volume regulation: the role of released transmitters and plasma membrane receptors. *J Cell Physiol*, *216*(1), 14-28. https://doi.org/10.1002/jcp.21406

Fuchs-Telem, D., Pessach, Y., Mevorah, B., Shirazi, I., Sarig, O., & Sprecher, E. (2011). Erythrokeratoderma variabilis caused by a recessive mutation in GJB3. *Clin Exp Dermatol*, *36*(4), 406-411. https://doi.org/10.1111/j.1365-2230.2010.03986.x

Gabriel, H. D., Jung, D., Bützler, C., Temme, A., Traub, O., Winterhager, E., & Willecke, K. (1998). Transplacental uptake of glucose is decreased in embryonic lethal connexin26-deficient mice. *J Cell Biol*, *140*(6), 1453-1461. https://doi.org/10.1083/jcb.140.6.1453

Gehi, R., Shao, Q., & Laird, D. W. (2011). Pathways regulating the trafficking and turnover of pannexin1 protein and the role of the C-terminal domain. *J Biol Chem*, *286*(31), 27639-27653. https://doi.org/10.1074/jbc.M111.260711

Gholamitabar Tabari, M., Ali Jorsaraei, S. G., Ghasemzadeh-Hasankolaei, M., Asghar Ahmadi, A., & Ghasemi, M. (2019). Comparison of Germ Cell Gene Expression in Spontaneous Monolayer versus Embryoid Body Differentiation of Mouse Embryonic Stem Cells toward Germ Cells. *International Journal of Fertility and Sterility*, *Vol 13*, 139-147. https://doi.org/https://doi.org/10.22074/ijfs.2019.5557

Gilbert S, F. (2000). Developmental Biology. In (6 ed.). Sinauer Associates.

Gilbert, S. F. (2000a). Developmental Biology. In *Endoderm* (6 ed.). Sinauer Associates.

Gilbert, S. F. (2000b). Developmental Biology. In. Sinauer Associates.

Gordeeva, O. (2019). TGFβ Family Signaling Pathways in Pluripotent and Teratocarcinoma Stem Cells' Fate Decisions: Balancing Between Self-Renewal, Differentiation, and Cancer. *Cells*, *8*(12). https://doi.org/10.3390/cells8121500

Graw, J. (2010). Eye development. *Curr Top Dev Biol*, *90*, 343-386. https://doi.org/10.1016/S0070-2153(10)90010-0

Guo, T., Feng, Y. L., Xiao, J. J., Liu, Q., Sun, X. N., Xiang, J. F., . . . Xie, A. Y. (2018). Harnessing accurate non-homologous end joining for efficient precise deletion in

CRISPR/Cas9-mediated genome editing. *Genome Biol*, *19*(1), 170. https://doi.org/10.1186/s13059-018-1518-x

Gässler, A., Quiclet, C., Kluth, O., Gottmann, P., Schwerbel, K., Helms, A., . . . Vogel, H. (2020). Overexpression of Gjb4 impairs cell proliferation and insulin secretion in primary islet cells. *Mol Metab*, *41*, 101042. https://doi.org/10.1016/j.molmet.2020.101042

Hainz, N., Beckmann, A., Schubert, M., Haase, A., Martin, U., Tschernig, T., & Meier, C. (2018). Human stem cells express pannexins. *BMC Res Notes*, *11*(1), 54. https://doi.org/10.1186/s13104-018-3125-z

Hartfield, E. M., Rinaldi, F., Glover, C. P., Wong, L. F., Caldwell, M. A., & Uney, J. B. (2011). Connexin 36 expression regulates neuronal differentiation from neural progenitor cells. *PLoS One*, *6*(3), e14746. https://doi.org/10.1371/journal.pone.0014746

Hillis, G. S., Duthie, L. A., Mlynski, R., McKay, N. G., Mistry, S., MacLeod, A. M., . . . Haites, N. E. (1997). The expression of connexin 43 in human kidney and cultured renal cells. *Nephron*, *75*(4), 458-463. https://doi.org/10.1159/000189585

Hirabayashi, Y., Yoon, B. I., Tsuboi, I., Huo, Y., Kodama, Y., Kanno, J., . . . Inoue, T. (2007a). Membrane channel connexin 32 maintains Lin(-)/c-kit(+) hematopoietic progenitor cell compartment: analysis of the cell cycle. *J Membr Biol*, *217*(1-3), 105-113. https://doi.org/10.1007/s00232-007-9042-z

Hirabayashi, Y., Yoon, B. I., Tsuboi, I., Huo, Y., Kodama, Y., Kanno, J., . . . Inoue, T. (2007b). Protective role of connexin 32 in steady-state hematopoiesis, regeneration

state, and leukemogenesis. *Exp Biol Med (Maywood)*, *232*(5), 700-712. https://doi.org/https://doi.org/10.3181%2F00379727-232-2320700

Hsu, P. D., Lander, E. S., & Zhang, F. (2014). Development and applications of CRISPR-Cas9 for genome engineering. *Cell*, *157*(6), 1262-1278. https://doi.org/10.1016/j.cell.2014.05.010

Huettner, J. E., Lu, A., Qu, Y., Wu, Y., Kim, M., & McDonald, J. W. (2006). Gap junctions and connexon hemichannels in human embryonic stem cells. *Stem Cells*, *24*(7), 1654-1667. https://doi.org/10.1634/stemcells.2005-0003

Ishikawa, M., Iwamoto, T., Fukumoto, S., & Yamada, Y. (2014). Pannexin 3 inhibits proliferation of osteoprogenitor cells by regulating Wnt and p21 signaling. *J Biol Chem*, *289*(5), 2839-2851. https://doi.org/10.1074/jbc.M113.523241

Ishikawa, M., & Yamada, Y. (2017). The Role of Pannexin 3 in Bone Biology. *J Dent Res*, *96*(4), 372-379. https://doi.org/10.1177/0022034516678203

Iwamoto, T., Nakamura, T., Doyle, A., Ishikawa, M., de Vega, S., Fukumoto, S., & Yamada, Y. (2010). Pannexin 3 regulates intracellular ATP/cAMP levels and promotes chondrocyte differentiation. *J Biol Chem*, *285*(24), 18948-18958. https://doi.org/10.1074/jbc.M110.127027

Joberty, G., Fälth-Savitski, M., Paulmann, M., Bösche, M., Doce, C., Cheng, A. T., . . . Grandi, P. (2020). A Tandem Guide RNA-Based Strategy for Efficient CRISPR Gene Editing of Cell Populations with Low Heterogeneity of Edited Alleles. *CRISPR J*, *3*(2), 123-134. https://doi.org/10.1089/crispr.2019.0064

Johnson, M. T., Carpenter, E. J., Tian, Z., Bruskiewich, R., Burris, J. N., Carrigan, C. T., . . . Wong, G. K. (2012). Evaluating methods for isolating total RNA and predicting

the success of sequencing phylogenetically diverse plant transcriptomes. *PLoS One*, *7*(11), e50226. https://doi.org/10.1371/journal.pone.0050226

Johnstone, S. R., Billaud, M., Lohman, A. W., Taddeo, E. P., & Isakson, B. E. (2012). Posttranslational modifications in connexins and pannexins. *J Membr Biol*, *245*(5-6), 319-332. https://doi.org/10.1007/s00232-012-9453-3

Jurić, M., Zeitler, J., Vukojević, K., Bočina, I., Grobe, M., Kretzschmar, G., . . . Filipović, N. (2020). Expression of Connexins 37, 43 and 45 in Developing Human Spinal Cord and Ganglia. *Int J Mol Sci*, *21*(24). https://doi.org/10.3390/ijms21249356

Kanai-Azuma, M., Kanai, Y., Gad, J. M., Tajima, Y., Taya, C., Kurohmaru, M., . . . Hayashi, Y. (2002). Depletion of definitive gut endoderm in Sox17-null mutant mice. *Development*, *129*(10), 2367-2379. https://doi.org/https://doi.org/10.1242/dev.129.10.2367

Ke, Q., Li, L., Cai, B., Liu, C., Yang, Y., Gao, Y., . . . Xiang, A. P. (2013). Connexin 43 is involved in the generation of human-induced pluripotent stem cells. *Hum Mol Genet*, *22*(11), 2221-2233. https://doi.org/10.1093/hmg/ddt074

Ke, Q., Li, L., Yao, X., Lai, X., Cai, B., Chen, H., . . . Li, W. (2017). Enhanced generation of human induced pluripotent stem cells by ectopic expression of Connexin 45. *Sci Rep*, *7*(1), 458. https://doi.org/10.1038/s41598-017-00523-y

Kelly, J. J., Esseltine, J. L., Shao, Q., Jabs, E. W., Sampson, J., Auranen, M., . . . Laird, D. W. (2016). Specific functional pathologies of Cx43 mutations associated with oculodentodigital dysplasia. *Mol Biol Cell*, *27*(14), 2172-2185. https://doi.org/10.1091/mbc.E16-01-0062

Kelly, J. J., Simek, J., & Laird, D. W. (2015). Mechanisms linking connexin mutations to human diseases. *Cell Tissue Res*, *360*(3), 701-721. https://doi.org/10.1007/s00441-014-2024-4

Khodosevich, K., Zuccotti, A., Kreuzberg, M. M., Le Magueresse, C., Frank, M., Willecke, K., & Monyer, H. (2012). Connexin45 modulates the proliferation of transit-amplifying precursor cells in the mouse subventricular zone. *Proc Natl Acad Sci U S A*, *109*(49), 20107-20112. https://doi.org/10.1073/pnas.1217103109

Kiecker, C., Bates, T., & Bell, E. (2016). Molecular specification of germ layers in vertebrate embryos. *Cell Mol Life Sci*, *73*(5), 923-947. https://doi.org/10.1007/s00018-015-2092-y

Kojima, T., Kokai, Y., Chiba, H., Yamamoto, M., Mochizuki, Y., & Sawada, N. (2001). Cx32 but not Cx26 is associated with tight junctions in primary cultures of rat hepatocytes. *Exp Cell Res*, *263*(2), 193-201. https://doi.org/10.1006/excr.2000.5103

Kokotas, H., Papagiannaki, K., Grigoriadou, M., Petersen, M. B., & Katsarou, A. (2012). Erythrokeratodermia variabilis: report of two cases and a novel missense variant in GJB4 encoding connexin 30.3. *Eur J Dermatol*, *22*(2), 182-186. https://doi.org/10.1684/ejd.2011.1617

Koval, M., Molina, S. A., & Burt, J. M. (2014). Mix and match: investigating heteromeric and heterotypic gap junction channels in model systems and native tissues. *FEBS Lett*, *588*(8), 1193-1204. https://doi.org/10.1016/j.febslet.2014.02.025

Krüger, O., Plum, A., Kim, J. S., Winterhager, E., Maxeiner, S., Hallas, G., . . . Willecke, K. (2000). Defective vascular development in connexin 45-deficient mice.

Development, *127*(19), 4179-4193. https://doi.org/https://doi.org/10.1242/dev.127.19.4179

Kumar, A., Placone, J. K., & Engler, A. J. (2017). Understanding the extracellular forces that determine cell fate and maintenance. *Development*, *144*(23), 4261-4270. https://doi.org/10.1242/dev.158469

Laird, D. W., Naus, C. C., & Lampe, P. D. (2017). SnapShot: Connexins and Disease. *Cell*, *170*(6), 1260-1260.e1261. https://doi.org/10.1016/j.cell.2017.08.034

Lam, A. Q., Freedman, B. S., Morizane, R., Lerou, P. H., Valerius, M. T., & Bonventre, J. V. (2014). Rapid and efficient differentiation of human pluripotent stem cells into intermediate mesoderm that forms tubules expressing kidney proximal tubular markers. *J Am Soc Nephrol*, *25*(6), 1211-1225. https://doi.org/10.1681/ASN.2013080831

Lampe, P. D., & Lau, A. F. (2004). The effects of connexin phosphorylation on gap junctional communication. *Int J Biochem Cell Biol*, *36*(7), 1171-1186. https://doi.org/10.1016/S1357-2725(03)00264-4

Lampe, P. D., TenBroek, E. M., Burt, J. M., Kurata, W. E., Johnson, R. G., & Lau, A. F. (2000). Phosphorylation of connexin43 on serine368 by protein kinase C regulates gap junctional communication. *J Cell Biol*, *149*(7), 1503-1512. https://doi.org/10.1083/jcb.149.7.1503

Lee, J. R., & White, T. W. (2009). Connexin-26 mutations in deafness and skin disease. *Expert Rev Mol Med*, *11*, e35. https://doi.org/10.1017/S1462399409001276

Lee, V. R., Barr, K. J., Kelly, J. J., Johnston, D., Brown, C. F. C., Robb, K. P., . . . Penuela, S. (2018). Pannexin 1 regulates adipose stromal cell differentiation and fat accumulation. *Sci Rep*, *8*(1), 16166. https://doi.org/10.1038/s41598-018-34234-9

Liao, Y., Day, K. H., Damon, D. N., & Duling, B. R. (2001). Endothelial cell-specific knockout of connexin 43 causes hypotension and bradycardia in mice. *Proc Natl Acad Sci U S A*, *98*(17), 9989-9994. https://doi.org/10.1073/pnas.171305298

Lin, F. X., Zheng, G. Z., Chang, B., Chen, R. C., Zhang, Q. H., Xie, P., . . . Li, X. D. (2018). Connexin 43 Modulates Osteogenic Differentiation of Bone Marrow Stromal Cells Through GSK-3beta/Beta-Catenin Signaling Pathways. *Cell Physiol Biochem*, *47*(1), 161-175. https://doi.org/10.1159/000489763

Lin, Y., & Chen, G. (2014). *Stembook. In: Community TSCR, editor*. IOS Press.

Lindsley, R. C., Gill, J. G., Kyba, M., Murphy, T. L., & Murphy, K. M. (2006). Canonical Wnt signaling is required for development of embryonic stem cell-derived mesoderm. *Development*, *133*(19), 3787-3796. https://doi.org/10.1242/dev.02551

Lo, B., & Parham, L. (2009). Ethical issues in stem cell research. *Endocr Rev*, *30*(3), 204-213. https://doi.org/10.1210/er.2008-0031

Lotz, S., Goderie, S., Tokas, N., Hirsch, S. E., Ahmad, F., Corneo, B., . . . Fasano, C. A. (2013). Sustained levels of FGF2 maintain undifferentiated stem cell cultures with biweekly feeding. *PLoS One*, *8*(2), e56289. https://doi.org/10.1371/journal.pone.0056289

Lucke, T., Choudhry, R., Thom, R., Selmer, I. S., Burden, A. D., & Hodgins, M. B. (1999). Upregulation of connexin 26 is a feature of keratinocyte differentiation in

hyperproliferative epidermis, vaginal epithelium, and buccal epithelium. *J Invest Dermatol*, *112*(3), 354-361. https://doi.org/10.1046/j.1523-1747.1999.00512.x

López-Bigas, N., Olivé, M., Rabionet, R., Ben-David, O., Martínez-Matos, J. A., Bravo, O., . . . Estivill, X. (2001). Connexin 31 (GJB3) is expressed in the peripheral and auditory nerves and causes neuropathy and hearing impairment. *Hum Mol Genet*, *10*(9), 947-952. https://doi.org/10.1093/hmg/10.9.947

Maes, M., Cogliati, B., Crespo Yanguas, S., Willebrords, J., & Vinken, M. (2015). Roles of connexins and pannexins in digestive homeostasis. *Cell Mol Life Sci*, *72*(15), 2809-2821. https://doi.org/10.1007/s00018-015-1961-8

Mandal, P. K., Ferreira, L. M., Collins, R., Meissner, T. B., Boutwell, C. L., Friesen, M., . . . Cowan, C. A. (2014). Efficient ablation of genes in human hematopoietic stem and effector cells using CRISPR/Cas9. *Cell Stem Cell*, *15*(5), 643-652. https://doi.org/10.1016/j.stem.2014.10.004

Mannino, G., Vicario, N., Parenti, R., Giuffrida, R., & Lo Furno, D. (2020). Connexin expression decreases during adipogenic differentiation of human adipose-derived mesenchymal stem cells. *Mol Biol Rep*, *47*(12), 9951-9958. https://doi.org/10.1007/s11033-020-05950-1

Mansergh, F. C., Daly, C. S., Hurley, A. L., Wride, M. A., Hunter, S. M., & Evans, M. J. (2009). Gene expression profiles during early differentiation of mouse embryonic stem cells. *BMC Dev Biol*, *9*, 5. https://doi.org/10.1186/1471-213X-9-5

Matsui, Y., Zsebo, K., & Hogan, B. L. (1992). Derivation of pluripotential embryonic stem cells from murine primordial germ cells in culture. *Cell*, *70*(5), 841-847. https://doi.org/10.1016/0092-8674(92)90317-6

McLean, A. B., D'Amour, K. A., Jones, K. L., Krishnamoorthy, M., Kulik, M. J., Reynolds, D. M., . . . Dalton, S. (2007). Activin a efficiently specifies definitive endoderm from human embryonic stem cells only when phosphatidylinositol 3-kinase signaling is suppressed. *Stem Cells*, *25*(1), 29-38. https://doi.org/10.1634/stemcells.2006-0219

Michalski, K., Syrjanen, J. L., Henze, E., Kumpf, J., Furukawa, H., & Kawate, T. (2020). The Cryo-EM structure of pannexin 1 reveals unique motifs for ion selection and inhibition. *Elife*, *9*. https://doi.org/10.7554/eLife.54670

Montecino-Rodriguez, E., Leathers, H., & Dorshkind, K. (2000). Expression of connexin 43 (Cx43) is critical for normal hematopoiesis. *Blood*, *96*(3), 917-924. https://doi.org/https://doi.org/10.1182/blood.V96.3.917

Moore, J. C., Tsang, S. Y., Rushing, S. N., Lin, D., Tse, H. F., Chan, C. W., & Li, R. A. (2008). Functional consequences of overexpressing the gap junction Cx43 in the cardiogenic potential of pluripotent human embryonic stem cells. *Biochem Biophys Res Commun*, *377*(1), 46-51. https://doi.org/10.1016/j.bbrc.2008.09.076

Mossahebi-Mohammadi, M., Quan, M., Zhang, J. S., & Li, X. (2020). FGF Signaling Pathway: A Key Regulator of Stem Cell Pluripotency. *Front Cell Dev Biol*, *8*, 79. https://doi.org/10.3389/fcell.2020.00079

Mullen, A. C., & Wrana, J. L. (2017). TGF-β Family Signaling in Embryonic and Somatic Stem-Cell Renewal and Differentiation. *Cold Spring Harb Perspect Biol*, *9*(7). https://doi.org/10.1101/cshperspect.a022186

Murgia, A., Orzan, E., Polli, R., Martella, M., Vinanzi, C., Leonardi, E., . . . Zacchello, F. (1999). Cx26 deafness: mutation analysis and clinical variability. *J Med Genet*, *36*(11), 829-832. https://doi.org/http://dx.doi.org/10.1136/jmg.36.11.829

Nagasaka, R., Matsumoto, M., Okada, M., Sasaki, H., Kanie, K., Kii, H., . . . Kato, R. (2017). Visualization of morphological categories of colonies for monitoring of effect on induced pluripotent stem cell culture status. *Regen Ther*, *6*, 41-51. https://doi.org/10.1016/j.reth.2016.12.003

Nagy, J. I., Ionescu, A. V., Lynn, B. D., & Rash, J. E. (2003). Connexin29 and connexin32 at oligodendrocyte and astrocyte gap junctions and in myelin of the mouse central nervous system. *J Comp Neurol*, *464*(3), 356-370. https://doi.org/10.1002/cne.10797

Nelles, E., Bützler, C., Jung, D., Temme, A., Gabriel, H. D., Dahl, U., . . . Willecke, K. (1996). Defective propagation of signals generated by sympathetic nerve stimulation in the liver of connexin32-deficient mice. *Proc Natl Acad Sci U S A*, *93*(18), 9565-9570. https://doi.org/10.1073/pnas.93.18.9565

Nishii, K., Shibata, Y., & Kobayashi, Y. (2014). Connexin mutant embryonic stem cells and human diseases. *World J Stem Cells*, *6*(5), 571-578. https://doi.org/10.4252/wjsc.v6.i5.571

Nishimoto, M., Fukushima, A., Okuda, A., & Muramatsu, M. (1999). The gene for the embryonic stem cell coactivator UTF1 carries a regulatory element which selectively interacts with a complex composed of Oct-3/4 and Sox-2. *Mol Cell Biol*, *19*(8), 5453-5465. https://doi.org/10.1128/mcb.19.8.5453

Noort, R. J., Christopher, G. A., & Esseltine, J. L. (2021). Pannexin 1 Influences Lineage Specification of Human iPSCs. *Frontiers in Cell and Developmental Biology*, *9*, 876. https://doi.org/0.3389/fcell.2021.659397

Nostro, M. C., Cheng, X., Keller, G. M., & Gadue, P. (2008). Wnt, activin, and BMP signaling regulate distinct stages in the developmental pathway from embryonic stem cells to blood. *Cell Stem Cell*, *2*(1), 60-71. https://doi.org/10.1016/j.stem.2007.10.011

Okita, K., Ichisaka, T., & Yamanaka, S. (2007). Generation of germline-competent induced pluripotent stem cells. *Nature*, *448*(7151), 313-317. https://doi.org/10.1038/nature05934

Orellana, J. A., Froger, N., Ezan, P., Jiang, J. X., Bennett, M. V., Naus, C. C., . . . Sáez, J. C. (2011). ATP and glutamate released via astroglial connexin 43 hemichannels mediate neuronal death through activation of pannexin 1 hemichannels. *J Neurochem*, *118*(5), 826-840. https://doi.org/10.1111/j.1471-4159.2011.07210.x

Oyamada, M., Takebe, K., Endo, A., Hara, S., & Oyamada, Y. (2013). Connexin expression and gap-junctional intercellular communication in ES cells and iPS cells. *Front Pharmacol*, *4*, 85. https://doi.org/10.3389/fphar.2013.00085

Pagliuca, F. W., Millman, J. R., Gürtler, M., Segel, M., Van Dervort, A., Ryu, J. H., . . . Melton, D. A. (2014). Generation of functional human pancreatic β cells in vitro. *Cell*, *159*(2), 428-439. https://doi.org/10.1016/j.cell.2014.09.040

Parekkadan, B., Berdichevsky, Y., Irimia, D., Leeder, A., Yarmush, G., Toner, M., . . . Yarmush, M. L. (2008). Cell-cell interaction modulates neuroectodermal

specification of embryonic stem cells. *Neurosci Lett*, *438*(2), 190-195. https://doi.org/10.1016/j.neulet.2008.03.094

Pei, H., Zhai, C., Li, H., Yan, F., Qin, J., Yuan, H., . . . Pei, X. (2017). Connexin 32 and connexin 43 are involved in lineage restriction of hepatic progenitor cells to hepatocytes. *Stem Cell Res Ther*, *8*(1), 252. https://doi.org/10.1186/s13287-017-0703-2

Peng, Q., Yue, C., Chen, A. C. H., Lee, K. C., Fong, S. W., Yeung, W. S. B., & Lee, Y. L. (2019). Connexin 43 is involved in early differentiation of human embryonic stem cells. *Differentiation*, *105*, 33-44. https://doi.org/10.1016/j.diff.2018.12.003

Penuela, S., Bhalla, R., Gong, X. Q., Cowan, K. N., Celetti, S. J., Cowan, B. J., . . . Laird, D. W. (2007). Pannexin 1 and pannexin 3 are glycoproteins that exhibit many distinct characteristics from the connexin family of gap junction proteins. *J Cell Sci*, *120*(Pt 21), 3772-3783. https://doi.org/10.1242/jcs.009514

Penuela, S., Bhalla, R., Nag, K., & Laird, D. W. (2009). Glycosylation regulates pannexin intermixing and cellular localization. *Mol Biol Cell*, *20*(20), 4313-4323. https://doi.org/10.1091/mbc.e09-01-0067

Penuela, S., Celetti, S. J., Bhalla, R., Shao, Q., & Laird, D. W. (2008). Diverse subcellular distribution profiles of pannexin 1 and pannexin 3. *Cell Commun Adhes*, *15*(1), 133-142. https://doi.org/10.1080/15419060802014115

Penuela, S., Gehi, R., & Laird, D. W. (2013). The biochemistry and function of pannexin channels. *Biochim Biophys Acta*, *1828*(1), 15-22. https://doi.org/10.1016/j.bbamem.2012.01.017

Penuela, S., Harland, L., Simek, J., & Laird, D. W. (2014). Pannexin channels and their links to human disease. *Biochem J*, *461*(3), 371-381. https://doi.org/10.1042/BJ20140447

Perrimon, N., Pitsouli, C., & Shilo, B. Z. (2012). Signaling mechanisms controlling cell fate and embryonic patterning. *Cold Spring Harb Perspect Biol*, *4*(8), a005975. https://doi.org/10.1101/cshperspect.a005975

Pettinato, G., Wen, X., & Zhang, N. (2014). Formation of well-defined embryoid bodies from dissociated human induced pluripotent stem cells using microfabricated cell-repellent microwell arrays. *Sci Rep*, *4*, 7402. https://doi.org/10.1038/srep07402

Pham, T. L., St-Pierre, M. E., Ravel-Chapuis, A., Parks, T. E. C., Langlois, S., Penuela, S., . . . Cowan, K. N. (2018). Expression of Pannexin 1 and Pannexin 3 during skeletal muscle development, regeneration, and Duchenne muscular dystrophy. *J Cell Physiol*, *233*(10), 7057-7070. https://doi.org/10.1002/jcp.26629

Plum, A., Hallas, G., Magin, T., Dombrowski, F., Hagendorff, A., Schumacher, B., . . . Willecke, K. (2000). Unique and shared functions of different connexins in mice. *Curr Biol*, *10*(18), 1083-1091. https://doi.org/10.1016/s0960-9822(00)00690-4

Plum, A., Winterhager, E., Pesch, J., Lautermann, J., Hallas, G., Rosentreter, B., . . . Willecke, K. (2001). Connexin31-deficiency in mice causes transient placental dysmorphogenesis but does not impair hearing and skin differentiation. *Dev Biol*, *231*(2), 334-347. https://doi.org/10.1006/dbio.2000.0148

Prummel, K. D., Nieuwenhuize, S., & Mosimann, C. (2020). The lateral plate mesoderm. *Development*, *147*(12). https://doi.org/10.1242/dev.175059

Przybyla, L., & Voldman, J. (2012). Probing embryonic stem cell autocrine and paracrine signaling using microfluidics. *Annu Rev Anal Chem (Palo Alto Calif)*, *5*, 293-315. https://doi.org/10.1146/annurev-anchem-062011-143122

Qin, J., Chang, M., Wang, S., Liu, Z., Zhu, W., Wang, Y., . . . Pei, X. (2016). Connexin 32-mediated cell-cell communication is essential for hepatic differentiation from human embryonic stem cells. *Sci Rep*, *6*, 37388. https://doi.org/10.1038/srep37388

Qu, R., Dong, L., Zhang, J., Yu, X., Wang, L., & Zhu, S. (2020). Cryo-EM structure of human heptameric Pannexin 1 channel. *Cell Res*, *30*(5), 446-448. https://doi.org/10.1038/s41422-020-0298-5

Raveh-Amit, H., Berzsenyi, S., Vas, V., Ye, D., & Dinnyes, A. (2013). Tissue resident stem cells: till death do us part. *Biogerontology*, *14*(6), 573-590. https://doi.org/10.1007/s10522-013-9469-9

Raymond, A., Liu, B., Liang, H., Wei, C., Guindani, M., Lu, Y., . . . Nagarajan, L. (2014). A role for BMP-induced homeobox gene MIXL1 in acute myelogenous leukemia and identification of type I BMP receptor as a potential target for therapy. *Oncotarget*, *5*(24), 12675-12693. https://doi.org/10.18632/oncotarget.2564

Reaume, A. G., de Sousa, P. A., Kulkarni, S., Langille, B. L., Zhu, D., Davies, T. C., . . . Rossant, J. (1995). Cardiac malformation in neonatal mice lacking connexin43. *Science*, *267*(5205), 1831-1834. https://doi.org/10.1126/science.7892609

Rodda, D. J., Chew, J. L., Lim, L. H., Loh, Y. H., Wang, B., Ng, H. H., & Robson, P. (2005). Transcriptional regulation of nanog by OCT4 and SOX2. *J Biol Chem*, *280*(26), 24731-24737. https://doi.org/10.1074/jbc.M502573200

Rosler, E. S., Fisk, G. J., Ares, X., Irving, J., Miura, T., Rao, M. S., & Carpenter, M. K. (2004). Long-term culture of human embryonic stem cells in feeder-free conditions. *Dev Dyn*, *229*(2), 259-274. https://doi.org/10.1002/dvdy.10430

Sahli, K. A., Flora, G. D., Sasikumar, P., Maghrabi, A. H., Holbrook, L. M., AlOuda, S. K., . . . Gibbins, J. M. (2021). Structural, functional, and mechanistic insights uncover the fundamental role of orphan connexin-62 in platelets. *Blood*, *137*(6), 830-843. https://doi.org/10.1182/blood.2019004575

Salomon, D., Masgrau, E., Vischer, S., Ullrich, S., Dupont, E., Sappino, P., . . . Meda, P. (1994). Topography of mammalian connexins in human skin. *J Invest Dermatol*, *103*(2), 240-247. https://doi.org/10.1111/1523-1747.ep12393218

Sang, Q., Zhang, Z., Shi, J., Sun, X., Li, B., Yan, Z., . . . Wang, L. (2019). A pannexin 1 channelopathy causes human oocyte death. *Sci Transl Med*, *11*(485). https://doi.org/10.1126/scitranslmed.aav8731

Sargiannidou, I., Vavlitou, N., Aristodemou, S., Hadjisavvas, A., Kyriacou, K., Scherer, S. S., & Kleopa, K. A. (2009). Connexin32 mutations cause loss of function in Schwann cells and oligodendrocytes leading to PNS and CNS myelination defects. *J Neurosci*, *29*(15), 4736-4749. https://doi.org/10.1523/JNEUROSCI.0325-09.2009

Saund, R. S., Kanai-Azuma, M., Kanai, Y., Kim, I., Lucero, M. T., & Saijoh, Y. (2012). Gut endoderm is involved in the transfer of left-right asymmetry from the node to the lateral plate mesoderm in the mouse embryo. *Development*, *139*(13), 2426-2435. https://doi.org/10.1242/dev.079921

Scemes, E., Suadicani, S. O., Dahl, G., & Spray, D. C. (2007). Connexin and pannexin mediated cell-cell communication. *Neuron Glia Biol*, *3*(3), 199-208. https://doi.org/10.1017/S1740925X08000069

Scherer, S. S., & Kleopa, K. A. (2012). X-linked Charcot-Marie-Tooth disease. *J Peripher Nerv Syst*, *17 Suppl 3*, 9-13. https://doi.org/10.1111/j.1529-8027.2012.00424.x

Schindelin, J., Arganda-Carreras, I., Frise, E., Kaynig, V., Longair, M., Pietzsch, T., . . . Cardona, A. (2013). Fiji: an open-source platform for biological-image analysis. *Nat Methods*, *9*(7), 676-682. https://doi.org/10.1038/nmeth.2019

Schmidt, R., & Plath, K. (2012). The roles of the reprogramming factors Oct4, Sox2 and Klf4 in resetting the somatic cell epigenome during induced pluripotent stem cell generation. *Genome Biol*, *13*(10), 251. https://doi.org/10.1186/gb-2012-13-10-251

Scott, C. A., Tattersall, D., O'Toole, E. A., & Kelsell, D. P. (2012). Connexins in epidermal homeostasis and skin disease. *Biochim Biophys Acta*, *1818*(8), 1952-1961. https://doi.org/10.1016/j.bbamem.2011.09.004

Serre-Beinier, V., Bosco, D., Zulianello, L., Charollais, A., Caille, D., Charpantier, E., . . . Meda, P. (2009). Cx36 makes channels coupling human pancreatic beta-cells, and correlates with insulin expression. *Hum Mol Genet*, *18*(3), 428-439. https://doi.org/10.1093/hmg/ddn370

Shahbazi, M. N. (2020). Mechanisms of human embryo development: from cell fate to tissue shape and back. *Development*, *147*(14). https://doi.org/10.1242/dev.190629

Shahriyari, L., & Komarova, N. L. (2013). Symmetric vs. asymmetric stem cell divisions: an adaptation against cancer? *PLoS One*, *8*(10), e76195. https://doi.org/10.1371/journal.pone.0076195

Shao, Q., Esseltine, J. L., Huang, T., Novielli-Kuntz, N., Ching, J. E., Sampson, J., & Laird, D. W. (2019). Connexin43 is Dispensable for Early Stage Human Mesenchymal Stem Cell Adipogenic Differentiation But is Protective against Cell Senescence. *Biomolecules*, *9*(9). https://doi.org/10.3390/biom9090474

Shao, Q., Lindstrom, K., Shi, R., Kelly, J., Schroeder, A., Juusola, J., . . . Laird, D. W. (2016). A Germline Variant in the PANX1 Gene Has Reduced Channel Function and Is Associated with Multisystem Dysfunction. *J Biol Chem*, *291*(24), 12432-12443. https://doi.org/10.1074/jbc.M116.717934

Sharma, A., Toepfer, C. N., Ward, T., Wasson, L., Agarwal, R., Conner, D. A., . . . Seidman, C. E. (2018). CRISPR/Cas9-Mediated Fluorescent Tagging of Endogenous Proteins in Human Pluripotent Stem Cells. *Curr Protoc Hum Genet*, *96*, 21.11.21-21.11.20. https://doi.org/10.1002/cphg.52

Sharma, R., Shafer, M. E. R., Bareke, E., Tremblay, M., Majewski, J., & Bouchard, M. (2017). Bmp signaling maintains a mesoderm progenitor cell state in the mouse tailbud. *Development*, *144*(16), 2982-2993. https://doi.org/10.1242/dev.149955

Sharovskaya, Y. Y., Philonenko, E. S., Kiselev, S. L., & Lagarkova, M. A. (2012). De novo reestablishment of gap junctional intercellular communications during reprogramming to pluripotency and differentiation. *Stem Cells Dev*, *21*(14), 2623-2629. https://doi.org/10.1089/scd.2011.0707

Shi, G., & Jin, Y. (2010). Role of Oct4 in maintaining and regaining stem cell pluripotency. *Stem Cell Res Ther*, *1*(5), 39. https://doi.org/10.1186/scrt39

Simunovic, M., & Brivanlou, A. H. (2017). Embryoids, organoids and gastruloids: new approaches to understanding embryogenesis. *Development*, *144*(6), 976-985. https://doi.org/10.1242/dev.143529

Singh, V. K., Saini, A., Kalsan, M., Kumar, N., & Chandra, R. (2016). Describing the Stem Cell Potency: The Various Methods of Functional Assessment and. *Front Cell Dev Biol*, *4*, 134. https://doi.org/10.3389/fcell.2016.00134

Song, B., Fan, Y., He, W., Zhu, D., Niu, X., Wang, D., . . . Sun, X. (2015). Improved hematopoietic differentiation efficiency of gene-corrected beta-thalassemia induced pluripotent stem cells by CRISPR/Cas9 system. *Stem Cells Dev*, *24*(9), 1053-1065. https://doi.org/10.1089/scd.2014.0347

Soufi, A., & Dalton, S. (2016). Cycling through developmental decisions: how cell cycle dynamics control pluripotency, differentiation and reprogramming. *Development*, *143*(23), 4301-4311. https://doi.org/10.1242/dev.142075

Sui, L., Mfopou, J. K., Geens, M., Sermon, K., & Bouwens, L. (2012). FGF signaling via MAPK is required early and improves Activin A-induced definitive endoderm formation from human embryonic stem cells. *Biochem Biophys Res Commun*, *426*(3), 380-385. https://doi.org/10.1016/j.bbrc.2012.08.098

Söhl, G., Joussen, A., Kociok, N., & Willecke, K. (2010). Expression of connexin genes in the human retina. *BMC Ophthalmol*, *10*, 27. https://doi.org/10.1186/1471-2415-10-27

Söhl, G., Nielsen, P. A., Eiberger, J., & Willecke, K. (2003). Expression profiles of the novel human connexin genes hCx30.2, hCx40.1, and hCx62 differ from their

putative mouse orthologues. *Cell Commun Adhes*, *10*(1), 27-36. https://doi.org/10.1080/15419060302063

Takahashi, K., Tanabe, K., Ohnuki, M., Narita, M., Ichisaka, T., Tomoda, K., & Yamanaka, S. (2007). Induction of pluripotent stem cells from adult human fibroblasts by defined factors. *Cell*, *131*(5), 861-872. https://doi.org/10.1016/j.cell.2007.11.019

Tam, P. P., & Loebel, D. A. (2007). Gene function in mouse embryogenesis: get set for gastrulation. *Nat Rev Genet*, *8*(5), 368-381. https://doi.org/10.1038/nrg2084

Tang, X., Fu, J., Chen, Z., Luo, L., Li, D. W., & Liu, Y. (2021). Generation of a homozygous CRISPR/Cas9-mediated knockout H9 hESC subline for the MERTK locus. *Stem Cell Res*, *53*, 102310. https://doi.org/10.1016/j.scr.2021.102310

Taniguchi Ishikawa, E., Gonzalez-Nieto, D., Ghiaur, G., Dunn, S. K., Ficker, A. M., Murali, B., . . . Cancelas, J. A. (2012). Connexin-43 prevents hematopoietic stem cell senescence through transfer of reactive oxygen species to bone marrow stromal cells. *Proc Natl Acad Sci U S A*, *109*(23), 9071-9076. https://doi.org/10.1073/pnas.1120358109

Tchieu, J., Zimmer, B., Fattahi, F., Amin, S., Zeltner, N., Chen, S., & Studer, L. (2017). A Modular Platform for Differentiation of Human PSCs into All Major Ectodermal Lineages. *Cell Stem Cell*, *21*(3), 399-410.e397. https://doi.org/10.1016/j.stem.2017.08.015

Temme, A., Buchmann, A., Gabriel, H. D., Nelles, E., Schwarz, M., & Willecke, K. (1997). High incidence of spontaneous and chemically induced liver tumors in mice deficient for connexin32. *Curr Biol*, *7*(9), 713-716. https://doi.org/10.1016/s0960-9822(06)00302-2

Teubner, B., Michel, V., Pesch, J., Lautermann, J., Cohen-Salmon, M., Söhl, G., . . . Willecke, K. (2003). Connexin30 (Gjb6)-deficiency causes severe hearing impairment and lack of endocochlear potential. *Hum Mol Genet*, *12*(1), 13-21. https://doi.org/10.1093/hmg/ddg001

Thomson, J. A., Itskovitz-Eldor, J., Shapiro, S. S., Waknitz, M. A., Swiergiel, J. J., Marshall, V. S., & Jones, J. M. (1998). Embryonic stem cell lines derived from human blastocysts. *Science*, *282*(5391), 1145-1147. https://doi.org/10.1126/science.282.5391.1145

Thomson, J. A., & Odorico, J. S. (2000). Human embryonic stem cell and embryonic germ cell lines. *Trends Biotechnol*, *18*(2), 53-57. https://doi.org/10.1016/s0167-7799(99)01410-9

Uhlén, M., Fagerberg, L., Hallström, B. M., Lindskog, C., Oksvold, P., Mardinoglu, A., . . . Pontén, F. (2015). Proteomics. Tissue-based map of the human proteome. *Science*, *347*(6220), 1260419. https://doi.org/10.1126/science.1260419

Umar, S. (2010). Intestinal stem cells. *Curr Gastroenterol Rep*, *12*(5), 340-348. https://doi.org/10.1007/s11894-010-0130-3

van der Velden, H. M., & Jongsma, H. J. (2002). Cardiac gap junctions and connexins: their role in atrial fibrillation and potential as therapeutic targets. *Cardiovasc Res*, *54*(2), 270-279. https://doi.org/10.1016/s0008-6363(01)00557-0

van Veen, A. A., van Rijen, H. V., & Opthof, T. (2001). Cardiac gap junction channels: modulation of expression and channel properties. *Cardiovasc Res*, *51*(2), 217-229. https://doi.org/10.1016/s0008-6363(01)00324-8

Vanden Abeele, F., Bidaux, G., Gordienko, D., Beck, B., Panchin, Y. V., Baranova, A. V., . . . Prevarskaya, N. (2006). Functional implications of calcium permeability of the channel formed by pannexin 1. *J Cell Biol*, *174*(4), 535-546. https://doi.org/10.1083/jcb.200601115

Verma, N., Zhu, Z., & Huangfu, D. (2017). CRISPR/Cas-Mediated Knockin in Human Pluripotent Stem Cells. *Methods Mol Biol*, *1513*, 119-140. https://doi.org/10.1007/978-1-4939-6539-7_9

Vozzi, C., Dupont, E., Coppen, S. R., Yeh, H. I., & Severs, N. J. (1999). Chamber-related differences in connexin expression in the human heart. *J Mol Cell Cardiol*, *31*(5), 991-1003. https://doi.org/10.1006/jmcc.1999.0937

Wakui, T., Matsumoto, T., Matsubara, K., Kawasaki, T., Yamaguchi, H., & Akutsu, H. (2017). Method for evaluation of human induced pluripotent stem cell quality using image analysis based on the biological morphology of cells. *J Med Imaging (Bellingham)*, *4*(4), 044003. https://doi.org/10.1117/1.JMI.4.4.044003

Wang, P., Rodriguez, R. T., Wang, J., Ghodasara, A., & Kim, S. K. (2011). Targeting SOX17 in human embryonic stem cells creates unique strategies for isolating and analyzing developing endoderm. *Cell Stem Cell*, *8*(3), 335-346. https://doi.org/10.1016/j.stem.2011.01.017

Wang, Z. X., Teh, C. H., Kueh, J. L., Lufkin, T., Robson, P., & Stanton, L. W. (2007). Oct4 and Sox2 directly regulate expression of another pluripotency transcription factor, Zfp206, in embryonic stem cells. *J Biol Chem*, *282*(17), 12822-12830. https://doi.org/10.1074/jbc.M611814200

Wicki-Stordeur, L. E., Dzugalo, A. D., Swansburg, R. M., Suits, J. M., & Swayne, L. A. (2012). Pannexin 1 regulates postnatal neural stem and progenitor cell proliferation. *Neural Dev*, *7*, 11. https://doi.org/10.1186/1749-8104-7-11

Wicki-Stordeur, L. E., Sanchez-Arias, J. C., Dhaliwal, J., Carmona-Wagner, E. O., Shestopalov, V. I., Lagace, D. C., & Swayne, L. A. (2016). Pannexin 1 Differentially Affects Neural Precursor Cell Maintenance in the Ventricular Zone and Peri-Infarct Cortex. *J Neurosci*, *36*(4), 1203-1210. https://doi.org/10.1523/JNEUROSCI.0436-15.2016

Wilgenbus, K. K., Kirkpatrick, C. J., Knuechel, R., Willecke, K., & Traub, O. (1992). Expression of Cx26, Cx32 and Cx43 gap junction proteins in normal and neoplastic human tissues. *Int J Cancer*, *51*(4), 522-529. https://doi.org/10.1002/ijc.2910510404

Willecke, K., Temme, A., Teubner, B., & Ott, T. (1999). Characterization of targeted connexin32-deficient mice: a model for the human Charcot-Marie-Tooth (X-type) inherited disease. *Ann N Y Acad Sci*, *883*, 302-309. https://doi.org/https://doi.org/10.1111/j.1749-6632.1999.tb08592.x

Wiszniewski, L., Limat, A., Saurat, J. H., Meda, P., & Salomon, D. (2000). Differential expression of connexins during stratification of human keratinocytes. *J Invest Dermatol*, *115*(2), 278-285. https://doi.org/10.1046/j.1523-1747.2000.00043.x

Wolpert, L. (2015). *Principles of development* (5th ed.). Oxford University Press.

Wong, R. C., Dottori, M., Koh, K. L., Nguyen, L. T., Pera, M. F., & Pébay, A. (2006). Gap junctions modulate apoptosis and colony growth of human embryonic stem cells

maintained in a serum-free system. *Biochem Biophys Res Commun*, *344*(1), 181-188. https://doi.org/10.1016/j.bbrc.2006.03.127

Wörsdörfer, P., Bosen, F., Gebhardt, M., Russ, N., Zimmermann, K., Komla Kessie, D., . . . Willecke, K. (2017). Abrogation of Gap Junctional Communication in ES Cells Results in a Disruption of Primitive Endoderm Formation in Embryoid Bodies. *Stem Cells*, *35*(4), 859-871. https://doi.org/10.1002/stem.2545

Wörsdörfer, P., Maxeiner, S., Markopoulos, C., Kirfel, G., Wulf, V., Auth, T., . . . Willecke, K. (2008). Connexin expression and functional analysis of gap junctional communication in mouse embryonic stem cells. *Stem Cells*, *26*(2), 431-439. https://doi.org/10.1634/stemcells.2007-0482

Yang, W., Lampe, P. D., Kensel-Hammes, P., Hesson, J., Ware, C. B., Crisa, L., & Cirulli, V. (2019). Connexin 43 Functions as a Positive Regulator of Stem Cell Differentiation into Definitive Endoderm and Pancreatic Progenitors. *iScience*, *19*, 450-460. https://doi.org/10.1016/j.isci.2019.07.033

Zhang, X., Huang, C. T., Chen, J., Pankratz, M. T., Xi, J., Li, J., . . . Zhang, S. C. (2010). Pax6 is a human neuroectoderm cell fate determinant. *Cell Stem Cell*, *7*(1), 90-100. https://doi.org/10.1016/j.stem.2010.04.017

Zhao, J., Jiang, W. J., Sun, C., Hou, C. Z., Yang, X. M., & Gao, J. G. (2013). Induced pluripotent stem cells: origins, applications, and future perspectives. *J Zhejiang Univ Sci B*, *14*(12), 1059-1069. https://doi.org/10.1631/jzus.B1300215

Zhu, Z., & Huangfu, D. (2013). Human pluripotent stem cells: an emerging model in developmental biology. *Development*, *140*(4), 705-717. https://doi.org/10.1242/dev.086165

Zorn, A. M., & Wells, J. M. (2009). Vertebrate endoderm development and organ formation. *Annu Rev Cell Dev Biol*, *25*, 221-251. https://doi.org/10.1146/annurev.cellbio.042308.113344

6 Appendix A

Subject **HREB - Approval of Ethics Renewal 510179**
From <administrator@hrea.ca>
To Esseltine Jessica(Principal Investigator) <jesseltine@mun.ca>
Cc <administrator@hrea.ca>
Date 2020-10-06 08:59

roundcube
open source webmail software

Researcher Portal File #: 20191777

Dear Dr. Jessica Esseltine:

This e-mail serves as notification that your ethics renewal for study HREB # 2018.210 – Connexins and Pannexins in Stem Cell Pluripotency and Cell Fate Decisions – has been **approved**. Please log in to the Researcher Portal to view the approved event.

Ethics approval for this project has been granted for a period of twelve months effective from 13 Nov 2020 to 13 Nov 2021.

Please note, it is the responsibility of the Principal Investigator (PI) to ensure that the Ethics Renewal form is submitted prior to the renewal date each year. Though the Research Ethics Office makes every effort to remind the PI of this responsibility, the PI may not receive a reminder. The Ethics Renewal form can be found on the Researcher Portal as an "Event".

Thank you,

Research Ethics Office

(e) info@hrea.ca
(t) 709-777-6974
(f) 709-777-8776
(w) www.hrea.ca
Office Hours: 8:30 a.m. – 4:30 p.m. (NL TIME) Monday-Friday